

University of Nevada, Reno

**Water Quality Modeling Approach to Investigate Nutrient Criteria on the South
Fork Humboldt Reservoir, Nevada**

A thesis submitted in partial fulfillment of the
requirements for the degree of Masters of Science in
Hydrology

By

David William Smith

Dr. John J. Warwick / Thesis Advisor

December, 2011



University of Nevada, Reno
Statewide • Worldwide

THE GRADUATE SCHOOL

We recommend that the thesis
prepared under our supervision by

DAVID WILLIAM SMITH

entitled

**Water Quality Modeling Approach To Investigate Nutrient Criteria On The South
Fork Humboldt Reservoir, Nevada**

be accepted in partial fulfillment of the
requirements for the degree of

MASTER OF SCIENCE

Dr. John J. Warwick, Advisor

Dr. Christian H. Fritsen, Committee Member

Dr. V. Dean Adams, Graduate School Representative

Marsha H. Read, Ph. D., Associate Dean, Graduate School

December, 2011

ABSTRACT

The development of nutrient criteria for reservoir-river systems requires the consideration of downstream impacts, a difficult variable to quantify in arid environments with highly productive periphyton conditions. The South Fork Humboldt Reservoir (Elko County, Nevada) represents a river impoundment operated by bottom release and observed to increase nutrient loadings to highly eutrophic tail-waters (benthic Chl-a values $>500 \text{ mg/m}^2$). The USEPA mechanistic model AQUATOX 3.1 has been used to simulate the South Fork Reservoir and River algal nutrient loading functional response, and to determine coupled system changes for nutrient criteria development. The calibrated and validated reservoir model was used to simulate scenarios of 10 percent incremental changes to reservoir phosphorous loadings, with the equivalent covariance relationship of phosphorous to nitrogen and sediment loadings. The results indicate hypothetical ranges of eutrophic conditions for nutrient-criteria variables of phosphorous, nitrogen, secchi depth and chlorophyll-a (Chl-a). The reservoir scenario of 40 percent increase of observed loadings resulted in a decrease of average secchi depth, from 5.27 to 4.20 meters, and an increase of average Chl-a values from 2.11 to 2.29 $\mu\text{g/L}$ respectively. Reservoir scenario outflows were used as model boundary conditions for the calibrated and validated downstream river model. River scenarios results of 20 reservoir outflows indicate the immediate tailwater reach is somewhat insensitive to changes in reservoir loadings, demonstrating outflows conditions are potentially dominated by long-term in-reservoir sediment diagenesis processes.

ACKNOWLEDGMENTS

First, I would like to express my gratitude to my adviser Dr. John J. Warwick, for providing unrelenting guidance and support even with logistical challenges of career advancement across the country. Thank you to committee member Dr. Chris H. Fritsen, for supportive direction and guidance on technical writing and the fantastic opportunity to work with the SMEL lab on the South Fork Humboldt Reports. I would also like to Dr. Dean Adams, for a great introduction to surface water quality models, and for his support for project objectives.

I would also like to thank the organizations of the Nevada Department of Environmental Protection, especially Randy Pahl, Dave Simpson, and John Heggeness for data collection and financial support. The South Fork Humboldt State Park employees, for their unrelenting logistical and sampling support. Also, the Nevada Department of Wildlife for the willingness to share critical reservoir data.

Research, field work, data analysis and modeling were greatly helped through the guidance of Ramon Naranjo, Clint Davis, Jeramie Memmott, Lucas Williamson, and Arica Crootof. Without the support of my committee, organizations, and friends this project would not have been possible.

TABLE OF CONTENTS

ACKNOWLEDGMENTS	ii
TABLE OF CONTENTS.....	iii
LIST OF FIGURES	v
LIST OF TABLES	xi
1. INTRODUCTION	1
1.1 Nutrient Criteria Development Status Nevada	1
1.2 Linking Reservoir and River Simulations.....	5
2. BACKGROUND	8
2.1 Study Site: South Fork Humboldt Reservoir	8
2.2 South Fork Reservoir Eutrophication Status.....	12
2.3 South Fork River Eutrophication Status	15
3. FIELD DATA METHODS.....	16
3.1 Field Data Collection: 2009-2010 South Fork Reservoir	16
3.2 Field Data Collection: 2009-2010 South Fork Humboldt River.....	18
3.3 Discharge, Stage, Temperature and Weather Data Collection	20
4. FIELD DATA RESULTS.....	22
4.1 South Fork Reservoir 2009-2010.....	22
4.2 South Fork Humboldt River 2009-2010	28
5. USEPA - AQUATOX 3.1.....	32
5.1 Model Description	32
5.2 Reservoir Model.....	33
5.3 Phytoplankton, Periphyton and Zooplankton Calculations	36
5.4 Sediment Diagenesis.....	38
5.5 River Model	40
6. AQUATOX 3.1 Sensitivity Analysis, Calibration, and Validation	42
6.1 SFH Reservoir and River Model Sensitivity Analysis	42
6.2 SFH River and Reservoir Model Calibration Parameters.....	44

6.2.1	Phytoplankton and Periphyton Calibration Parameters	44
6.2.2	Zooplankton Calibration Parameters	49
6.2.3	Sediment Diagenesis Calibration Parameters	50
6.3	AQUATOX 3.1 Model Calibration and Validation.....	51
6.3.1	Reservoir Model Calibration Results.....	53
6.3.2	Reservoir Model Validation Results.....	66
6.3.3	River Model Calibration Results	72
6.3.4	River Model Validation Results.....	80
7.	NUTRIENT LOADING SCENARIOS	84
8.	CONCLUSIONS & RECOMMENDATIONS.....	93
9.	REFERENCES	96
	APPENDIX A-2009-2010 SFH System Data.....	103
	APPENDIX B- Reservoir and River Model Initial Conditions	105
	APPENDIX C- Reservoir Parameter Values	107
	APPENDIX D- River Parameters	112
	APPENDIX E- Scenario Nutrient Loading Values	114

LIST OF FIGURES

Figure 1: EPA Aggregated Ecoregion III geographical area, with Nevada being encompassed in the Central Basin and Range Ecoregion (13) (U.S. EPA, 2001 (U.S. EPA, 2001).....	2
Figure 2: SFH Reservoir bathymetry and sample locations noted by SFR# (Fritsen, 2011).	9
Figure 3: USGS gauge daily mean flow statistics of 10320000 (Inlet flow: shaded gray area outlines the 10 th and 90 th flow percentile, and black mean historical flows) and 10319900 (Outlet flow: shaded blue area outlines the 10 th and 90 th flow percentile and blue mean historical) flows units are in cubic meters per second (USGS, 2011).....	10
Figure 4: Arithmetic mean Chl-a values of the SFH Reservoir epilimnion and reservoir outflows. Error bars represent Chl-a value mean standard error. (Fritsen, et. al., 2011;USGS, 2011).....	13
Figure 5: South Fork Humboldt River sample locations for 2009 and 2010, and location of 2010 reservoir vertical profile (SFR1).....	19
Figure 6: Observed and modeled South Fork Reservoir epilimnion water temperature, and observed air temperatures.	22
Figure 7: A) USGS gage 10319900 observed inlet flows, in cubic meters per second (cms), to the SFH Reservoir. B) USGS gage 10320000 observed outlet flows (cms) from the SFH Reservoir. (USGS, 2011).....	23
Figure 8: Dissolved oxygen concentrations, calculated as the arithmetic mean of the epilimnion and hypolimnion. Error bars represent minimum and maximum values.	24
Figure 9: SFH Reservoir 2009 phytoplankton biovolume percentages of major taxonomic groups.....	26
Figure 10: Zooplankton estimated biomass of the SFH Reservoir.....	27
Figure 11: Image of SFH Reservoir gravity core sample collected on September 23 rd , 2009 (tape-measure values are in inches).	28
Figure 12: Hourly temperature data of the SFH River 0.75 km and 20 km away from the dam outlet.....	29
Figure 13: Benthic Chl-a concentrations from 2009 and 2010 0.75 km downstream of the SFH Reservoir. Circles are the arithmetic mean of ~24 samples, error bars represent mean standard error.....	30
Figure 14: Periphyton taxonomic biovolumes, 0.75 km downstream of the dam. Values obtained from (Davis, et al., 2011)	31
Figure 15: Conceptual framework of AQUATOX 3. (US EPA, 2010).....	33
Figure 16: Di Toro's (2001) conceptual model of sediment diagenesis model for the SFH Reservoir. (U.S. EPA, 2009a).....	39

Figure 17: Sensitivity analysis results for cyanobacteria of the SFH Reservoir simulation. Black center line indicates nominal or default parameter values. Blue bars extending from the default line represent +10% adjustment of parameters, red bars equal a -10% parameter adjustment. Only the top 10 most sensitive parameter values are displayed..	43
Figure 18: Sensitivity analysis results for PO ₄ sediment diagenesis flux of the SFH Reservoir simulation. Black center line indicates nominal or default parameter values. Blue bars extending from the default line represent +10% adjustment of parameters, red bars equal a -10% parameter adjustment. Only the top 10 most sensitive parameter values are displayed.	44
Figure 19: SFH Reservoir Monte Carlo calibration results for cyanobacteria. Circles indicate cyanobacteria observed biomass, with error bars representing the minimum and maximum observed values. Grey lines represent 100 Monte Carlo iterations, with the black line indicating the parameter set with the lowest RMSE and BIAS values.	53
Figure 20: Volume calibration results for the SFH Reservoir. Black line is the simulated reservoir volume model results, blue line represents observed reservoir volume, and blue circles represent observed hypolimnion volumes.	59
Figure 21: Dissolved Oxygen calibration results for the SFH Reservoir. Black line is the simulated model results, blue circles represent observed layer arithmetic means, and error bars indicate minimum and maximum observed values.	59
Figure 22: Results of reservoir calibration for SD. Black line is the simulated model results, blue circles represent observed arithmetic means, and error bars indicate minimum and maximum observed values.	60
Figure 23: Results of reservoir calibration for PO ₄ . Black line is the simulated model results, blue circles represent arithmetic means, and error bars indicate minimum and maximum observed values.....	60
Figure 24: Results of reservoir calibration for NH ₄ . Black line is the simulated model results, blue circles represent arithmetic means, and error bars indicate minimum and maximum observed values.....	61
Figure 25: Results of reservoir calibration for NO _x . Black line is the simulated model results, blue circles represent arithmetic means, and error bars indicate minimum and maximum observed values.....	61
Figure 26: Results of reservoir calibration for TP. Black line is the simulated model results, blue circles represent arithmetic means, and error bars indicate minimum and maximum observed values.....	62
Figure 27: Results of reservoir calibration simulations for TN. Black line is the simulated model results, blue circles represent arithmetic means, and error bars indicate minimum and maximum observed values.	62

Figure 28: Results of calibration simulations for Chl-a. Black line is the simulated model results, blue circles represent arithmetic means, and error bars indicate minimum and maximum observed values.	63
Figure 29: Results of calibration simulations for cyanobacteria. Black line is the simulated model results, blue circles represent arithmetic means, and error bars indicate minimum and maximum observed values.	63
Figure 30: Results of calibration simulations for diatoms. Black line is the simulated model results, blue circles represent arithmetic means, and error bars indicate minimum and maximum observed values.	64
Figure 31: Results of calibration simulations for chlorophytes. Black line is the simulated model results, blue circles represent arithmetic means, and error bars indicate minimum and maximum observed values.	64
Figure 32: Results of calibration simulations for Cladocerans. Black line is the simulated model results, blue circles represent arithmetic means, and error bars indicate minimum and maximum observed values.	65
Figure 33: Results of calibration simulations for Copepod. Black line is the simulated model results, blue circles represent arithmetic means, and error bars indicate minimum and maximum observed values.	65
Figure 34: DO calibration (2009) and validation (2010) results for the SFH Reservoir. Black line is the simulated reservoir volume model results, red line represents observed reservoir volume, and red error bars represent minimum and maximum observed values.	68
Figure 35: Secchi Depth calibration (2009) and validation (2010) results for the SFH Reservoir. Black line is the simulated SD model results, red line represents observed SD values, and red error bars represent minimum and maximum values.....	68
Figure 36: Chl-a calibration (2009) and validation (2010) results for the SFH Reservoir. Black line is the simulated Chl-a model results, red circle represents observed Chl-a values, and red error bars represent minimum and maximum.....	69
Figure 37: PO ₄ calibration (2009) and validation (2010) results for the SFH Reservoir. Black line is the simulated PO ₄ model results, red circle represents observed Chl-a, and red error bars represent minimum and maximum.....	69
Figure 38: NH ₄ calibration (2009) and validation (2010) results for the SFH Reservoir. Black line is the simulated NH ₄ model results, red circle represents observed NH ₄ , and red error bars represent minimum and maximum.....	70
Figure 39: NO _x calibration (2009) and validation (2010) results for the SFH Reservoir. Black line is the simulated NO _x model results, red circle represents observed NO _x , and red error bars represent minimum and maximum.....	70

Figure 40: TP calibration (2009) and validation (2010) results for the SFH Reservoir. Black line is the simulated TP model results, red circle represents observed TP, and red error bars represent minimum and maximum.	71
Figure 41: TN calibration (2009) and validation (2010) results for the SFH Reservoir. Black line is the simulated TN model results, red circle represents observed TN, and red error bars represent minimum and maximum.	71
Figure 42: Results of river calibration simulations for run velocity. Blue circles represent the observed arithmetic mean, and error bars represent the observed mean standard error.	76
Figure 43: Results of river calibration simulations for DO. Blue circles represent the discrete DO observations from a Hydrolab Sonde.	76
Figure 44: Results of river calibration simulations for diel DO. Blue line represents continuously observed DO values from YSI sonde deployment.	77
Figure 45: Results of river calibration simulations for PO ₄ . Blue circles represent the observed arithmetic mean, and error bars represent the observed mean standard error. ..	77
Figure 46: Results of river calibration simulations for NH ₄ . Blue circles represent the observed arithmetic mean, and error bars represent the observed mean standard error. ..	78
Figure 47: NO _x calibration results for the SFH River simulation. Blue circles represent the observed arithmetic mean, and error bars represent the observed mean standard error.	78
Figure 48: Chl-a calibration results for the SFH River simulation. Blue circles represent the observed arithmetic mean, and error bars represent the observed mean standard error.	79
Figure 49: Periphyton diatoms calibration results for the SFH River simulation. Blue circles represent the observed arithmetic mean, and error bars represent the observed mean standard error.	79
Figure 50: <i>Cladophora</i> calibration results for the SFH River simulation. Blue circles represent the observed arithmetic mean, and error bars represent the observed mean standard error.	80
Figure 51: Flow velocity Validation results for the SFH River. Black line is the simulated flow model results, , and red error bars represent the mean standard error of observed values.	81
Figure 52: DO calibration (2009) and validation (2010) results for the SFH River. Grey line is the simulated river DO, red circles represent observed river DO values.	82
Figure 53: PO ₄ calibration (2009) and validation (2010) results for the SFH River. Grey line is the simulated river model results, red circle represents observed PO ₄ values, and red error bars represent the mean standard error of observed samples.	82

Figure 54: NH ₄ calibration (2009) and validation (2010) results for the SFH River. Grey line is the simulated river model results, red circle represents observed NH ₄ values, and red error bars represent the mean standard error of observed samples.	83
Figure 55: NO _x calibration (2009) and validation (2010) results for the SFH River. Grey line is the simulated river model results, red circle represents observed NH ₄ values, and red error bars represent the mean standard error of observed samples.	83
Figure 56: Benthic Chl-a calibration (2009) and validation (2010) results for the SFH River. Grey line is the simulated river model results, red circle represents observed Chl-a values, and red error bars represent the mean standard error of observed samples.	84
Figure 57: TP vs. TN regression analysis for nutrient multiplier covariance. Black circles represent NDEP observed nutrient samples, and red line is the linear regression of the dataset.	86
Figure 58: TP vs. TSS regression analysis for nutrient multiplier covariance. Black circles represent NDEP observed nutrient samples, and red line is the linear regression of the dataset.	86
Figure 59: TP scenario loading results for April 7 th to Oct. 1 st 2009. Boxplots center line is median, outer box represents the 25 th and 75 th percentiles, and whiskers are 1.5 times the Inter Quartile Range (IQR). Lake TP trophic level boundaries based on (Carlson and Simpson, 1996). Red dashed line indicates EPA reference condition of 0.030 mgP/L for the Great Basin and Range Ecoregion (U.S. EPA, 2001).	88
Figure 60: SD scenario loading results for April 7 th to Oct. 1 st 2009. Boxplots center line is median, outer box represents the 25 th and 75 th percentiles, and whiskers are highest data points within 1.5 times the Inter Quartile Range (IQR). Trophic level boundaries are based on (Carlson and Simpson, 1996). Red dashed line indicates EPA reference condition of 2.3 meters for the Great Basin and Range Ecoregion (U.S. EPA, 2001).	89
Figure 61: Chl-a scenario loading results for April 7 th to Oct. 1 st 2009. Boxplots center line is median, outer box represents the 25 th and 75 th percentiles, whiskers are highest data points within 1.5 times the IQR, and red plus signs indicate statistical outliers. Lake TP trophic level boundaries based on (Carlson and Simpson, 1996). Red dashed line indicates EPA reference condition of 3.5 µg/L for the Great Basin and Range Ecoregion (U.S. EPA, 2001).	90
Figure 62: 3-dimensional view of the SFH load scenarios for the 2009 phytoplankton growing season. Black line indicates the calibrated model results.	90
Figure 63: 3-dimensional view of the SFH river loading scenarios for the 2009 season. Black line indicates the calibrated model results.	92
Figure 64: Average daily wind speed obtained from the Elko Regional Airport NWS Weather Station (http://mesowest.utah.edu/index.html).	103
Figure 65: Average daily radiation from the Crain Springs BLM Weather Station (http://mesowest.utah.edu/index.html).	103

Figure 66: Scenario results for PO ₄ loading to the SFH Reservoir. 2009 simulation is represented by the OBS values.	114
Figure 67: Scenario results for NH ₄ loading to the SFH Reservoir. 2009 simulation is represented by the OBS values.	114
Figure 68: Scenario results for NO _x loading to the SFH Reservoir. 2009 simulation is represented by the OBS values.	115

LIST OF TABLES

Table 1: Reference conditions for lakes and reservoirs in the Central Basin and Range reproduced from (U.S. EPA, 2001). Parameters represent Total Kjeldhal Nitrogen (TKN), nitrate-nitrite (NO _x), total nitrogen (TN), total phosphorous (TP), secchi disk depth (SD) and chlorophyll-a (Chl-a).	3
Table 2: Comparison of Carlson’s Trophic State Index from Sater et. al (1994) and Fritsen et. al., (2011) of Chl-a and SD. Values represent composite samples to a depth of 4 meters. TSI values represent reproduced from Fritsen et. al., (2011). Values in 2009 are repeated June and August for comparison with values from 1993.	14
Table 3: Comparison of laboratory methods of chemical analysis of South Fork Reservoir and River Samples for samples collected in 2009 and 2010.	17
Table 4: SFH Reservoir Chl-a, SD and nutrient data reported as the arithmetic mean of epilimnion samples. POC samples are from site location SFR5 and used as a surrogate for POC loadings to the reservoir. Values represented by a hyphen indicate samples were not completed.	25
Table 5: Dissolved nutrients of the SFH River near the reservoir inlet and 0.75 km downstream of the outlet. TP and TN data were not collected for river samples in 2009 and 2010.	30
Table 6: AQUATOX 3.1 factors relating velocities to those of the average reach. (U.S. EPA, 2009a)	41
Table 7: SFH Reservoir parameter estimation results for phytoplankton. Maximum and minimum values indicate initial literature ranges in uniform distribution for Monte Carlo random sampling. Additional parameters included for the phytoplankton state variables are left as default values.	56
Table 8: Reservoir calibration goodness-of-fit for the epilimnion (Epil) and hypolimnion (Hypo).	57
Table 9: Reservoir model validation goodness-of-fit for the epilimnion (Epil) and hypolimnion (Hypo).	67
Table 10: SFH River parameter estimation results for periphyton. Maximum and minimum values indicate initial literature ranges in uniform distribution for Monte Carlo random sampling. Additional parameters included for the periphyton state variables are left as default values.	74
Table 11: River model calibration goodness-of-fit results.	75
Table 12: SFH River model validation goodness-of-fit results.	81
Table 13: Scenario loading multipliers for dissolved nutrients, TSS, and OM loadings. “Observed” represents the calibrated SFH Reservoir model observed nutrient loadings. 87	
Table 14: Average growing season values of water quality derived from loading scenarios.	91

Table 15: South Fork Reservoir average pH, calculated thermocline depth and average hypolimnion temperature from 2009-2010.....	104
Table 16: SFH reservoir and river model initial conditions (Fritsen, et. al., 2011).	105
Table 17: SFH reservoir and river initial conditions (continued).	106
Table 18: Default phytoplankton parameters values used in SFH Reservoir modeling study (USEPA, 2009).....	107
Table 19: Zooplankton parameter values for the SFH Reservoir model.	108
Table 20: Remineralization parameters used within the SFH Reservoir model.....	109
Table 21: Sediment diagenesis parameters for the reservoir model.	110
Table 22: Sediment diagenesis parameters for the reservoir model (continued).....	111
Table 23: Default periphyton parameters for the SFH river model (USEPA, 2009).....	112
Table 24: Remineralization parameters used within the SFH River model.....	113

1. INTRODUCTION

1.1 NUTRIENT CRITERIA DEVELOPMENT STATUS NEVADA

The eutrophication of inland waters is a primary concern of municipal, state and tribal agencies that ensure the health and socioeconomic benefits of surface water. Waterways in desert environments, such as Nevada, are especially vulnerable to excessive algal growth due to increased productivity, temperatures, light and nutrient availability (Bunn et al., 2006). The U.S. Environmental Protection Agency (EPA) oversees water resources the compliance of states to identify and develop criteria for addressing water quality issues set forth by the Clean Water Act (U.S. EPA, 1972). Subsequently, national water quality assessments have revealed the role of nutrient enrichment, specifically nitrogen and phosphorous, as integral contributors to algal eutrophication of both Nevada (NDEP, 2009) and the Nation's surface waters (Dubrovsky et al., 2010; Smith et al., 1999; U.S. EPA, 1998).

The Nevada Department of Environmental Protection (NDEP) is the representing state agency accountable to assess and identify surface water impairment for numerical water quality standard development. State numerical standards are approved by the EPA and based on nutrients, total phosphorous (TP) and total nitrogen (TN), and their relationship to algal degradation of surface water. Classical TP and TN nutrient criteria represent a scientifically defensible threshold, with exceedance values resulting in chemical and/or biological harm to the aquatic environment (U.S. EPA, 2010). Exceedance of state standards also indicates the designated use of a waterway can no

longer be achieved, and in extreme cases may threaten human health with contact or ingestion (Whitton and Potts, 2000).

NDEP has set nutrient standards for rivers and streams throughout Nevada, including anti-degradation standards based on algal biomass in lake value for algal eutrophication (NDEP, 2008). Encouragement by the EPA for states to “accelerate” the setting of nutrient criteria formation (Grumbles, 2007), and litigation against the EPA in Florida (Obreza et al., 2010), have motivated state agencies to accelerate the creation of standards for lakes and reservoirs in addition to rivers and streams. NDEP has responded by developing site-specific criteria for the South Fork Humboldt (SFH) Reservoir, located outside of Elko, NV to meet these recent EPA directives (Pahl, 2011). The EPA recommends three strategies in nutrient criteria development: (1) stressor-response relationships, (2) ecoregion reference-based conditional approaches (Figure 1), and (3) mechanistic modeling of ecological systems (U.S. EPA, 2010).



Figure 1. EPA Aggregated Ecoregion III geographical area, with Nevada being encompassed in the Central Basin and Range Ecoregion (13) (U.S. EPA, 2001 (U.S. EPA, 2001).

EPA stressor-response criteria focus on regression and statistical analysis of historical data to interpret relationships of nutrients and algal biomass with the understood limitations that log-regressions of nutrients and algal interactions have considerable uncertainty and are costly to collect for site specific applications (Welch and Jacoby, 2004). Additionally, observation data collected from the SFH Reservoir only exists for the time periods of 1992-1993 and 2009-2010, lacking the wide ranges of eutrophic conditions required for regression analysis (Sater et. al, 1994; Fritsen et. al, 2011).

Preliminary recommendations of lake and reservoir nutrient criteria were released by the EPA in 2001, specifying ecoregions within the U.S. for reference-based approach to nutrient criteria development. The 1990 to 2000 study examines reference based conditions for aggregated ecoregions throughout the U.S. and highlights empirically derived nutrient criteria as a starting point for stressor and response criteria throughout Nevada (Table 1).

Table 1. Reference conditions for lakes and reservoirs in the Central Basin and Range reproduced from (U.S. EPA, 2001). Parameters represent Total Kjeldhal Nitrogen (TKN), nitrate-nitrite (NO_x), total nitrogen (TN), total phosphorous (TP), secchi disk depth (SD) and chlorophyll-a (Chl-a).

Parameter	No. of lakes N*	Reported Values		25th Percentiles based on all seasons data for the decade
		Min	Max	
TP mgP/L	49	0.011	0.742	0.03
TN mgP/L	7	0.5	2.37	0.51
SD meters	36	0.1	4.9	2.3
Chl-a ug/L	4	1.7	5.5	1.9
TKN mgN/L	42	0.07	2.69	0.34
NO _x mgN/L	10	0.01	0.68	0.01

The 2001 EPA report did not make the distinction between lakes and artificial impoundments, such as reservoirs. Unique characteristics and manual operation of reservoirs for flow augmentation, flood mitigation, power generation and water withdrawal locations have significant impacts on reservoir and downstream nutrient and algal dynamics (Cooke, 2005). The EPA emphasizes the need to define and quantify the relationships between reservoir nutrients and downstream water quality conditions (U.S. EPA, 1998). The application of EPA reference conditions and observational data alone may not capture the true nutrient/algal dynamics of the SFH Reservoir or quantify possible effects on downstream water quality. Therefore, using the third EPA approach (mechanistic modeling of nutrient criteria) represents possible advantages in criteria development for the SFH Reservoir.

The mechanistic modeling approach to developing nutrient criteria relies on numerical simulations to represent simplified processes of algal and nutrient interactions and simulate ecological process and dynamics (U.S. EPA, 2010). Mechanistic models have the advantage of supplementing observational data of stressor-response variables and simulating ecosystem responses to changes in nitrogen and phosphorus loadings (U.S. EPA, 1998). Lastly, the EPA requires the consideration of downstream impacts of meeting nutrient criteria in reservoirs; making the application of linked mechanistic models of both riverine and reservoir systems advantageous for nutrient criteria selection.

1.2 LINKING RESERVOIR AND RIVER SIMULATIONS

Reservoir management and impoundment structural design can have significant effects on downstream river systems (Blinn et al., 1998; Cooke, 2005; Ward and Stanford, 1983). Effects have been documented to include increased nutrient loadings, oxygen depletion, temperature alterations, flow regime changes and aquatic life disturbances (Cooke, et al., 2005). Reservoir management reviews indicate reservoir operations and downstream water quality concerns were found to be unmistakably linked (Kennedy, 2005), though the use of integrated, holistic management seldom occurs. Reservoir operation often requires hydrologic models for release optimization for hydropower or remediation from eutrophication. Models typically fail to examine the system of linked reservoir and tailwater segments, adding to the degradation of downstream water quality (Chaves et al., 2003; Jager and Smith, 2008).

Applications of linked reservoir and tailwater models to simulate threatened aquatic life along with dissolved oxygen (DO) and thermal requirements have been published (Bartholow et al., 2001; Ernst and Owens, 2009; Jager and Smith, 2008; Nurnberg, 2007). Unfortunately, such modeling occurs only when regulated impacts are conspicuously linked (Dhar and Datta, 2008; Saito and Koski, 2006), while more indirect releases of nutrients that impact algal communities have been largely uninvestigated.

Studies of downstream eutrophication demonstrate cause-effect relationships with reservoir release structures and operation (Camargo et al., 2005; Marshall et al., 2006; Munn and Brusven, 2004). No mechanistic modeling investigations, within the knowledge of the author, have been published that include a simultaneous link for

investigating eutrophic effects of reservoir release and cause-effect impacts on river tailwaters. Clearly, the sampling costs of acquiring both river and reservoir datasets for an integrated modeling approach and the lack of extreme tailwater productivity may have to date precluded simulating such associations.

The Desert Research Institute (DRI) conducted an investigation of the SFH Reservoir and a downstream river algal assessment in 2009. Subsequently in 2010, a limited dataset for model validation purposes was collected capturing annual dynamics of the reservoir-river system. The linked nature of the two datasets and problematic reservoir internal loadings may indicate early stages of nutrient recycling and enhanced eutrophication through time and clearly a unique system for model investigations (Davis et al., 2011; Fritsen et al., 2011).

The formation of a mechanistic model to examine reservoir nutrient criteria paired with river response to reservoir changes is the logical next step in the investigation. The EPA recommends the use of many receiving water models for nutrient criteria investigations, including EUTROMOD, PHOSMOD, BATHTUB and AQUATOX 3.1 (U.S. EPA, 1998). AQUATOX 3.1 was selected for the SFH Reservoir modeling purposes to mechanistically simulate algal dynamics and related nutrient cycling. In addition, AQUATOX 3.1 has the added ability to simulate riverine processes. The purpose of the linked system modeling approach is to simulate how varied nutrient loadings to the reservoir will impact internal reservoir loadings and the eutrophication status for the reservoir and downstream river reaches. Using data collected from the 2009-2010 DRI investigations, four objectives were undertaken:

1. Calibrate the EPA model AQUATOX 3.1 using the 2009 dataset for the reservoir and linked river segments, with river boundary-conditions being specified from reservoir model outputs.
2. Validate the model with additional sample collection data from 2010.
3. Evaluate scenarios of varied nutrient loadings, modeling of management optimization for simulating reservoir response.
4. Examine the influences of reservoir nutrient loadings on both reservoir conditions and the downstream riverine periphyton community.

Results will also provide a mechanism to quantify the impacts of selecting nutrient criteria for the aquatic health of both reservoir and river systems.

2. BACKGROUND

2.1 STUDY SITE: SOUTH FORK HUMBOLDT RESERVOIR

The SFH watershed is located in the central Northeastern region of Nevada, covering approximately 2,325 km². The watershed land cover is dominated by desert scrub, with the SFH River corridor is being managed as agriculture pasture and grazing land. Flow of the SFH River is dictated by spring snow-melt from the Ruby Mountains and flows northeast to the South Fork Reservoir impoundment located 16 km south of Elko, Nevada.

The reservoir is located within the South Fork Nevada State Park and is operated year-round for recreation purposes including: fishing, swimming and watercraft activities. The reservoir is formed by a 550 meter earthen dam located on the north end of the reservoir (Figure 2), and stores a maximum water volume of 50×10^6 m³ covering 6.7 km² of grazing pastures prior to structural completion in 1988. Filling of the reservoir was completed in 1995 and under normal operating conditions, the reservoir is approximately 5 km long and 1.5 km wide with an average depth of 7.5 meters (NDSP, 2008).

The SFH reservoir is operated as a bottom release reservoir by the Nevada Division of Water Resources, with the release elevation located 14.7 meters below normal reservoir stage of 1,595 meters elevation. Flow is controlled via two Howell-Bunger® cone valves, 1.22 meters in diameter, and regulated by downstream water rights to match reservoir inlet flows (Perry, 2007).

The river substrate is a sand-gravel-cobble bed, with a well-defined average channel width of 15 meters. The SFH River also has a lack of vegetation near the banks and experiences minimal shading from solar radiation throughout the tail-water reach.

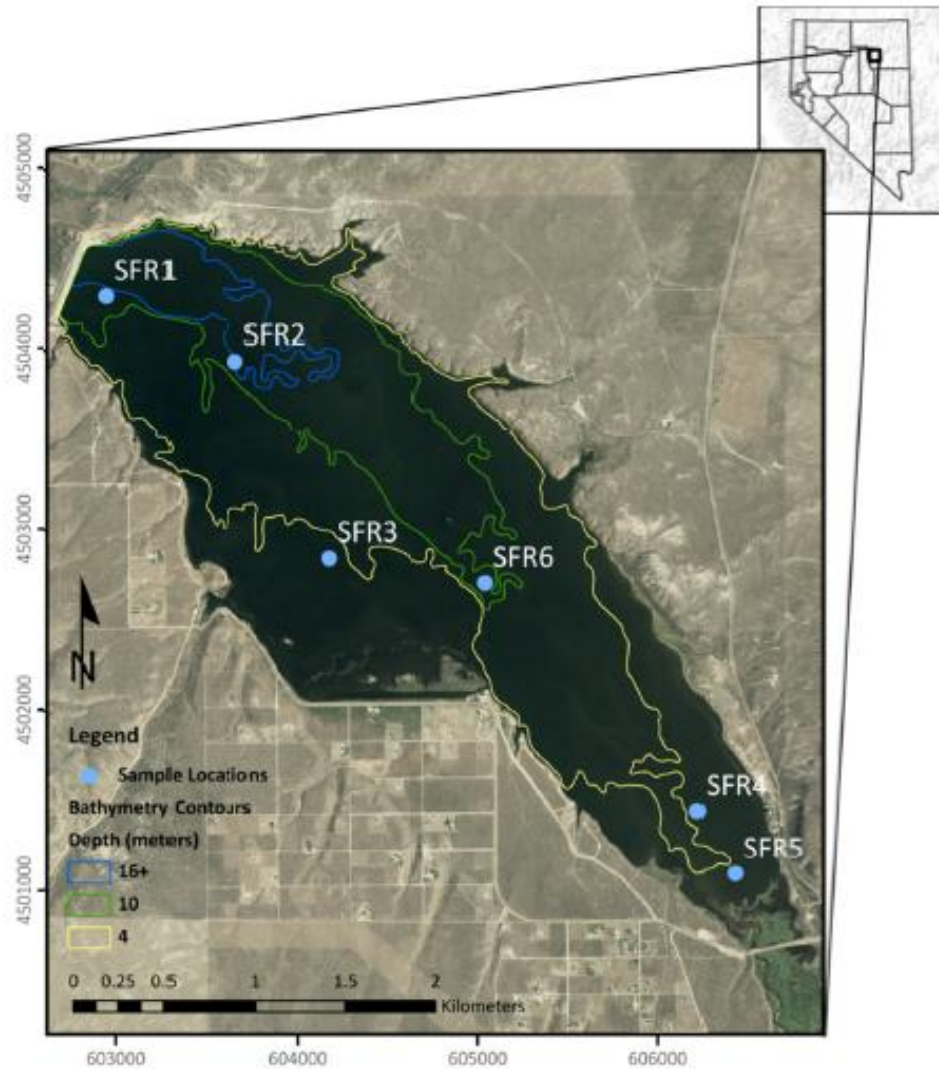


Figure 2. SFH Reservoir bathymetry and sample locations noted by SFR# (Fritsen, 2011).

Two United States Geological Survey (USGS) stream gauges above (10319900 SFH River above Ten-mile Creek) and below the reservoir (10320000 SFH River above Dixie Creek) are used by the Nevada Division of Water Resources to match flows of the

reservoir inlet and outlet (USGS, 2011). The reservoir has yearly deeded water storage right of $6.4 \times 10^6 \text{ m}^3$ to account for reservoir stage losses due to evaporation (NDSP, 2008).

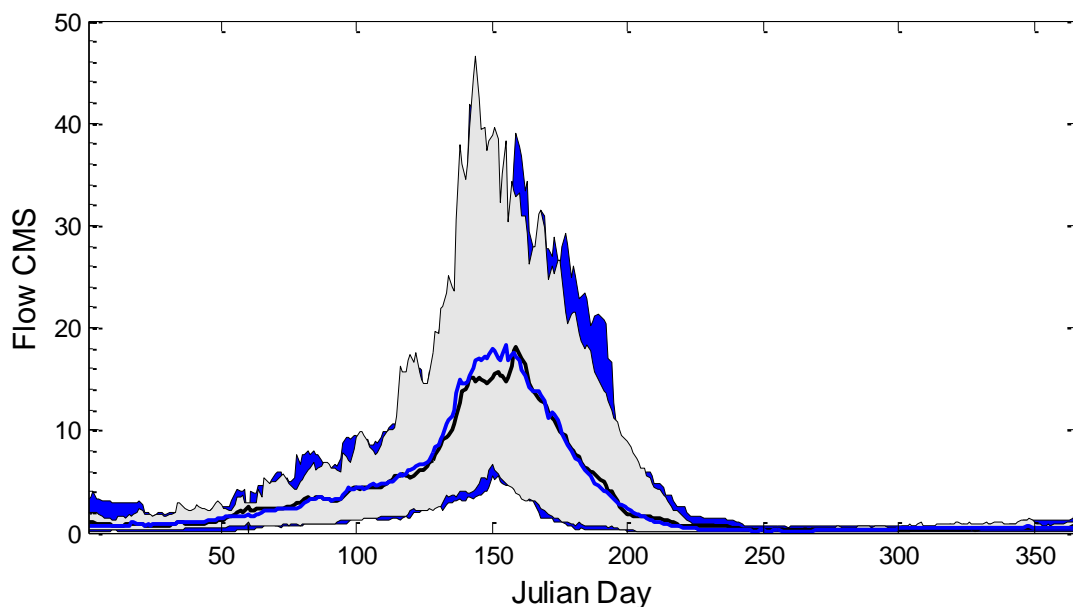


Figure 3. USGS gauge daily mean flow statistics of 10320000 (Inlet flow: shaded gray area outlines the 10th and 90th flow percentile, and black mean historical flows) and 10319900 (Outlet flow: shaded blue area outlines the 10th and 90th flow percentile and blue mean historical) flows units are in cubic meters per second (USGS, 2011).

Outflow of the reservoir continues as the SFH River to the confluence with the Humboldt River approximately 30 km downstream. The SFH River below the dam has two additional tributaries of Ten-mile Creek and Dixie Creek, 0.90 km and 5.75 km respectively downstream. Both streams contribute flow to the SFH River, the streams may be considered ephemeral and contribute little flow after peak snow-melt conditions.

Two reports, commissioned by NDEP, have been completed to understand and quantify the nutrient/algal relationships from the reservoir completion in 1988. The first study by (Sater et al., 1994) focused on characterizing basic limnological features with

periodic reservoir sampling from 1991 to 1993. However, during sampling the reservoir was in the late stages of filling and experienced shallower depths and potentially different ecosystem characteristics. The second study (Fritsen, et al., 2011) emphasizes nutrient algal relationships and the downstream effects with concentrated reservoir sampling for the 2009 algal growing season (April to August). The combined research of the SFH Reservoir highlights the characteristic of thermal stratification, with the maximum reservoir depth 18.5 meters in close proximity to the submerged outlet.

Thermal stratification of the SFH Reservoir is typically observed in late spring, with increased development of stratification with higher temperatures followed by turnover in the fall (Fritsen, et al., 2011). In addition, inverse-stratification has been observed with complete ice cover of the reservoir in winter (Sater, et al., 1994). Summer stratification results in the resistance of the reservoir to mixing of warm surface waters of the epilimnion and the cold bottom layer known as the hypolimnion. The epilimnion layer experiences warmer temperatures and atmospheric exchange, while the lower hypolimnion is isolated with cold and anoxic conditions in later summer months due to oxygen demand from the breakdown of settled organic matter (OM) (Wetzel, 2001).

The effect of stratification, oxygen depletion, and OM deposition is the enhanced ability of sediments to be a source of dissolved nutrients for eutrophication of the SFH Reservoir (Fritsen, et al., 2011). Observed reservoir dissolved oxygen (DO) concentrations below 1 mg/L result in the flux of soluble nutrients of orthophosphorous (PO_4), ammonium (NH_4), and nitrification to nitrite-nitrate (NO_x) to the overlying water column (Fritsen, et al., 2011). Numerous case studies have shown the potential

degradation of anoxic hypolimnion water (Hupfer and Lewandowski, 2008; Koiv et al., 2011) and the potential for self-enhancing eutrophication (Larsen et al., 1981; Ozkundakci et al., 2011).

2.2 SOUTH FORK RESERVOIR EUTROPHICATION STATUS

The duration of time river water spends within impounds can have profound effects on the biological and chemical process of eutrophication within impoundments, considered one of the most important factors in reservoir water quality, leading to nutrient retention in river-reservoir systems (Jorgensen, 2003).

The hydrologic residence time (HRT) is equal to the average amount of time an incoming water particle spends in the reservoir prior to being discharged, is critical to the eutrophic status of lakes and reservoirs. While many methods exist to calculate the HRT of lentic water bodies (Rueda et al., 2006), a commonly used and simplistic equation of V , volume of a water body (m^3), divided by the Q , flow rate (m^3/day) out of the reservoir is equal to HRT , the hydrologic residence time (days):

$$HRT = V/Q \tag{1}$$

The HRT of the South Fork Reservoir was calculated as 181 days for the 2009 calendar year and a historic average residence time of 223 days from 1989 to 2009 (Fritsen, et al., 2011). Influences of spring snow melt tend to flush the reservoir from May through July. River flow outside the snow melt seasons results in higher instantaneous HRTs in April and August to September of 2009 (Figure 4). Algal biomass was observed to be the highest during these months (Fritsen, et al., 2011).

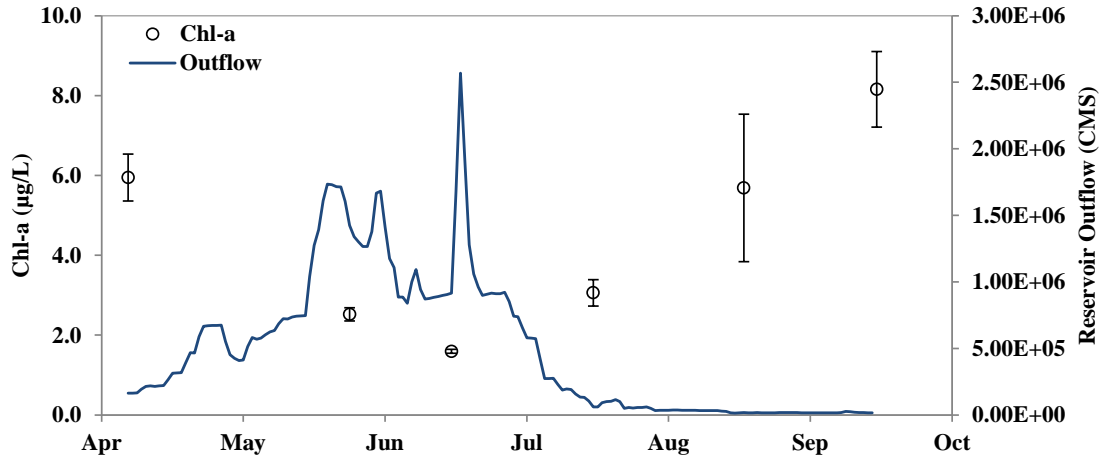


Figure 4. Arithmetic mean Chl-a values of the SFH Reservoir epilimnion and reservoir outflows. Error bars represent Chl-a value mean standard error. (Fritsen, et. al., 2011; USGS, 2011)

Reservoir composite samples have been used to investigate the eutrophic status of the SFH Reservoir, totaling 15 mean samples from 1991 to 2009. Composites represent simple arithmetic means of vertical sample locations typically within the first four meters of depth (Fritsen, et al., 2011). The mean reservoir Chl-a value is 4.90 µg/L, with a minimum value of 1.15 µg/L in October of 1992, and a maximum concentration of 11.79 µg/L in March of 1993. Secchi Depth (SD) values range over this period from a minimum of 1.0 meter in 1993, to a maximum of 6.9 meters in June of 2009 and are highly influenced by suspended sediment during the 1994 study (Sater, et al., 1994).

Table 2. Comparison of Carlson's Trophic State Index from Sater et. al (1994) and Fritsen et. al., (2011) of Chl-a and SD. Values represent composite samples to a depth of 4 meters. TSI values represent reproduced from Fritsen et. al., (2011). Values in 2009 are repeated for June and August for comparison with 1993.

Month and Year Compared	Sater et. al. (1994)					Month in 2009	Fritsen et. al. (2011)				
	TSI	Chl-a $\mu\text{g/L}$	SD m	TP mgP/L	TN mgN/L		TSI	Chl-a $\mu\text{g/L}$	SD m	TP mgP/L	TN mgN/L
Jun 1992	43	3.6	1.3	0.061	1.613	Jun	37	2.02	6.9	0.022	0.277
Aug 1992	36	1.8	1.5	0.074	1.688	Aug	51	8.06	5.2	0.078	0.707
Jun 1993	49	6.9	1.0	0.038	1.089	Jun	37	2.02	6.9	0.022	0.277
Jul 1993	50	7.5	1.3	0.037	1.478	Jul	40	2.6	5.9	0.016	0.344
Aug 1993	52	9.3	1.3	0.042	1.487	Aug	51	8.06	5.2	0.078	0.707

A comparison of active water quality information in Sater, et. al. (1994) and Fritsen et. al. (2011) indicates there has been improvement in the Carlson's Trophic State Index (TSI) (an index indication of eutrophic status).

$$TSI = 9.81 * \ln(Chla) + 30.6 \quad (2)$$

Where Chl-a is equal to the mean summer reservoir concentration ($\mu\text{g/L}$):

TN decreased between 1992 and 2009, while TP values in August increased from 1992 also appear to have decreased, with the exception of values being similar in August of 1992 and 2009 (Table 2). SD measurements increased by an average depth of 5.12 meters from 1992 to 2009. The TSI index suggests the reservoir had slightly poorer water quality in 1992-1993, yet water quality improved to a meso-oligotrophic status in 2009. Filling of the reservoir from 1991 to 1993 must be considered as influencing the water quality improvement, due to substantial differences in volume, depth, and HRT of the reservoir.

2.3 SOUTH FORK RIVER EUTROPHICATION STATUS

Lakes and reservoirs with outlet flow and sediment nutrient fluxes commonly use a remediation technique known as hypolimnetic release to ameliorate possible reservoir eutrophication effects. The technique is successfully applied when the withdrawal location is within the hypolimnion and 1-2 meters above the sediment surface (Cooke, 2005). This technique acts to flush out concentrated waters of the hypolimnion, removing nutrients available for phytoplankton uptake and within reservoir eutrophication. The SFH Dam design is conventional to numerous reservoir case studies demonstrating the successful mitigation of eutrophication by hypolimnetic withdrawal (Nurnberg, 2007); common negative effects of hypolimnetic withdrawal is the degradation of downstream water quality including tailwater eutrophication (Cooke, 2005). Negative release effects include circumstances of concentrated nutrient withdrawals, however timely release from different depths in the water column can be used to alleviate the impacts of excessive nutrient transfer to downstream rivers (Nurnberg, 2007). The South Fork design does not allow for selective withdrawal from other stratified zones within the water column, resulting in potential impacts downstream.

The tail-water of the SFH Reservoir experiences extreme periphyton eutrophication, likely a result of concentrated dissolved nutrients and low turbidity reservoir outflows (Bunn, et al., 2006; Fritsen, et al., 2011). Davis et al., (2011) document the excessive periphyton growth with a maximum benthic Chl-a concentration exceeding 500 mg/m^2 , diel DO swings from $4 \text{ mgO}_2/\text{L}$ to $20 \text{ mgO}_2/\text{L}$, and describes SFH River tail-water as being one of the most productive streams documented. The linking of

reservoir and river tail-water within a mechanistic model will help to quantify possible further degradation or improvement of the downstream river based on nutrient criteria selection.

3. FIELD DATA METHODS

3.1 FIELD DATA COLLECTION: 2009-2010 SOUTH FORK RESERVOIR

Field data from the SFH Reservoir and River was collected during two separate field campaigns. The first, from April to September of 2009, was associated with the SFH Reservoir report and resulting information was used as calibration data for the nutrient criteria water quality model investigation (Fritsen, et al., 2011). The second campaign, from June to August of 2010, resulted in data used for validation of the calibrated water quality model. The focus of this section is to emphasize data collection methods used for the water quality model and differences of collection and analysis of the 2009 and 2010 datasets.

Reservoir sampling in 2009 focused on documenting algal and nutrient dynamics (Fritsen et. al., 2011). Samples of the reservoir were completed at six locations (Figure 2) on the dates of: April 7th, May 27th, June 19th, July 21st, August 24th, and September 23rd of 2009. At sample locations, vertical profiles of DO, pH, and temperature were determined using a YSI 6600V2 water quality sonde. Secchi disk depth was determined at these locations by lowering the disk and recording the maximum observable distance. Discrete samples were collected for algal taxa identification, TP, TN, dissolved nutrients, Chl-a, Ash Free Dry Mass (AFDM) and particulate organic carbon (POC). Vertical

samples were collected with a 5 liter Niskin sampler and transferred to amber HDPE Nalgene bottles and immediately iced at 4°C for analysis.

Reservoir validation data consisted of four sample collections on June 17th, July 14th, August 4th, and September 21st of 2010. Reservoir sample locations (Figure 2) were kept identical to previous study locations, with collection of only one vertical reservoir profile at SFR1. Additional samples of TN, TP, and Chl-a were collected from epilimnion and hypolimnion at locations SFR3 and SFR4. Water quality parameters of DO, pH and temperature, were collected with a calibrated Hydrolab5® sonde, collecting vertical profiles of sites SFR1, SFR3 and SFR4. Discrete vertical samples were collected via a Non-Metallic Kemmerer Sampler and placed in opaque 250ml bottles and stored at 4°C until analysis.

Table 3. Comparison of laboratory methods of chemical analysis of South Fork Reservoir and River Samples for samples collected in 2009 and 2010.

Analysis	2009	2010
	Fritsen, et. al (2011)	Validation data, 2010
TP	Lachat QuickChem Method 10-115-01-4-B (Tucker and Jones, 2007a)	Standard Methods 18th Ed. 4500P-B,5 4500P-E
PO ₄	Lachat QuickChem Method 10-115-01-1-M (Liao, 2002)	Automated Colorimetric US EPA Method 365.1
TN	Lachat QuickChem Method 10-107-04-4-B (Tucker and Jones, 2007b)	Standards Methods 18th Ed. 4500-N _{org} D
NH ₄	Lachat QuikChem Method 10-107-06-2-C (Prokopy, 2003)	Automated Colorimetric Cadmium US EPA Method 350.1
NO _x	QuikChem Method 10-107-04-1-C (Pritzlaff, 2000)	Automated Phenate US EPA Method 353.2
Chl-a	Turner Designs 10AU Fluorometer (Welschmeyer, 1994)	Spectrophotometer Standard Methods 18th Ed. 10200
POC	Perkin-Elmer 24000 Series II CHN/O Analyzer (Karl et al., 1991)	Not Analyzed

Analyses of samples collected in 2009 were completed at the Desert Research Institute (DRI) Systems Microbial Ecology Laboratory (SMEL). Samples collected in 2010 were analyzed at the DRI Water Quality Laboratory (PO_4 , NH_4 , and NO_x), the DRI SMEL lab (Chl-a) and the Nevada State Public Health Lab (TN, TP and Chl-a). Laboratory methods used for 2009 and 2010 chemical analysis are included in Table 3.

Reservoir samples were additionally analyzed for phytoplankton and zooplankton taxonomic identification. Phytoplankton discrete samples and vertical zooplankton tows were preserved in 0.5% gluteraldehyde solution and analyzed with an Olympus BX-60 epifluorescence microscope. Enumeration of individuals or natural units (NU) occurred after settling for 24 hours in an Utermohl Chamber with over 400 individual targets of phytoplankton identification. Samples were counted with a minimum of 15 microscopic field views, and biovolume was calculated as outlined in (Hillebrand et al., 1999).

SFH reservoir sediments were collected on September 23rd 2009 with a 25 kg gravity corer (3.2 cm diameter) at reservoir location SFR2. The sediment core was immediately sectioned in 2.54 cm increments and stored at 4°C until analysis. Samples were homogenized, dried at 100°C for 24 hours to obtain the average sediment density, (kg/m^3).

3.2 FIELD DATA COLLECTION: 2009-2010 SOUTH FORK HUMBOLDT RIVER

The SFH River was sampled the reservoir inlet, and at 0.75 km, 10 km and 19.5 km downstream of the dam outlet (Figure 5). Water quality samples collected on April 14th, May 26th, June 11th, July 15th, and August 18th of 2009. Study site locations were identical for 2009 to 2010, with 2010 samples collected on June 17th, July 14th, August 4th

and September 21st. Procedures for the analysis of water quality samples are further discussed in (Davis, et al., 2011), with laboratory methods represented in Table 3. In addition to water quality grab samples, a YSI 6600 sonde was deployed at the three tailwater locations for observations of DO, pH and temperature dynamics for 27 hour deployment durations.

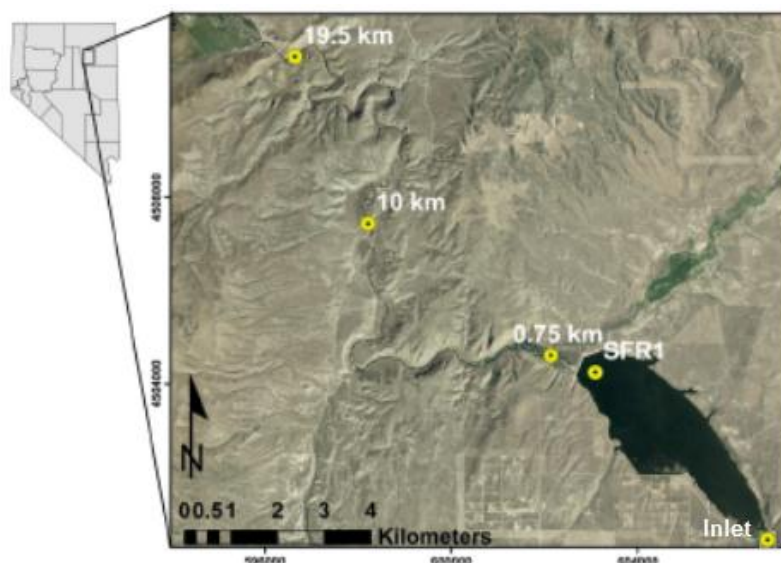


Figure 5. South Fork Humboldt River sample locations for 2009 and 2010, and location of 2010 reservoir vertical profile (SFR1).

Benthic Chl-a concentrations, Ash Free Dry Mass (AFDM), and periphyton taxa were documented on June 11th, July, 16th, and August 18th of 2009 and August 11th in 2010. Sampling used randomized selection of three points within 10 meter reaches, for a total of 24 samples in 80 meters. The size was taken into account by sampling one to two cobbles and three to five gravel sized rocks. Substrates were sampled and rocks were scrubbed by wire brushes into plastic containing units, and dislodged material was transferred to opaque Nalgene bottles and placed on ice. Episammic samples were collected if the substrate was sand or mud, with 47 mm petri dishes and a spatula for

sample collection. River water was vacuum filtered with 0.45 μm GF/F filters and used to rinse rock samples and equipment during sample collection. Rock dimensions along three axes were measured for cobble surface area, using the methods of (Dall, 1979).

Periphyton taxonomic identification followed methods of (Acker, 2002; Clason et al., 2002) after preservation with 0.5% gluteraldehyde solution. Identification and biovolume calculations were performed by using an Olympus BX-60 epifluorescence microscope. Soft-algae samples were counted and enumerated with the use of a Palmer-Maloney microscope, and biovolumes were calculated as outlined in (Hillebrand, et al., 1999). Further details of these methods included in (Davis, et al., 2011).

Laboratory processing of river samples occurred within 24 hours of collection. Filamentous particles were homogenized within a blender, inverted for thorough mixing, and delivered by pipette to a filter for analysis of Chl-a and AFDM. Chl-filters were placed immediately on dry ice and stored at -80°C until analysis. AFDM samples were analyzed according to methods outlined in (Clesceri et al., 1998) and calculated as the weight difference of pre and post 500°C combustion. Chlorophyll-a analysis was completed by a Turner Designs 10AU fluorometer as discussed in (Welschmeyer, 1994) and (Fritsen, et al., 2011).

3.3 DISCHARGE, STAGE, TEMPERATURE AND WEATHER DATA COLLECTION

Water discharge measurements for the SFH River were available from the USGS online National Water Information System (NWIS) (<http://waterdata.usgs.gov/nwis>) from sites 10319900 SFH River above Tenmile Creek and 10320000 SFH River above Dixie

Creek. Daily mean discharge and 10th and 90th percentile of site flows were compiled for the 2009 and 2010 calendar years.

The Nevada Division of Water Resources operates a continuous stage data-logger of the SFH Reservoir, located near the dam outlet. Data were obtained online source (<http://www.water.nv.gov/data/southfork/>), with linear interpolation applied for incomplete data. The Nevada Department of Wildlife (NDOW), collected continuous epilimnion surface water temperature data from the reservoir at a location near the dam during 2009. In situ temperature data from 2010 was lost due to vandalism of temperature recorders. Therefore, surface water temperatures were estimated using methods of interpolation (Neumann et al., 2003). Continuous hypolimnion temperature data were not available, and linearly interpolated from vertical profile sample dates occurring in 2009 and 2010. In addition, waterproof Ibutton® temperature recorders were deployed at the three river site locations from July to August of 2010 for daily mean temperature data collection.

Weather data for the study period was obtained from the University of Utah, MESO WEST online database (<http://mesowest.utah.edu/index.html>). Daily mean temperature, relative humidity, and wind speed were selected from the Elko Regional Airport National Weather Service (NWS) station (16 km from the SFH Reservoir). Shortwave radiation data was available from the Bureau of Land Management (BLM) Crane Springs weather station located 30km southwest of the reservoir.

4. FIELD DATA RESULTS

4.1 SOUTH FORK RESERVOIR 2009-2010

Reservoir water temperatures ranged from a low of 8.5°C in April, 2009, to a high of 24.0°C in July of 2009. The reservoir experienced ice cover in winter of 2009 and 2010, although observational data was not collected during these periods. Continuous daily surface temperatures were collected from April to October of 2009. Data outside this period were modeled by multiple linear regression (Neumann, et al., 2003) and corresponds well with ambient air temperatures for the area (Figure 6).

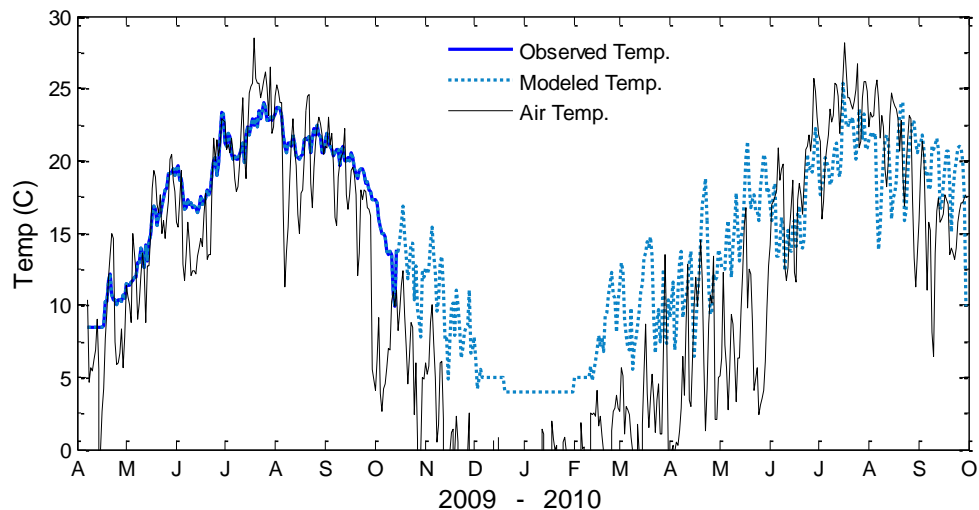


Figure 6. Observed and modeled South Fork Reservoir epilimnion water temperature, and observed air temperatures.

Characteristics of the reservoir include inlet and outlet flows typically observed within the 10th and 90th percentile of historical flows (Figure 7). Although, both the inlet and outlet flows exceeded the 90th percentile in June of both 2009 and 2010. Flows were comparable to the historical mean flows outside of the high flow period caused by heavy

rain events. Other site characteristics include an annual average radiation value of 516 ly/day and an average wind speed of 2.52 m/s (Appendix-A).

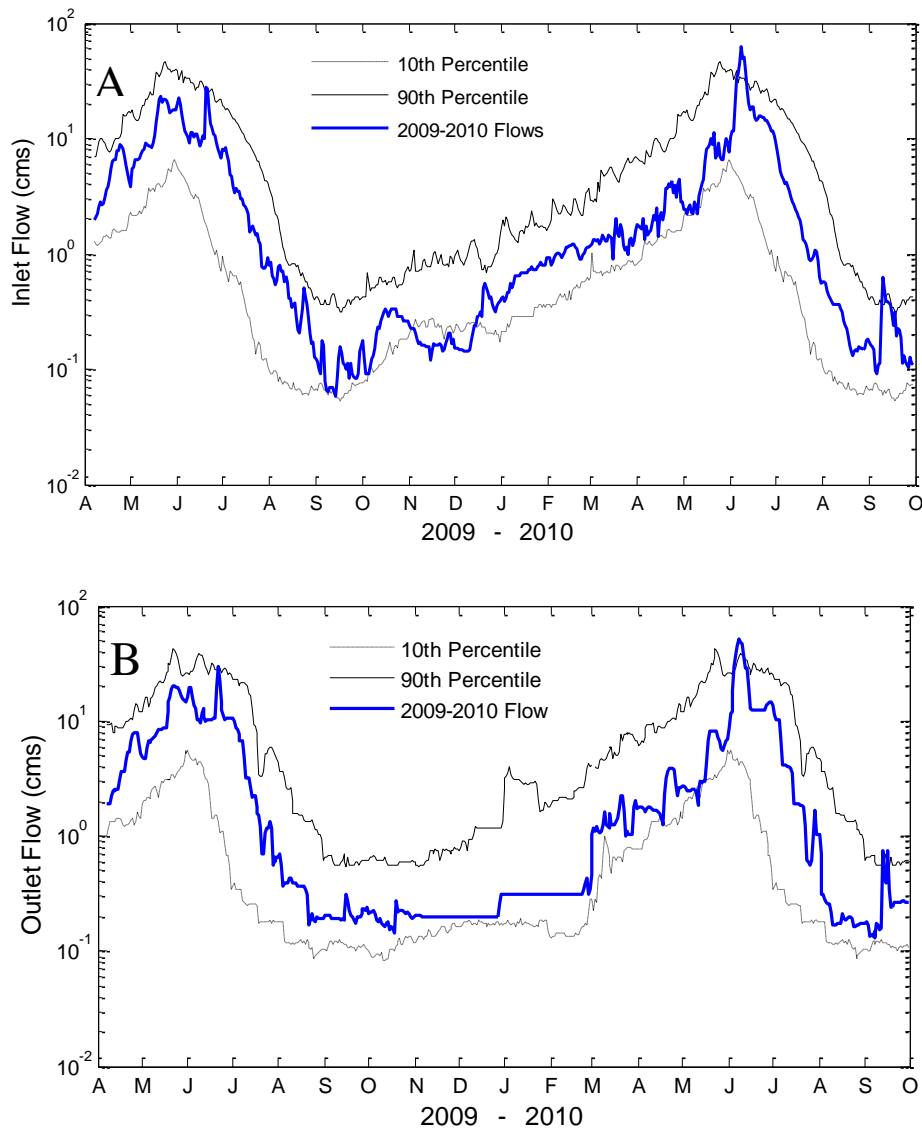


Figure 7. A) USGS gage 10319900 observed inlet flows, in cubic meters per second (cms), to the SFH Reservoir. B) USGS gage 10320000 observed outlet flows (cms) from the SFH Reservoir. (USGS, 2011)

Temperature profiles were analyzed with a derivative analysis to locate the reservoir thermocline, or the stratification boundary of the epilimnion and hypolimnion. The thermocline represents the location of hypolimnion and epilimnion separation and

resistance to mixing was highest at this calculated depth (Appendix-A). Analysis revealed reservoir stratification sometime between the sampling dates of April 7th and May 27th in 2009. Stratification was enhanced through the summer and was observed on the final sampling trip, August 22nd.

The epilimnion remained at or near saturation of DO, while the hypolimnion became anoxic during the period. Maximum values of DO were observed in April. Values of pH varied little with vertical depth throughout the sampling period. From April 2009 to August 2010, pH ranged from an average of 8.27, a minimum of 7.96 and maximum of 8.57 (Appendix-A).

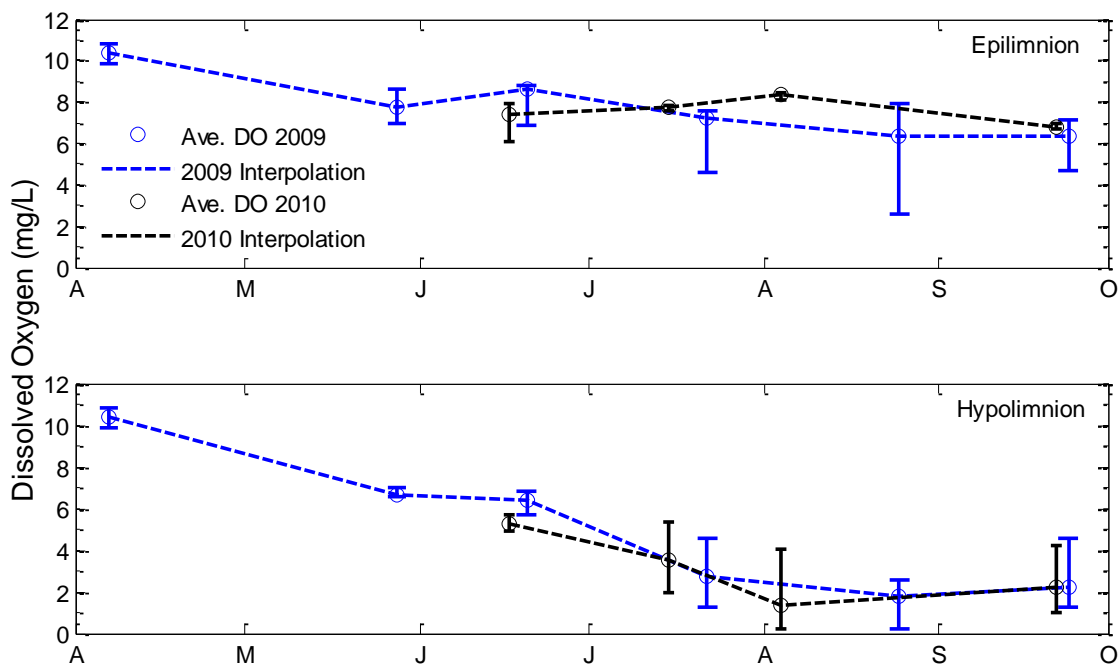


Figure 8. Dissolved oxygen concentrations, calculated as the arithmetic mean of the epilimnion and hypolimnion. Error bars represent minimum and maximum values.

Chl-a values of the reservoir ranged from a low of 0.50 $\mu\text{g/L}$ in July of 2010 to a high of 9.13 $\mu\text{g/L}$ August 2010 (Table 4). Sample concentrations represent the arithmetic mean of epilimnion vertical profiles collected from all sample locations. June and July experienced the lowest concentrations, and highest values were observed in August and September of 2009 and 2010. Similarly, SD values were the deepest, indicating improved water clarity, in June and July of 2009 and July of 2010. SD values were the shallowest in the April 2009 and June of 2010 (Table 4).

Epilimnion nutrients followed a pattern of low concentrations from April to July, increased in August to September of both 2009 and 2010. Particulate organic carbon concentrations in the epilimnion were highest in April and September of 2009, with lower values decreasing in the summer months (Table 4).

Table 4. SFH Reservoir Chl-a, SD and nutrient data reported as the arithmetic mean of epilimnion samples. POC samples are from site location SFR5 and used as a surrogate for POC loadings to the reservoir. Values represented by a hyphen indicate samples were not completed.

Reservoir Sample Date	Chl-a $\mu\text{g/L}$	SD m	TP mgP/L	PO ₄ mgP/L	TN mgN/L	NH ₄ mgN/L	NO _x mgN/L	POC mgC/L
4/7/2009	5.22	2.7	-	0.013	-	0.002	0.001	0.7559
5/27/2009	2.10	3.7	0.042	0.042	0.477	0.004	0.005	0.4575
6/9/2009	1.49	6.8	0.037	0.037	0.272	0.002	0.006	0.4033
7/21/2009	3.25	5.8	0.026	0.026	0.342	0.020	0.003	0.3862
8/24/2009	4.54	4.6	0.076	0.076	0.400	0.028	0.004	0.6822
9/23/2009	7.34	3.2	0.074	0.074	0.619	0.026	0.004	0.9657
6/17/2010	0.70	1.8	0.053	0.016	0.514	0.023	0.013	-
7/14/2010	0.50	5.6	0.034	0.011	0.542	0.021	0.013	-
8/4/2010	9.13	4.4	0.034	0.029	0.537	0.016	0.030	-
9/21/2010	2.38	5.2	0.054	0.027	0.600	0.099	0.025	-

The SFH reservoir phytoplankton community was mainly composed of three general taxonomic groups, cyanophyta (cyanobacteria), diatoms, and chlorophyta (green algae) (Figure 9). Diatoms dominated the phytoplankton community in April 2009 with greater than 95% of the biovolume, which decreased to 14% of the biovolume in August. Chlorophytes consistently accounted for 10% to 15% of total biovolume; after April of 2009, cyanobacteria represent greater than 40% of total biovolume of the reservoir (Fritsen, et al., 2011).

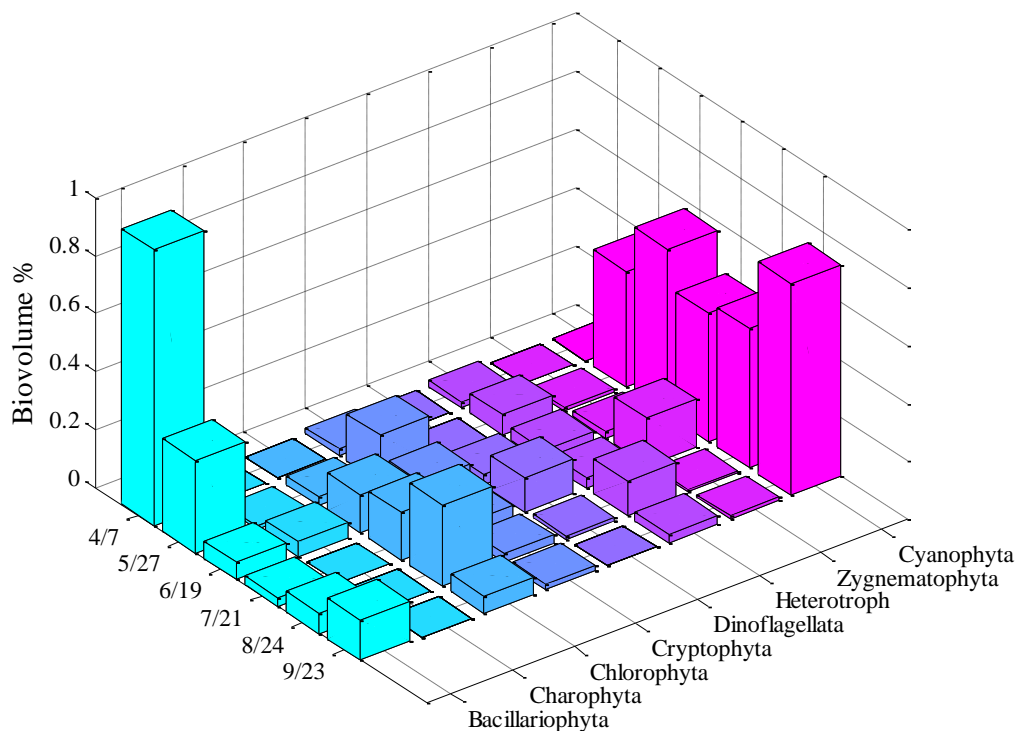


Figure 9. SFH Reservoir 2009 phytoplankton biovolume percentages of major taxonomic groups.

Reservoir zooplankton samples in September of 2009 with a total of 7.8×10^4 individuals/ m^3 and a minimum in May of 2.7×10^4 individuals/ m^3 (Fritsen, et al., 2011).

Zooplankton samples were dominated by cladocerans and Copepods throughout the

observational period. Dry weights of individuals were not calculated during to 2009 study. Conversion of individuals to dry mass was estimated by using the average individual weights as documented in (Hawkins and Evans, 1979) (Figure 10).

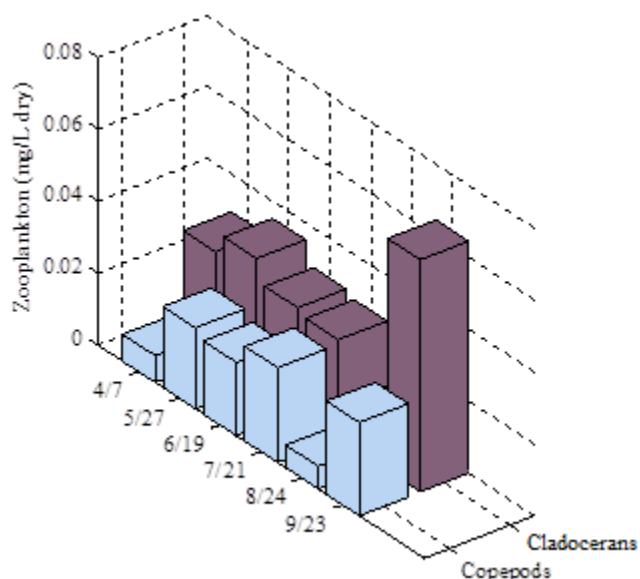


Figure 10. Zooplankton estimated biomass of the SFH Reservoir.

Additionally, reservoir sediment core samples resulted in a sediment sample approximately 0.3 meters in length, with distinct dark anoxic sediments and light gray clay paleosols of grazing land before reservoir construction (Figure 11). The results of the density analysis produced an arithmetic mean sediment density of 57.16 kg/m^3 . The density was used for model initial condition specification of initial conditions (Appendix-B) based on Redfield ratios (Redfield, 1958).



Figure 11. Image of SFH Reservoir gravity core sample collected on September 23rd, 2009 (tape-measure values are in inches).

4.2 SOUTH FORK HUMBOLDT RIVER 2009-2010

Three Ibutton® temperature data loggers were deployed in the SFH River below the reservoir at 0.75km, 10km, and 20km distance from the dam. Due to a malfunction, the data recorder located at 10km was corrupted and diel temperature fluctuations were available for only two locations (Figure 12). River temperatures located at 0.75km had larger daily temperature changes with a maximum of 26.4°C and a minimum of 3.75°C observed during deployment. River water temperatures 20km away from the dam had a lower amplitude diel temperature change, with a maximum of 25.1°C and minimum temperature of 9.3°C. In addition the reservoir was operated by top release only from mid-June to July 29th. Outflows occurred only through an emergency spillway during this time. The outflow was switched to bottom release on July 29th at 11:00 as indicated by the abrupt temperature drop shown in Figure 12.

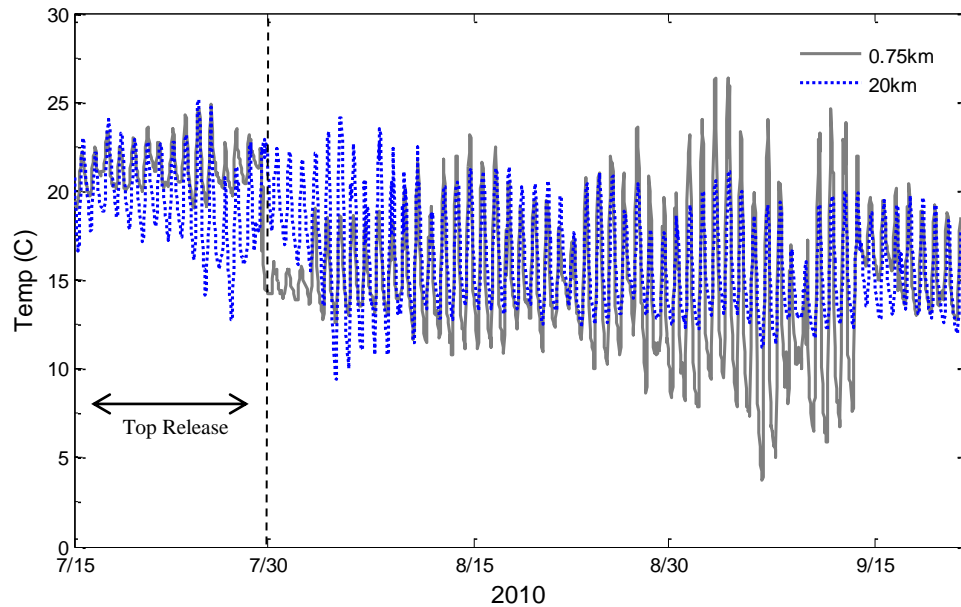


Figure 12. Hourly temperature data of the SFH River 0.75 km and 20 km away from the dam outlet.

Nutrients increased at the reservoir outlet, when compared to nutrient loadings to the reservoir (Table 5). A comparison of PO_4 values (Table 5) in 2009 and 2010 show a maximum outlet value in months of September and October at 0.086 mgP/L, while the highest values flowing into the reservoir were 0.049 mgP/L in June of 2009. Orthophosphorous in the reservoir outflows was nearly four times greater than in the inflow during August and September of both years. Both NH_4 and NO_x exhibited increases in concentrations with maximum outlet values of 0.073 mgN/L and 0.151 mgN/L, and inflow values of 0.021 mgN/L and 0.026 mgN/L respectively.

Table 5. Dissolved nutrients of the SFH River near the reservoir inlet and 0.75 km downstream of the outlet. TP and TN data were not collected for river samples in 2009 and 2010.

Reservoir Inlet				Reservoir Outlet (0.75km)			
Sample Date	PO ₄ mgP/L	NH ₄ mgN/L	NO _x mgN/L	Sample Date	PO ₄ mgP/L	NH ₄ mgN/L	NO _x mgN/L
4/13/2009	0.035	0.006	0.003	4/13/2009	0.007	0.002	0.002
5/26/2009	0.033	0.008	0.022	5/26/2009	0.038	0.032	0.014
6/11/2009	0.046	0.003	0.006	6/11/2009	0.024	0.042	0.015
6/18/2009	0.049	0.017	0.016	6/18/2009	0.049	0.060	0.028
7/15/2009	0.040	0.013	0.003	7/15/2009	0.020	0.006	0.002
8/18/2009	0.017	0.011	0.002	8/18/2009	0.086	0.030	0.037
6/17/2010	0.017	0.021	0.012	6/17/2010	0.023	0.062	0.026
7/10/2010	0.014	0.009	0.006	7/10/2010	0.042	0.073	0.075
8/5/2010	0.002	0.014	0.001	8/5/2010	0.085	0.026	0.151
9/21/2010	0.027	-	0.026	9/21/2010	0.086	0.067	0.088

Benthic Chl-a values were at exceptional levels with values exceeding 500 mg Chl-a/m² (Figure 13). Periphyton biomass was 577, 505 and 94 mg Chl-a/m² on June 12th, July 16th, and August 19th of 2009, respectively. Sampling was unfortunately delayed for logistical reasons to August 11th in 2010, and likely missed the maximum periphyton biomass, yet still had high values of 206 mg Chl-a/m².

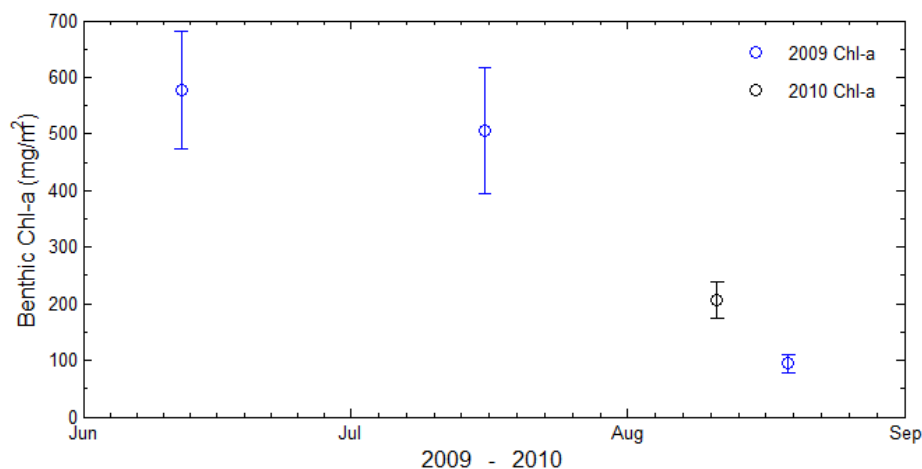


Figure 13. Benthic Chl-a concentrations from 2009 and 2010 0.75 km downstream of the SFH Reservoir. Circles are the arithmetic mean of ~24 samples, error bars represent mean standard error.

Bacillariophyta (diatoms), chlorophyta, and cyanobacteria were the major taxonomic groups from June to August of 2009 (Figure 14). Overall the reach was covered by nearly 50% diatoms and 50% chlorophytes for the study period with decreasing individuals from June to August. Chlorophytes are dominated by long filamentous periphyton identified as *Cladophora* and *Oedogonium*. Cyanobacteria periphyton, made up a maximum of 5% biovolume, contributing very little to the community total biovolume at the site 0.75 km downstream of the dam.

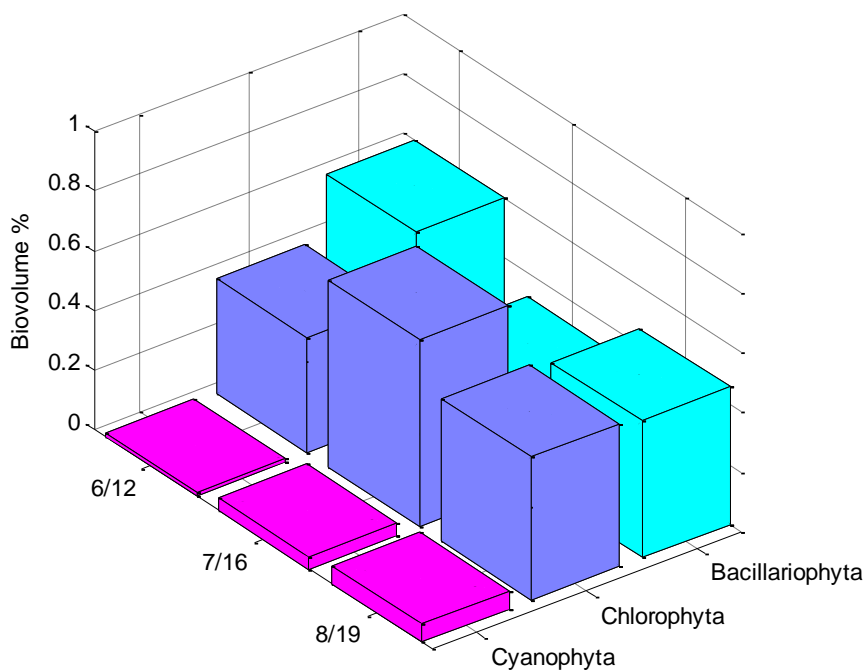


Figure 14. Periphyton taxonomic biovolumes, 0.75 km downstream of the dam. Values obtained from (Davis, et al., 2011)

5. USEPA - AQUATOX 3.1

5.1 MODEL DESCRIPTION

Mathematical models for surface water quality simulation vary greatly in model simulation variables, inputs, calculation methods and representation of physical processes. The EPA model AQUATOX 3.1 was selected to achieve study objectives since it is capable of simulating both riverine and reservoir ecosystems and it is recommended by the EPA for nutrient criteria investigations (U.S. EPA, 1998).

AQUATOX 3.1 is a biogeochemical, 1-dimensional mechanistic model simulating individual algal taxa of periphyton and phytoplankton with ecosystem trophic linkages for reservoirs and rivers (Richard A. Park et al., 2008). A comprehensive external review of AQUATOX 3.1 (Keehner, 2009) determined the model design is current with ecological literature and praises improvements of sensitivity and uncertainty analysis included in the model. AQUATOX 3.1 has been used in multiple river nutrient criteria investigations within the state of Minnesota (Carleton et al., 2009). Successful reservoir and river calibration and validation at multiple locations throughout the U.S. (Koelmans et al., 2001; Rashleigh et al., 2009; Sourisseau et al., 2008) substantiates the ability of AQUATOX to simulate the SFH system.

AQUATOX 3.1 is a public domain model using the conservation of mass principle to track changes in state-variables in multiple environmental settings. The principal user interface is through a graphical user interface (GUI) that facilitates importing data from Microsoft Excel. Model state-variables, or the components of an ecosystem that are simulated by first order differential equations (U.S. EPA, 2009a),

include: phosphorous, nitrogen, oxygen, light, dissolved oxygen, total suspended sediment (TSS), sediment oxygen and nutrient concentrations, organic matter, plants (phytoplankton and periphyton) and animal trophic linkages (Figure 15).

Simulation reporting time steps can be selected as daily or hourly steps with resulting calculations of trapezoidal integration or instantaneous output as determined by Runge-Kutta 4th and 5th order numerical solution (U.S. EPA, 2009a). The Runge-Kutta time-step solution avoids numerical instability by varying the step size of integration within the daily or hourly time step (White, 1986). In addition, the user selects the relative error of the simulation, selected as 0.001 for the SFH System, for improved accuracy and increased simulation time of model simulations.

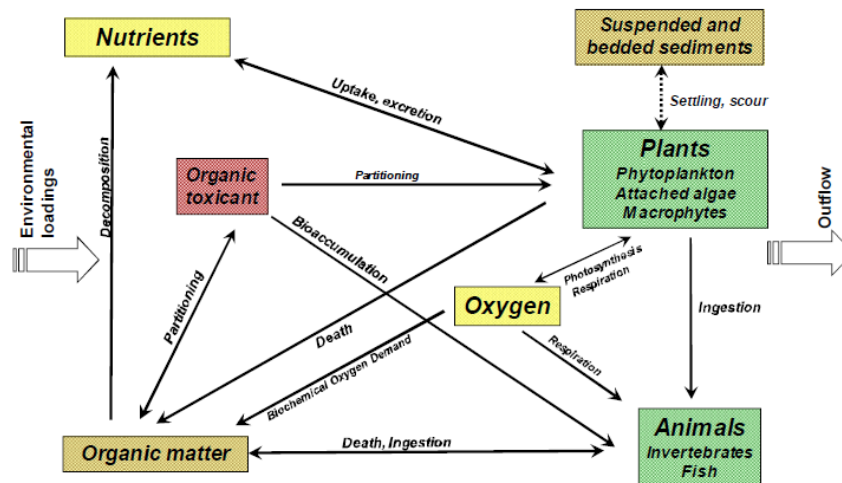


Figure 15. Conceptual framework of AQUATOX 3. (US EPA, 2010).

5.2 RESERVOIR MODEL

AQUATOX 3.1 represents reservoirs and lakes as simplified 1-dimensional continuously stirred tank reactors (CSTR) (Chapra, 1997) with changes in volume associated with water inflow (m^3/day), outflow (m^3/day), and evaporative losses

(m³/day). Evaporation is assumed to be constant throughout the simulation time period for all water bodies.

Stratification of the reservoir is simulated by user-specified or model calculated dates of stratification. April 20th was selected for the onset of stratification, and October 1st as the fall turnover date. Stratification was simulated by utilizing a user input time-varying depth of the hypolimnion, with the system represented by two 1-d, vertically stacked CSTRs (Straskraba and Gnauck, 1985). Outflows from the reservoir can be specified from the hypolimnion or epilimnion layer and vertical dispersion of state variables is represented by a function of temperature dynamics between layers (Thomann and Mueller, 1987):

$$\mathit{VertDispersion} = \mathit{Thick} * \left(\frac{\mathit{HypVolume}}{\mathit{ThermoclArea} * \mathit{Deltat}} * \frac{T_{\mathit{hypo}}^{t-1} - T_{\mathit{hypo}}^{t+1}}{T_{\mathit{epi}}^t - T_{\mathit{hypo}}^t} \right) \quad (3)$$

Where *VertDispersion* = Vertical Dispersion or exchange between the epilimnion and hypolimnion (m²/day); *Thick* = the mean depth (m); *HypVolume* = volume hypolimnion water (m³); *ThermoclArea* = area of the thermocline (m²); *Deltat* = time step (day); T_{hypo}^{t-1} , T_{hypo}^{t+1} , hypolimnion change in temperature during one time step; and T_{epi}^t , T_{hypo}^t , represent the epilimnion and hypolimnion temperatures (°C) respectively.

Reservoir and river inflowing boundary conditions for the SFH simulation include: inflow discharge (m³/day), temperature (°C), DO (mg/L), Carbonaceous Oxygen Demand (COD) (mg/L), suspended and dissolved detritus (mg/L dry), wind (m/s), light (ly/day) and pH. Boundary conditions of phytoplankton, zooplankton and animals are in the relative variables of (mg/L dry).

Reaeration of the reservoir is calculated as a function of wind speed as a minimum transfer velocity. Where *Reaeration* = mass transfer of oxygen (g/m³day); *Wind* = wind velocity 10 meters above the water (m/s); 864 = conversion factor (cm/s to m/day); *Thick* = thickness of mixed layer (m); *O2Sat* = saturation concentration of DO (g/m³), and *Oxygen* = concentration of DO (g/m³):

$$\mathbf{Reaeration} = \frac{(4E-4+4E-5*Wind^2)*864}{Thick} * (O2Sat - Oxygen) \quad (4)$$

Additionally, AQUATOX 3.1 models cyanobacteria only within the top 0.1m, therefore, if cyanobacteria biomass exceeds 1 mg/L dry the resulting productivity DO impact is only within the top 0.1 m, and does not impact the reaeration function (U.S. EPA, 2009a).

Nutrient state variables can be specified by the user as TN and TP or dissolved nutrients of PO₄, NO_x, and NH₄. Total nutrients (i.e., TN and TP) selected for loadings results in the model back-calculation of the amount of phosphorous and nitrogen in phytoplankton, suspended and dissolved detritus for given TN and TP values. If TN is selected as a state loading variable, NH₄ is specified as a constant value of 12% of bioavailable dissolved nitrogen and cannot be changed by the user. The user has the ability to specify the calculated TP and PO₄ relationship is provided by a input fraction of TP that is bioavailable (U.S. EPA, 2009a).

Dissolved and suspended detritus may represent significant portions of TN and TP calculations. Loadings of detritus are simulated as Organic Matter, though Biological Oxygen Demand (BOD) and Organic Carbon (OC) loadings are user-selectable. Only surrogate values of POC were available for the reservoir simulation, with the conversion

to OM loadings assumed to be $1.90 \cdot \text{OC}$ loadings (U.S. EPA, 2009a). The model uses ratio parameters of OM:nitrogen and OM:phosphorous for the nutrient composition of labile and refractory detritus loadings.

5.3 PHYTOPLANKTON, PERIPHYTON AND ZOOPLANKTON CALCULATIONS

AQUATOX 3.1 tracks changes in phytoplankton and periphyton state variables as changes in biomass with respect to time (U.S. EPA, 2009a). The change in biomass is calculated via a system of governing equations:

$$\frac{dBiomass_{phyto}}{dt} = \mathbf{Loading} + \mathbf{Photosynthesis} - \mathbf{Respiration} - \mathbf{Excretion} - \mathbf{Mortality} - \mathbf{Predation} \pm \mathbf{Sinking} - \mathbf{Washout} + \mathbf{Washin} \pm \mathbf{TurbDiff} + \frac{\mathbf{Slough}}{3} \quad (5)$$

$$\frac{dBiomass_{peri}}{dt} = \mathbf{Loading} + \mathbf{Photosynthesis} - \mathbf{Respiration} - \mathbf{Excretion} - \mathbf{Mortality} - \mathbf{Predation} + \mathbf{Sed}_{peri} - \mathbf{Slough} \quad (6)$$

Where: $\frac{dBiomass}{dt}$ = the change in biomass with respect to time of phytoplankton (phyto) and periphyton (peri) ($\text{g/m}^3 \cdot \text{day}$ and $\text{g/m}^2 \cdot \text{day}$, respectively); *Loading* = The boundary-condition loading of state variable of phytoplankton and periphyton ($\text{g/m}^3 \cdot \text{day}$ and $\text{g/m}^2 \cdot \text{day}$); *Photosynthesis* = photosynthesis rate ($\text{g/m}^3 \cdot \text{day}$ and $\text{g/m}^2 \cdot \text{day}$); *Respiration* = respiratory loss ($\text{g/m}^3 \cdot \text{day}$ and $\text{g/m}^2 \cdot \text{day}$); *Excretion* = photorespiration based on (R.A. Park et al., 1979) ($\text{g/m}^3 \cdot \text{day}$ and $\text{g/m}^2 \cdot \text{day}$); *Mortality* = nonpredation periphyton and phytoplankton mortality ($\text{g/m}^3 \cdot \text{day}$ and $\text{g/m}^2 \cdot \text{day}$); *Predation* = herbivory of state variables ($\text{g/m}^3 \cdot \text{day}$ and $\text{g/m}^2 \cdot \text{day}$); *Washout* = the downstream loss of phytoplankton state variable ($\text{g/m}^3 \cdot \text{day}$); *Washin* = upstream phytoplankton state variable loading ($\text{g/m}^3 \cdot \text{day}$); *Sinking* = gain or loss between epilimnion and

hypolimnion layers or due to bottom sedimentation ($\text{g/m}^3 \cdot \text{day}$); $TurbDiff$ = turbulent diffusion related to the vertical bulk mixing coefficient of (Thomann and Mueller, 1987) ($\text{g/m}^3 \cdot \text{day}$); $Slough$ = loss due to scouring of periphyton ($\text{g/m}^2 \cdot \text{day}$); Sed_{peri} = Gain from settling of phytoplankton to periphyton ($\text{g/m}^3 \cdot \text{day}$);

AQUATOX 3.1 contains multiple taxa of phytoplankton and periphyton for model simulation, with taxa initial conditions and simulated values of (mg/L dry). Phytoplankton and periphyton taxonomic identification for the SFH Reservoir were calculated as biovolume percent calculations; to facilitate the conversion of biovolume to biomass, by the equation:

$$PhytoBiomass = \left(\sum \frac{Chla * Biovol_{BG} * 45}{\frac{1000}{0.526}} + \sum \frac{Chla * Biovol_{Diatoms, Greens} * 45}{\frac{1000}{0.526}} \right) \quad (7)$$

Where: $PhytoBiomass$ = the total phytoplankton biomass (mg/L dry); $Chla$ = the reservoir arithmetic mean Chlorophyll-a concentration ($\mu\text{g/L}$); $Biovol_{BG, Diatoms, Greens}$ = biovolume percent of cyanobacteria, diatoms, and chlorophytes (percent); 0.526 = conversion factor of carbon to biomass (unitless). Carbon to Chl-a conversions can exhibit a wide range of values, AQUATOX 3.1 follows the methods of (Wool et al., 2004) for fixed values of conversion of 28 $\mu\text{gC}/\mu\text{gChl-a}$ for diatoms and chlorophytes, and 45 $\mu\text{gC}/\mu\text{gChl-a}$ for cyanobacteria.

Zooplankton and benthic macroinvertebrates are tracked as the changes in biomass with a general submodel parameterized for specific state variables of aquatic insects. The change in zooplankton biomass is calculated via a system of governing equations:

$$\frac{dBiomass}{dt} = Load + Consumption - Defecation - Respiration - Fishing - Excretion - Mortality - Predation - GameteLoss - Washout + Washin \pm Migration - Promotion + Recruit - Entrainment \quad (8)$$

Where: $\frac{dBiomass}{dt}$, is the change in zooplankton with respect to time ($g/m^3 \cdot day$); *Consumption* = the consumption of prey ($g/m^3 \cdot day$); *Defecation* = excretion of unassimilated prey ($g/m^3 \cdot day$); *Fishing* = the removal of the state variable by fish consumption ($g/m^3 \cdot day$); *GameteLoss* = loss of gametes during spawning ($g/m^3 \cdot day$); *Migration* = vertical migration of state variable ($g/m^3 \cdot day$); *Promotion* = variable emergence from size class ($g/m^3 \cdot day$); *Recruit* = recruitment from previous size class ($g/m^3 \cdot day$); *Entrainment* = transport of variable downstream ($g/m^3 \cdot day$);

Further descriptions of phytoplankton, periphyton and zooplankton sub-variable parameter calculations are discussed in (U.S. EPA, 2009a). Specific parameters used in the SFH Reservoir and River calibration are discussed in detail within chapter 6.

5.4 SEDIMENT DIAGENESIS

AQUATOX 3.1 includes multiple subroutines for the modeling of reservoir deposition of detritus and phytoplankton. The SFH Reservoir exhibits significant nutrient fluxes from the bottom sediment, with timing being a critical component of the flux (Fritsen, et al., 2011; Sater, et al., 1994). The DiToro, (2001) sediment diagenesis submodel was selected for the ability to match the timing and magnitude of nutrient fluxes from the SFH Reservoir sediments. The model uses principles of mass balance to

track OM deposition, decomposition, mineralization, pore water exchange and flux to the water column (Figure 16).

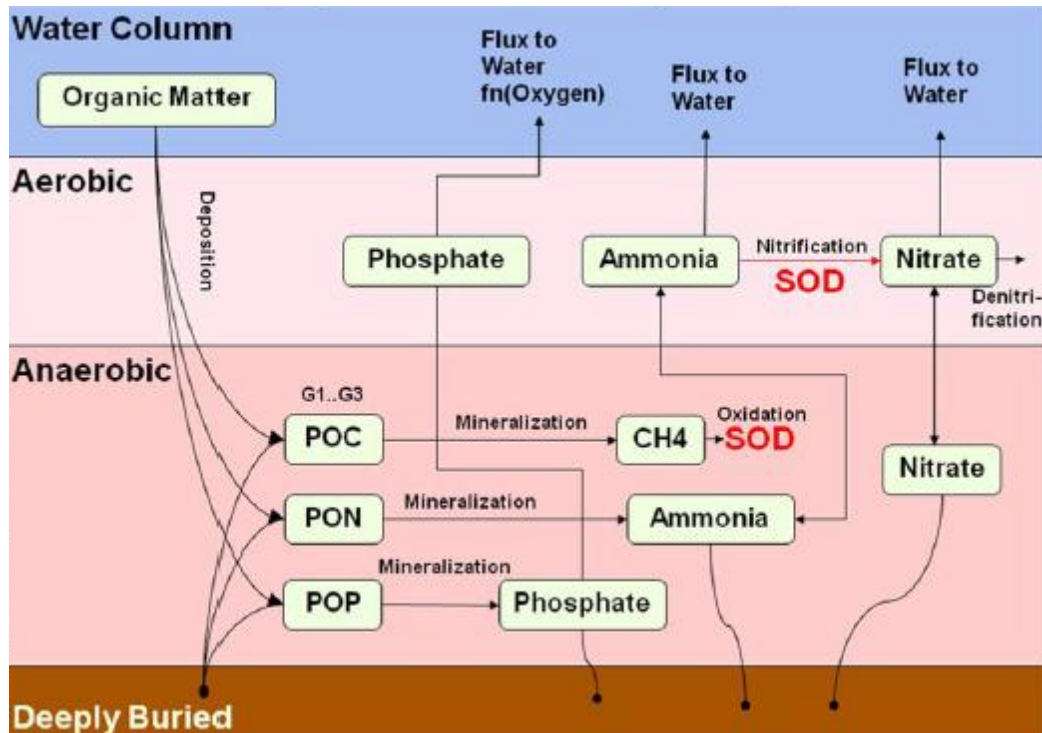


Figure 16. Di Toro's (2001) conceptual model of sediment diagenesis model for the SFH Reservoir. (U.S. EPA, 2009a).

Di Toro's model operates on the assumption of two homogeneous layers, H_1 an aerobic, thin top layer varying in thickness and H_2 , an anaerobic bottom layer at a fixed depth. Principles of mass balance are used in tracking state variable transfer between layers with analytical solutions of steady state equations. Where: H_1 and H_2 are the depths of zone 1 and 2 (m); $c_{(1)}, c_{(2)}$ concentration of state variable concentration in zones, respectively; dt = change in time; J is mass flux ($\text{mg}/\text{m}^2 \cdot \text{day}$); K_{L12} = mass transfer coefficient (m/day); w_2 = sedimentation velocity of state variable (m/day) (DiToro, 2001):

$$H_1 \frac{dc(1)}{dt} = J + K_{L12}(c(2) - c(1)) - (w_2 * c(1)) \quad (9)$$

$$H_2 \frac{dc(2)}{dt} = (w_2 * c(1)) + K_{L12}(c(2) - c(1)) - (w_2 * c(2)) \quad (10)$$

Settling organic matter is fractioned into particulate organic phosphorous (POP), particulate organic nitrogen (PON), and particulate organic carbon (POC). Sedimentation and burial of OM to layer H₂ enables model decomposition by first-order reaction kinetics and mineralization of POP to PO₄, PON to NH₄, and POC to methane, modeled as sediment oxygen demand (SOD). Movement of nutrients is tracked by equal mass exchanges from H₁ and H₂ by a diffusion transport coefficient K_L . Where K_L = diffusion velocity between layers (m/day); D_d = diffusion coefficient for pore water (m²/day); θ_{Dd} = constant for temperature adjustment for the diffusion coefficient (dimensionless); $Temp$ = temperature of water (°C); and H_2d = layer H₂ depth (m) (DiToro, 2001).

$$K_L = \frac{D_d * \theta_{Dd}^{Temp-20}}{H_2d} \quad (11)$$

5.5 RIVER MODEL

River simulation in AQUATOX 3.1 applies the CSTR methodology of reach volume and is computed by applying Manning's volume equation (U.S. EPA, 2009a).

$$ManningVol = \left(Q * \frac{Manning}{\sqrt{Slope * Width}} \right)^{\frac{3}{5}} * CLength * Width \quad (12)$$

Where Q = flow rate (m³/s); $Manning$ = Manning's roughness coefficient (s/m^{1/3}); $Slope$ = slope of channel (m/m); $Width$ = channel width (m); and; $CLength$ = length of reach

(m). Channel shape is assumed to be rectangular with habitat type of pool, riffle or run selected based on observed reach percentages. Habitat type is related to specific velocities based on the DSAMMt model (Caupp et al., 1998) (Table 6).

Table 6. AQUATOX 3.1 factors relating velocities to those of the average reach. (U.S. EPA, 2009a)

Flows (Q = discharge)	Run Velocity	Riffle Velocity	Pool Velocity
Q < 2.59e5 m ³ /day	1.00	1.60	0.36
2.59e5 m ³ /day < Q < 5.18e5 m ³ /day	1.00	1.30	0.46
5.18e5 m ³ /day < Q < 7.77e5 m ³ /day	1.00	1.10	0.56
Q > 7.77e5 m ³ /day	1.00	1.00	0.66

AQUATOX 3.1 river DO dynamics are controlled by an automatic reaeration coefficient based on relative water depth and channel velocity (Wool, et al., 2004).

Where: *TransitionDepth* = intermediate variable of depth (m) used for reaeration function determination; *Vel* = stream velocity (m/sec).

$$\mathbf{TransitionDepth = 4.411 * Vel^{2.9135}} \quad \mathbf{(13)}$$

The variable *TransitionDepth* is related to the Manning calculated stream depth (Eq. 12) and velocity for reaeration equation selection. If *TransitionDepth* < *Depth*, calculated stream depth (m), the O'Connor and Dobbins (1958, cited in Chapra (1997)) equation is used:

$$\mathbf{KRear = 3.93 * Vel^{0.50} * Depth^{-1.50}} \quad \mathbf{(14)}$$

However, if the stream depth is greater than 0.06 meters and less than 0.61 meters the Owens et. al. (1964, cited in Chapra (1997)) is used. Where *Depth* = mean stream depth (m):

$$KRear = 5.349 * Vel^{0.67} * Depth^{-1.85} \quad (15)$$

Also, if $Depth \leq TransitionDepth$ and > 0.60 meters the equation of Churchill et. al. (1962, cited in Chapra (1997)) is used:

$$KRear = 3.93 * Vel^{0.50} * Depth^{-1.67} \quad (16)$$

Wind speed can have the potential to have a greater reaeration coefficient than stream velocity and depth. In the case wind $KRear >$ velocity $KRear$ equation (5) is used.

6. AQUATOX 3.1 SENSITIVITY ANALYSIS, CALIBRATION, AND VALIDATION

6.1 SFH RESERVOIR AND RIVER MODEL SENSITIVITY ANALYSIS

The conventional use of mechanistic models involves three critical model procedures of sensitivity analysis, calibration, and validation for model development and assessment (Arhonditsis and Brett, 2004). Sensitivity analysis of AQUATOX 3.1 is particularly necessary due to the numerous parameters for state variables selected for simulation, with the total number of parameters for phytoplankton, zooplankton, and sediment diagenesis being 24, 29, and 59 respectively. Included within the model is an automated sensitivity analysis allowing the user to identify the parameters most sensitive to individual state variables for calibration. Sensitivity analysis included in AQUATOX 3.1 is performed as a nominal range sensitivity analysis, or threshold analysis. The analysis commonly used in model analysis to identify how parameters propagate through the model output (Cullen and Frey, 1999).

Model sensitivity analysis is initialized by the user selecting all relative parameters for individual state variables (i.e. cyanobacteria) simulation. The model is initially run for nominal, or a default parameter value solution, followed by varying of individual parameters by a user-entered percentage value. Results of the sensitivity analysis indicate the percent change of state variables, by a positive and negative percent change of individual parameter values. Results are graphically displayed as tornado diagrams, with the percent change of the state variable as a result of a 10% change in individual parameter values (Figure 17).

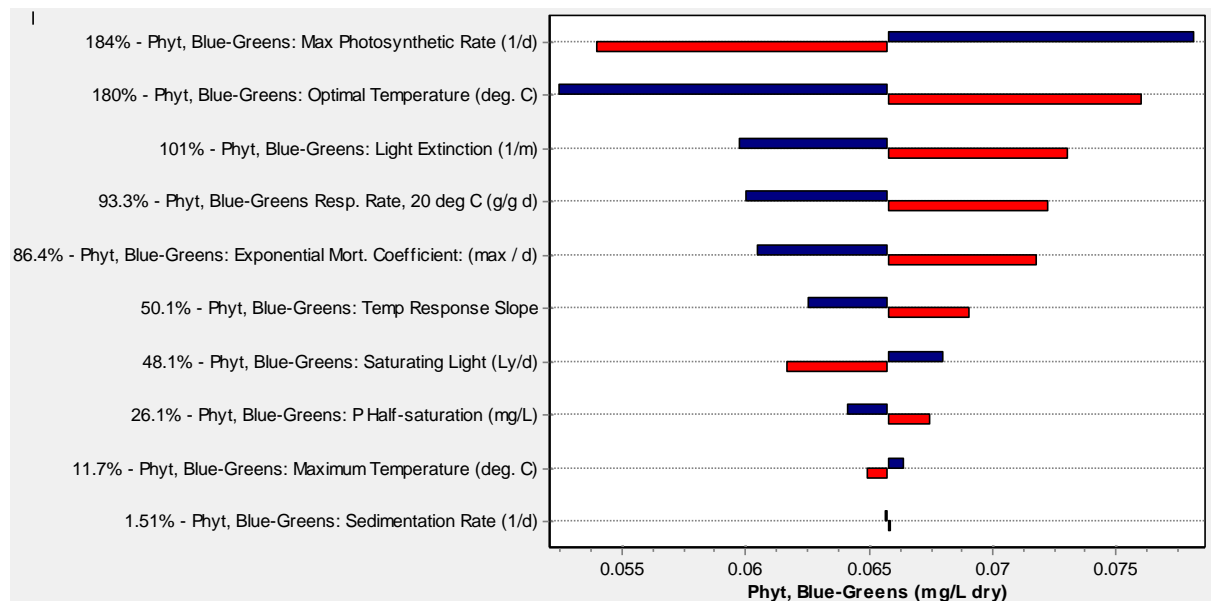


Figure 17. Sensitivity analysis results for cyanobacteria of the SFH Reservoir simulation. Black center line indicates nominal or default parameter values. Blue bars extending from the default line represent +10% adjustment of parameters, red bars equal a -10% parameter adjustment. Only the top 10 most sensitive parameter values are displayed.

Sensitivity analyses were performed for phytoplankton, periphyton, zooplankton and sediment diagenesis parameters. Sediment diagenesis parameters were identified for effects on dissolved nutrients of PO_4 , NO_x , and NH_4 in the hypolimnion (Figure 18). The

results of sensitivity analysis were used in combination with model calibration technical notes (U.S. EPA, 2009b) for the selection of calibration parameters.

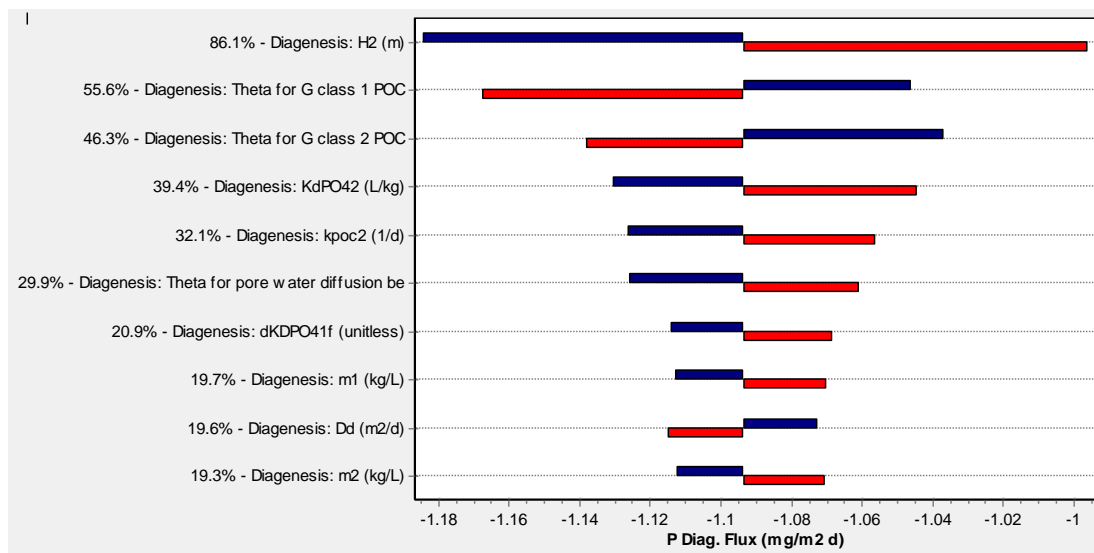


Figure 18. Sensitivity analysis results for PO₄ sediment diagenesis flux of the SFH Reservoir simulation. Black center line indicates nominal or default parameter values. Blue bars extending from the default line represent +10% adjustment of parameters, red bars equal a -10% parameter adjustment. Only the top 10 most sensitive parameter values are displayed.

6.2 SFH RIVER AND RESERVOIR MODEL CALIBRATION PARAMETERS

6.2.1 PHYTOPLANKTON AND PERIPHYTON CALIBRATION PARAMETERS

The results of the SFH Reservoir and River sensitivity analyses were used to select input parameters for model calibration of phytoplankton and periphyton. The calibration parameters for phytoplankton and periphyton state variables include: maximum photosynthesis, light saturation, optimum temperature, phosphorous half-saturation, nitrogen half-saturation, respiration rate and scour force (for periphyton state variables only).

The maximum photosynthesis rate parameter is a function expressed within phytoplankton and periphyton photosynthesis calculations for biomass (Eq. 6 and Eq. 7). Phytoplankton photosynthesis is directly related to the calibrated parameter of maximum photosynthetic rate (P_{max}) (1/day). Under optimal conditions photosynthesis will be calculated as the specified P_{max} rate multiplied by the state variable biomass (g/m^3 and g/m^2). However, P_{max} , and therefore photosynthesis, may be limited by reduction factors due to suboptimal conditions of nutrients, velocity, light, and temperature; parameters within the model simulation selected for calibration.

Nutrient limitations of phytoplankton and periphyton photosynthetic rates are based on Michaelis-Mention or Monod equations of uptake kinetics for nitrogen, phosphorous, and carbon (Hutchinson, 1957; U.S. EPA, 2009a).

$$P \text{ limit} = \frac{\text{Phosphorus}}{\text{Phosphorus} + KP} \quad (17)$$

$$N \text{ limit} = \frac{\text{Nitrogen}}{\text{Nitrogen} + KN} \quad (18)$$

$$C \text{ limit} = \frac{\text{Carbon}}{\text{Carbon} + KCO2} \quad (19)$$

Where: P , N , and $C \text{ limit}$ = the limitation due to phosphorous, nitrogen, and carbon (unitless); Phosphorus , Nitrogen , and Carbon = nutrient concentrations (gP/m^3 , gN/m^3 , and gC/m^3); and; KP , KN , and $KCO2$ = the calibration parameter of half-saturation constants of phosphorous (gP/m^3), nitrogen (gN/m^3), and carbon (gC/m^3) respectively. Half-saturation values of phosphorous were selected for phytoplankton calibration, while both KP and KN were sensitive to periphyton state variables. For

photosynthesis limitation, AQUATOX 3.1 follows the minimum limiting nutrient criteria of either P, N, or C for suboptimal nutrient calculations (Wool, et al., 2004)

Periphyton can also experience limitation of nutrients due to minimal flow velocities. A minimal velocity is needed for the replenishment of nutrients for periphyton biomass growth (McIntire and Colby, 1978).

$$VLimit = \min \left(1, RedStillWater + \frac{0.057 * Velocity}{1 + 0.057 * Velocity} \right) \quad (20)$$

Where: $VLimit$ = periphyton current limitation (unitless); $RedStillWater$ = photosynthesis reduction in current absence (unitless); and; $Velocity$ = current velocity (m/sec); Typical values of $RedStillWater$ in streams with flow is 0.2 (McIntire and Colby, 1978), and was used for the SFH River simulation.

Light is considered one of the most important and sensitive values for phytoplankton (Figure 17) and periphyton photosynthesis within AQUATOX 3.1. Light limitation of state variables is a function of light extinction at depth, or reduction of radiation, by dissolved and particulate detritus, water, and phytoplankton biomass. Phytoplankton is modeled as well-mixed throughout the entire reservoir and river reach volumes, while cyanobacteria are only modeled within the top 0.1 to 3.0 meters (U.S. EPA, 2009a). Light saturation values were selected for phytoplankton and periphyton calibration, where:

$$LtAtTop_{TimeStep} = e^{-\frac{Lt_{TimeStep}}{LtSat * LtCorr}} \quad (21)$$

$LtAtTop_{TimeStep}$ = Light limitation of phytoplankton and periphyton growth (unitless);
 $Lt_{TimeStep}$ = Photosynthetically Active Radiation (PAR) (ly/day); $LtSat$ = the calibration parameter of photosynthesis light saturation level (ly/day); and; $LtCorr$ = Daily time-step correction factor 1.0 for daily time-step and 1.25 for hourly. Light limitation is further related to total light extinction and calculated reduction at depth during daily photoperiods (U.S. EPA, 2009a).

AQUATOX 3.1 simulates the process of aerobic respiration in the absence of light for both periphyton and phytoplankton, resulting in the release of CO₂ and a small subsequent loss of biomass (Collins and Wlosinski, 1983), respiration is calculated by the equation:

$$\mathbf{Respiration} = \mathbf{Res20} * \mathbf{1.045}^{Temp-20} * \mathbf{Biomass} \quad (22)$$

Where: $Respiration$ = dark respiration rate (g/m³·day); $Res20$ = the calibrated parameter of phytoplankton or periphyton respiration at 20°C (g/g·day); $Temp$ = ambient water temperature, for (°C); and; $Biomass$ = phytoplankton (g/m³) or periphyton (g/m²) biomass.

Optimum temperature of phytoplankton and periphyton growth were also selected for calibration. A temperature correction factor is applied to the rate of photosynthesis for temperatures above and below an optimum temperature for phytoplankton and periphyton, where:

$$\mathbf{Tcorr} = \frac{\mathbf{(TMax+Acclimation)-Temp}}{\mathbf{(TMax+Acclimation)-(TOpt+Acclimation)}} \quad (23)$$

T_{corr} = correction factor applied to photosynthesis (unitless); T_{Max} = maximum temperature under which photosynthesis will occur ($^{\circ}\text{C}$); $Temp$ = ambient water temperature ($^{\circ}\text{C}$); $Acclimation$ = variable temperature acclimation, based on (Kitchell et al., 1972) ($^{\circ}\text{C}$); and; T_{Opt} = the calibrated parameter of photosynthesis optimum temperature ($^{\circ}\text{C}$);

The magnitude of flow velocities may also have a significant impact on the sloughing, or scouring, of periphyton by excessive force. The limitation of nutrients, light and temperature leads to the senescence of periphyton substrate binding cells. If the critical force of stream velocity exceeds the drag force of periphyton, sloughing occurs:

If: $DragForce > Suboptimal_{org} * FCrit_{org} * Adaptation$

then: $Slough = Biomass * FracSloughed$

else: $Slough = 0$ **(24)**

Where: $DragForce$ = flow force applied to periphyton biomass, based on (Asaeda and Son, 2000; U.S. EPA, 2009a); $Suboptimal_{org}$ = limitation of light, nutrients, and temperature effecting periphyton senescence (kg m/s^2); $FCrit_{org}$ = the calibrated parameter of force needed to scour periphyton (kg m/s^2); $Adaptation$ = adjustment factor to (Rosemond, 1993) (unitless); $Slough$ = periphyton biomass lost to sloughing (g/m^3); and; $FracSloughed$ = the percentage of biomass removed in a sloughing event (percent). The parameter $FCrit_{org}$ was calibrated for SFH River state variables of *Cladophora* and Diatoms.

6.2.2 ZOOPLANKTON CALIBRATION PARAMETERS

Two zooplankton groups of cladocerans and copepods were selected for simulation in the SFH Reservoir. Zooplankton variables were included to simulate phytoplankton predation. Zooplankton parameters selected for calibration included: optimum growth temperature, respiration rate, feeding half-saturation constant, maximum consumption rate, and minimum prey constraints for feeding. The parameter for optimum growth temperature ($^{\circ}\text{C}$) utilizes the same function of phytoplankton and periphyton optimum temperature correction (Eq. 23).

Zooplankton respiration is represented by a function of biomass and temperature influences, for the calculation of cladocerans and copepods basal respiratory loss:

$$\mathbf{StdResp_{pred} = BasalResp * TCorr * Biomass} \quad (25)$$

Where: $StdResp_{pred}$ = the basal respiratory loss, as a function of temperature ($\text{g}/\text{m}^3 \cdot \text{day}$); $BasalResp$ = the calibrated parameter of zooplankton respiration rate ($\text{g}/\text{g} \cdot \text{day}$); and; $TCorr$ = temperature correction function (Eq. 23) ($^{\circ}\text{C}$); $Biomass$ = zooplankton biomass (g/m^3);

Zooplankton consumption of phytoplankton is controlled by half-saturation feeding constant, represented by Monod equations similar to phytoplankton and periphyton P, N, and C half-saturation values (Eq. 18, 19, and 20), expressed in (gPhyto/m^3). Maximum consumption represents zooplankton maximum feeding rate ($\text{g}/\text{g} \cdot \text{day}$), and similarly a minimum amount of phytoplankton must be present before zooplankton feeding may proceed (g/m^3).

6.2.3 SEDIMENT DIAGENESIS CALIBRATION PARAMETERS

Sediment diagenesis is the modeled process of sediment nutrient flux, or the breakdown and conversion of OM to dissolved nutrients, and the release to the overlying water column (DiToro, 2001). Observations of sediment flux were not made in the 2009 SFH Reservoir report, therefore the calibration of sediment diagenesis parameters focuses on matching the hypolimnion concentrations of dissolved nutrients to the sediment flux. Sensitivity analysis was performed for the hypolimnion state variables of PO_4 , NO_x and NH_4 , resulting in the parameters of first-order decay rate of PON, freshwater reaction velocity of NH_4 and NO_3 , particulate phosphorous fractions of sediment layers 1 and 2, and theta pore water diffusion.

Critical to sediment flux, is the first-order decay rate of particulate organic matter (POM), which is partitioned into POP, POC, and PON fractions. The rate at which PON is mineralized into ammonia is controlled by the equation:

$$\mathbf{Mineralization}_{PON} = \mathbf{PON} * \mathbf{K}_{PON} * \boldsymbol{\theta}_{POM}^{Temp-20} \quad (26)$$

Where: $Mineralization_{PON}$ = the sediment bed decomposition of reactivity class of PON ($g/m^3 \cdot day$); PON = respective concentration in the sediment layer (g/m^3); K_{POM} = decay rate of PON (1/day); and; $\theta_{POM}^{Temp-20}$ = exponential temperature adjustment of decomposition (unitless).

The freshwater velocity of ammonia and nitrate, represent the mass rate (m/day) of transfer velocity between layers was also found to be sensitive and selected for calibration. Additionally, the process of nutrient diffusion between anaerobic and aerobic

layers was selected due to the highly sensitive relation to hypolimnion nutrient concentrations (Figure 18). The parameter, theta pore water diffusion coefficient (unitless), was also selected for calibration, as expressed in (Eq. 12).

Parameters selected for the calibration of phosphorous sediment flux included the K_dPO_4 1 and 2, or the partition coefficient of inorganic phosphorous in the aerobic layer one and anaerobic layer two. The parameter K_dPO_4 is used for the calculation of dissolved and particulate orthophosphorous:

$$f_{d\ PO_4, layer} = \frac{1}{1 + m_{layer} * K_{dPO_4}} \quad (27)$$

Where: $f_{d\ PO_4, layer}$ = the fraction of PO_4 in layer 1 or 2 (unitless); m_{layer} = layer solids concentration, user-input (kg/L); and; K_{dPO_4} = partition coefficient in layer (unitless).

6.3 AQUATOX 3.1 MODEL CALIBRATION AND VALIDATION

Calibration of the reservoir and river model state variables of phytoplankton, periphyton, zooplankton, and process of sediment diagenesis was facilitated by Monte Carlo simulation (random sampling of selected calibration parameters) assuming uniform parameter distributions. Uniform distributions were selected due to the inability to identify distributions of calibration parameter values, thus specifying equal likelihood of parameter values between specified ranges (Chapra, 1997). AQUATOX 3.1 performs Monte Carlo analysis by the Latin-hypercube based approach, with advantages of efficiently sampling all regions of distribution space resulting in fewer model iteration runs (McKay et al., 1979; Palisade Corporation, 1991). Monte Carlo simulations were limited to 100 iterations with each state variable simulated as an independent variable;

state variables include a maximum of seven parameters for random uniform sampling. Literature and model documentation recommendations of model parameter ranges were set as the minimum and maximum range for the generation of values sampled from uniform distributions. Monte Carlo analysis was therefore used as a simple way to explore parameter selections.

Monte Carlo results are saved as individual comma delimited output files for all iterations of randomly selected parameter sets. MATLAB was used to compile each iteration output file and to perform parameter estimation based on the objective function of normalized root mean squared error (NRMSE) and an additional objective function of Bias (BIAS), to avoid the inadequacies of using a single objective function (Diskin and Simon, 1977). The combination of two objective functions helped to minimize observed and simulated data error, and avoid bias with the calculations:

$$RMSE = \sqrt{\frac{1}{n} \sum_{i=1}^n (C_p - C_o)_i^2} \quad (28)$$

$$NRMSE = \frac{\sqrt{\frac{1}{n} \sum_{i=1}^n (C_p - C_o)_i^2}}{C_o_{max} - C_o_{min}} \quad (29)$$

$$BIAS = \frac{1}{n} \sum_{i=1}^n (C_{P_i} - C_{O_i}) \quad (30)$$

Where: n = sample number; i = the index of summation; C_p = predicted or modeled value; C_o = the observed value; and; C_o_{max}, min = the maximum and minimum observed values for normalization. NRMSE was selected over root mean squared error

(RMSE) due to the simultaneous calibration of state variables of both the epilimnion and hypolimnion layers, though RMSE was selected for calibration and validation goodness-of-fit results. An example of an objective function result for Monte Carlo simulations of cyanobacteria is presented in Figure 19.

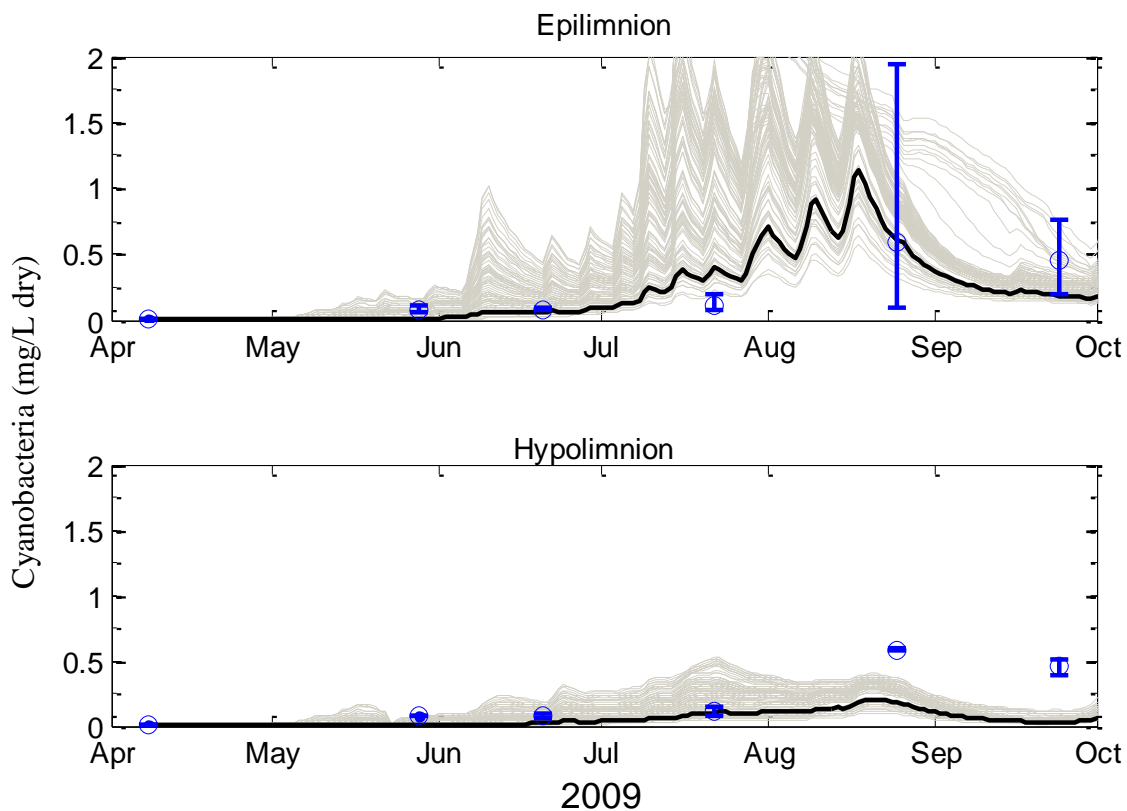


Figure 19. SFH Reservoir Monte Carlo calibration results for cyanobacteria. Circles indicate cyanobacteria observed biomass, with error bars representing the minimum and maximum observed values. Grey lines represent 100 Monte Carlo iterations, with the black line indicating the parameter set with the lowest RMSE and BIAS values.

6.3.1 RESERVOIR MODEL CALIBRATION RESULTS

The SFH reservoir model was calibrated for the period of April 4th to October 1st 2009, corresponding to the initial data collection phase of the SFH report (Fritsen, et al., 2011). The reservoir was modeled as a 1-d stacked stratifying system, with model inputs

of daily ambient epilimnion water temperature, radiation, and wind-speed collected for the observational period. Daily observations were not available for hypolimnion temperature, DO, pH, and dissolved nutrient loadings, though the model linearly interpolated between missing observed data points (U.S. EPA, 2009a). SFH reservoir samples of POC, collected from site SFR5 (Figure 2), were used as a surrogate for POC loadings to the reservoir.

Phytoplankton state variables of cyanobacteria, chlorophytes and diatoms were selected for reservoir simulation, based on taxa biovolume percentages being greater than 10 percent. Zooplankton state variables of cladocerans and copepods were included for their AQUATOX 3.1 specified trophic interaction of predation of cyanobacteria, diatom and chlorophyta phytoplankton variables. Simulations with and without zooplankton resulted in 5 to 20 percent difference in Chl-a at varying times in the simulation. Variables were also included to realistically simulate phytoplankton predation, in scenario loading simulations. The complete list of the SFH Reservoir model initial conditions are found in Appendix-B.

The SFH reservoir was calibrated for the state variables for dissolved nutrients (PO_4 , NO_x , and NH_4), SD, DO, phytoplankton (cyanobacteria, diatoms, and chlorophytes) and zooplankton (cladocerans and copepods). Calibration SFH reservoir state variables were approached in multiple iterative steps in the following order:

1. Phytoplankton calibration in order of highest to lowest biomass.
2. Epilimnion and hypolimnion dissolved nutrients, and DO calibration by the process of sediment diagenesis and reservoir nitrification rate.

3. Secchi Depth calibration.
4. Phytoplankton calibration in order of highest to lowest biomass.
5. Zooplankton calibration with phytoplankton as needed.

Phytoplankton growth and settling (death) was initially calibrated to be near observed conditions prior to the calibration of sediment diagenesis. Phytoplankton nutrient uptake had a significant effect on the calibration of other phytoplankton state variables, leading to the iterative calibration of phytoplankton from state variables highest biomass, of cyanobacteria, followed by diatoms and chlorophyta with the lowest respective biomass. Phytoplankton calibration consisted of multiple 100 iteration Monte Carlo simulations of the parameters: light saturation (1y/day), P half-saturation (mgP/L), optimum temperature ($^{\circ}\text{C}$), maximum photosynthesis (1/day), and respiration rate (g/g·day). Phytoplankton parameter uniform distribution boundaries were selected from literature (Table 7) and AQUATOX 3.1 default values.

Sediment diagenesis was calibrated by matching hypolimnion dissolved nutrient concentrations of PO_4 , NH_4 and NO_x for the calibration period and was followed by a recalibration of the phytoplankton and zooplankton variables. The results of parameter estimation for all reservoir model state variables can be found in Appendix-C.

Table 7. SFH Reservoir parameter estimation results for phytoplankton. Maximum and minimum values indicate initial literature ranges in uniform distribution for Monte Carlo random sampling. Additional parameters included for the phytoplankton state variables are left as default values.

Phyto. Parameters	<u>Cyanobacteria</u>		<u>Diatoms</u>		<u>Chlorophytes</u>	
	Value	Note	Value	Note	Value	Note
Lt Sat ly/day	218	Range: 36-306 (Whitton and Potts, 2000)	48.9	Range: 22.5-64 (Collins and Wlosinski, 1983; Hill, 1996)	103	Range: 50-110 (Collins and Wlosinski, 1983; U.S. EPA, 2009a)
P-Half Saturation mgP/L	0.019	Range: 0.006-0.03 (US EPA, 2009)	0.013	Range: 0.008-0.055 (Collins and Wlosinski, 1983; U.S. EPA, 2009a)	0.011	Range: 0.01-0.04 (Cercio and Cole, 1993)
Opt. Temp. °C	27.0	Default (Collins & Wlosinski, 1983)	20.0	Default (Collins and Wlosinski, 1983)	19.28	Range: 17-27.0 (Collins and Wlosinski, 1983)
Pmax 1/day	1.525	Range: 0.6-3.5 (Komatsu et al., 2006; U.S. EPA, 2009a)	0.652	Range: 0.6-3.5 (Komatsu, Fukushima, & Shiraishi, 2006; USEPA, 2009)	1.780	Range: 1.5-2.29 (Collins and Wlosinski, 1983; U.S. EPA, 2009a)
Resp. Rate 20°C g/g·day	0.004	Range: 0.003-.2 (US EPA, 2009) (Cercio and Cole, 1993)	0.061	Range: 0.01-0.08 (Collins and Wlosinski, 1983; Oklahoma Department of Environmental Quality, 1996)	0.4	Range: 0.1 to 0.5 (U.S. EPA, 2009a)

Calibration period goodness-of-fit results were assessed by RMSE and BIAS values of six reservoir observations in 2009 vs. model simulation results. All simulated state variables, with the exception of TN, DO and Chl-a (Table 8), had relative low RMSE values. BIAS values indicate an over-prediction bias of the epilimnion and hypolimnion values of PO₄, NH₄, NO_x, and TP, though bias of the hypolimnion nutrients were reduced. However, the high levels of BIAS NO_x and NH₄ are associated with the state variables with the lowest average observed concentrations. Graphical results indicate a simulated state variable within or near minimum and maximum observed values of the reservoir with the exception of TN (Figures 20-33). It is important to note that calibration focused upon accurately simulating dissolved nutrients in the reservoir due to the interest in also simulating downstream periphyton growth. The lack of

agreement between simulated and observed TN values is a result of model assumptions which cannot be changed by the user.

Table 8. Reservoir calibration goodness-of-fit for the epilimnion (Epil) and hypolimnion (Hypo).

SFH Reservoir State Variables	RMSE		BIAS	
	Epil	Hypo	Epil	Hypo
DO mgO ₂ /L	1.460	1.576	1.260	1.437
SD m	1.346	-	-0.699	-
PO ₄ mgP/L	0.025	0.094	-0.025	0.072
NH ₄ mgN/L	0.027	0.044	-0.024	-0.009
NO _x mgN/L	0.019	0.031	-0.016	0.015
TP mgP/L	0.020	0.318	-0.018	-0.006
TN mgN/L	0.361	0.035	0.346	0.310
Chl-a µg/L	2.521	1.963	1.583	0.901
Cyanobacteria mg/L dry	0.108	0.126	0.012	0.041
Diatoms mg/L dry	0.020	0.015	-0.004	-0.003
Chlorophytes mg/L dry	0.032	0.012	0.028	0.011
Cladocerans mg/L dry	0.024	-	-0.004	-
Copepods mg/L dry	0.018	-	0.017	-

The simulated volume of the SFH reservoir was near the observed values of the reservoir (Figure 20). Maximum simulated volume occurred earlier than observed and reservoir volume was overestimated from August to October. The simulation drift of modeled and observed volume, from August to October, is likely related to the use of a constant rate of evaporation which is an imposed model assumption.

Simulated DO values in the epilimnion and hypolimnion generally fell within the minimum and maximum values for observed samples (Figure 21). The observed depletion of the hypolimnion DO matched well with simulated values, though an observed rise in hypolimnion DO concentrations that were measured in September were not matched.

Secchi Disk observed values matched well throughout the observational period with a RMSE of 1.346 meters (Figure 22), though the simulation was typically within error bars of +/- 1 meter. Model simulations of dissolved nutrients fell between minimum and maximum observed values (Figure 23-25). An observed spike in NO_x concentration was not matched within the hypolimnion layer.

Total Phosphorous RMSE matched well for both the hypolimnion and epilimnion with respective values of 0.021 and 0.035 mgP/L (Figure 26). Total Nitrogen values were poorly matched (Figure 27), with RMSE layer values near 0.3 mgN/L for both layers. TN results are likely due to the inability to specify reservoir TN initial conditions due to April reservoir TN samples not reported in (Fritsen, et al., 2011). Also, the calculation of TN is the summation of all nitrogen within suspended and dissolved detritus and phytoplankton. Even with the adjustment of parameters controlling the fraction of particulate nitrogen, values were two orders of magnitude greater than reference values, and still unable to maintain TN levels. Data for dissolved organic matter and sediment was not available, and POC was used as a surrogate for suspended sediment, thus resulting in the inability to match TN values.

Chl-a and individual phytoplankton taxa compared well with observed data (Figures 28-31), and zooplankton simulations of cladocerans (Figure 32), and Copepods (Figure 33) fell close to observed data points. Zooplankton error bars were not calculable, though biomass generally fell within 20 percent of observed values.

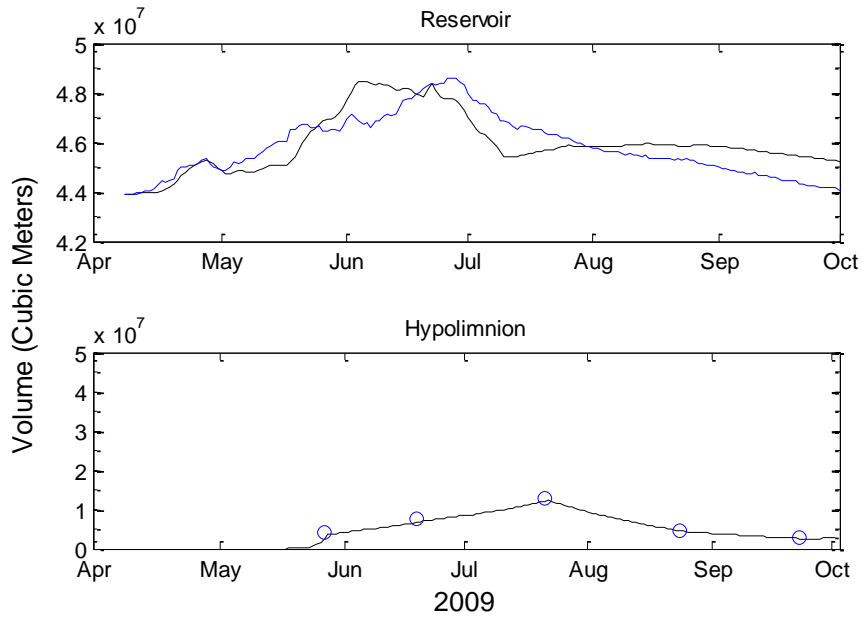


Figure 20. Volume calibration results for the SFH Reservoir. Black line is the simulated reservoir volume model results, blue line represents observed reservoir volume, and blue circles represent observed hypolimnion volumes.

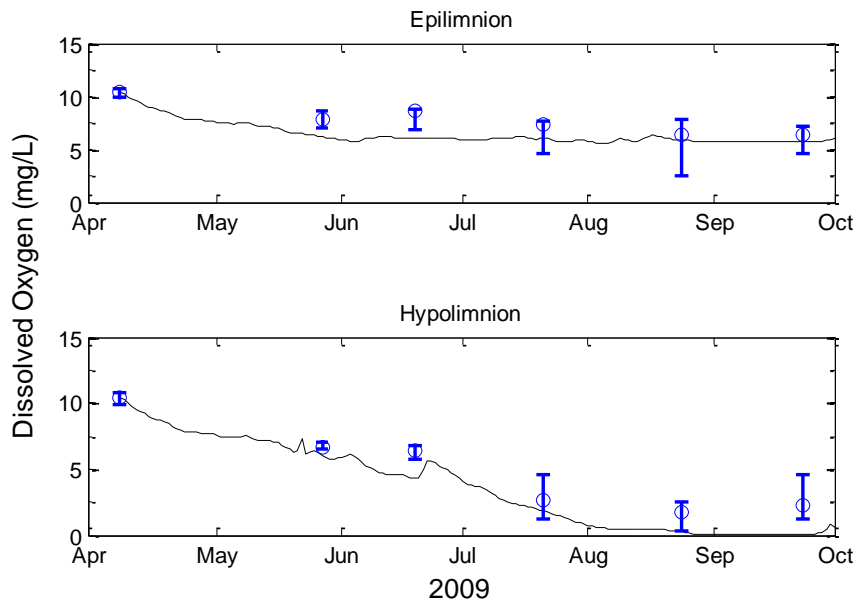


Figure 21. Dissolved Oxygen calibration results for the SFH Reservoir. Black line is the simulated model results, blue circles represent observed layer arithmetic means, and error bars indicate minimum and maximum observed values.

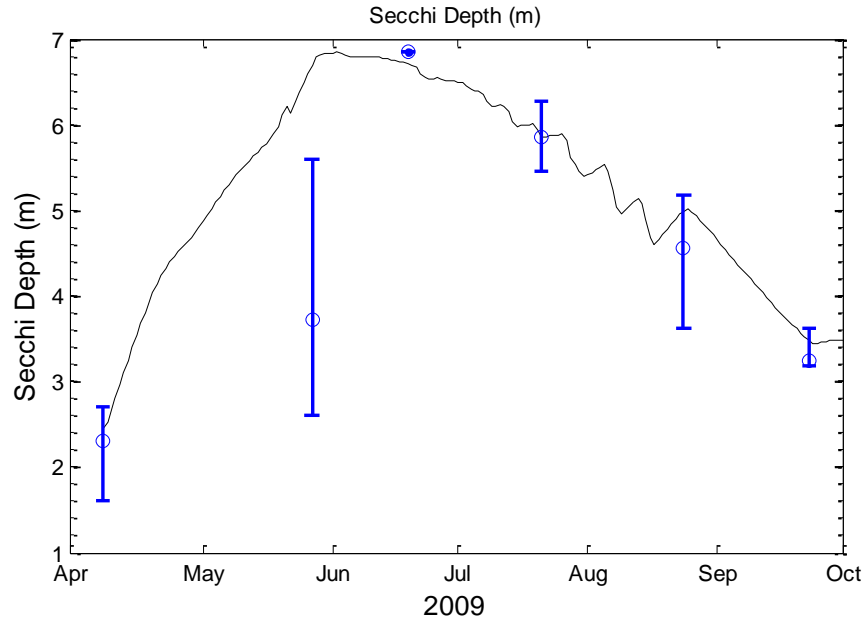


Figure 22. Results of reservoir calibration for SD. Black line is the simulated model results, blue circles represent observed arithmetic means, and error bars indicate minimum and maximum observed values.

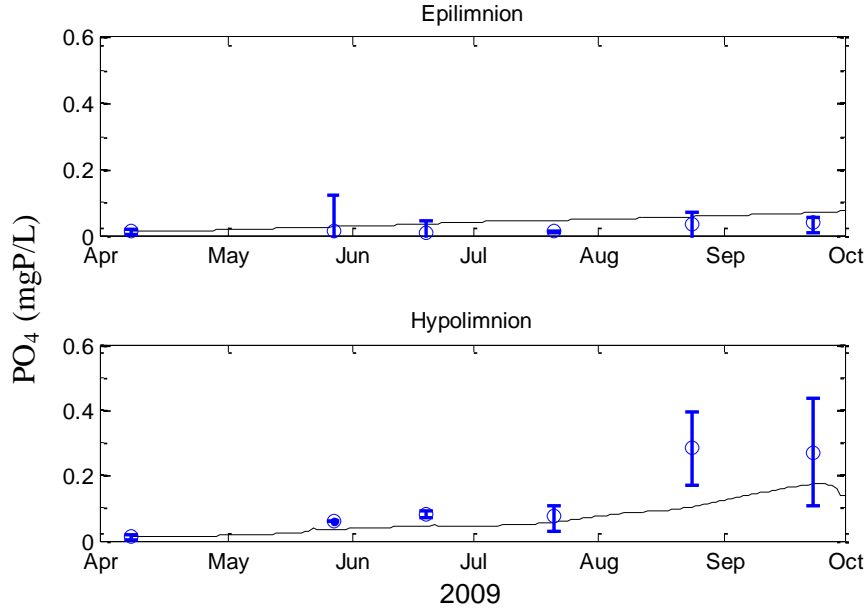


Figure 23. Results of reservoir calibration for PO₄. Black line is the simulated model results, blue circles represent arithmetic means, and error bars indicate minimum and maximum observed values.

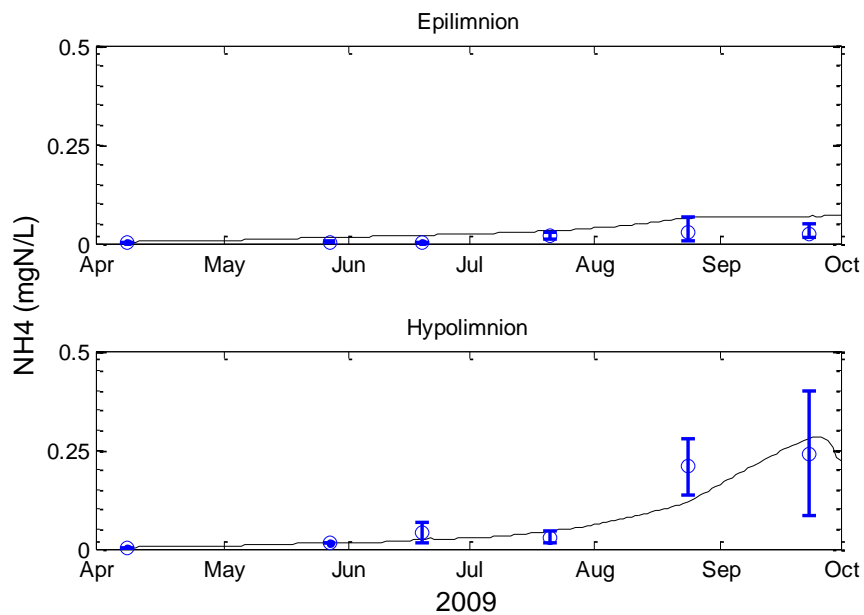


Figure 24. Results of reservoir calibration for NH_4 . Black line is the simulated model results, blue circles represent arithmetic means, and error bars indicate minimum and maximum observed values.

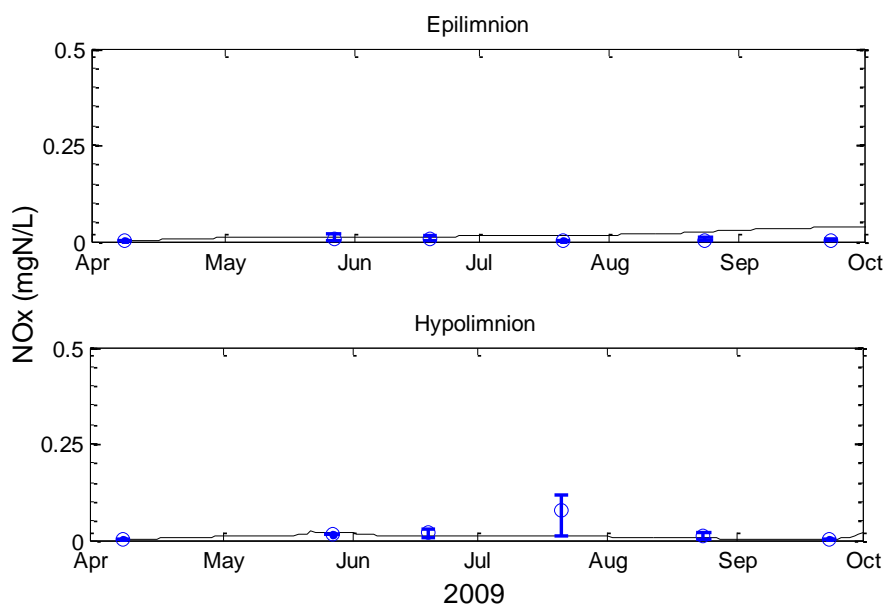


Figure 25. Results of reservoir calibration for NO_x . Black line is the simulated model results, blue circles represent arithmetic means, and error bars indicate minimum and maximum observed values.

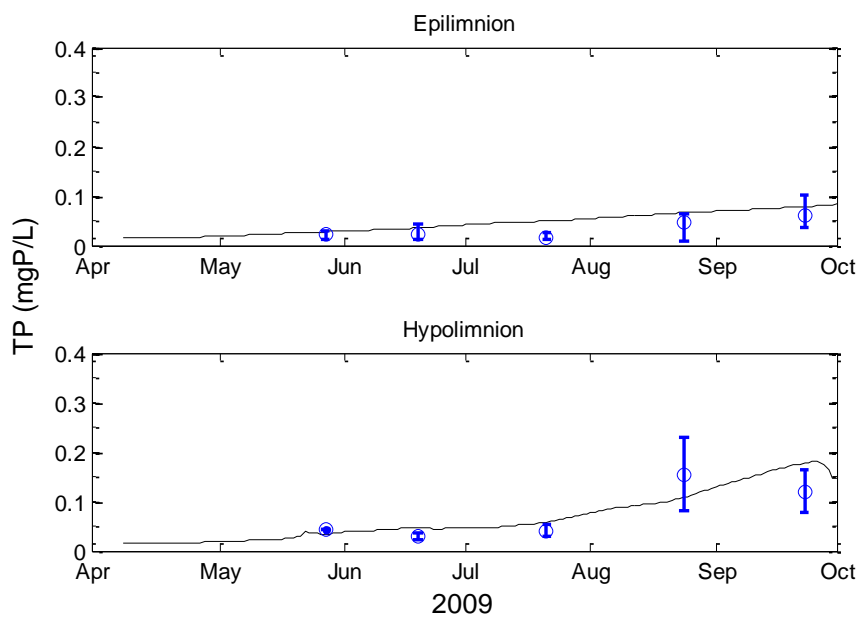


Figure 26. Results of reservoir calibration for TP. Black line is the simulated model results, blue circles represent arithmetic means, and error bars indicate minimum and maximum observed values.

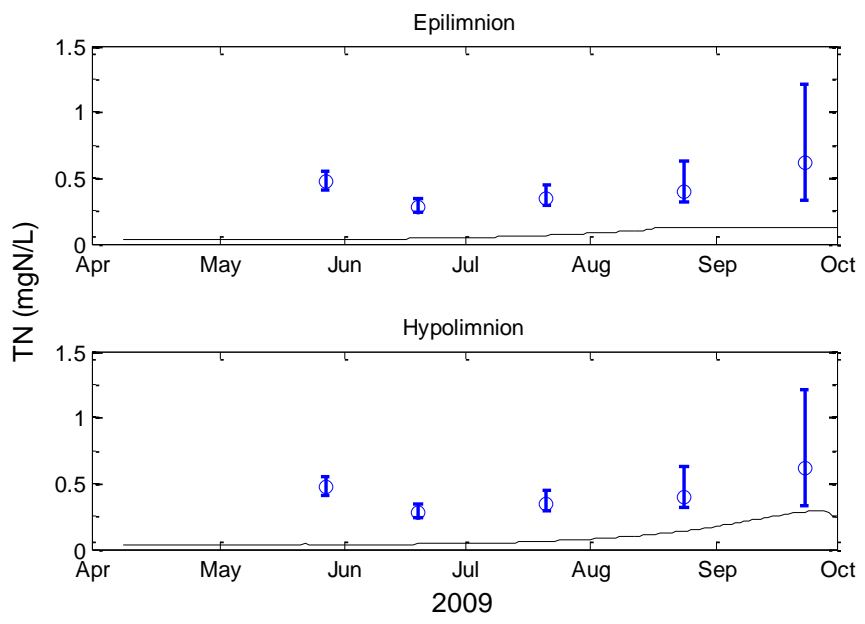


Figure 27. Results of reservoir calibration simulations for TN. Black line is the simulated model results, blue circles represent arithmetic means, and error bars indicate minimum and maximum observed values.

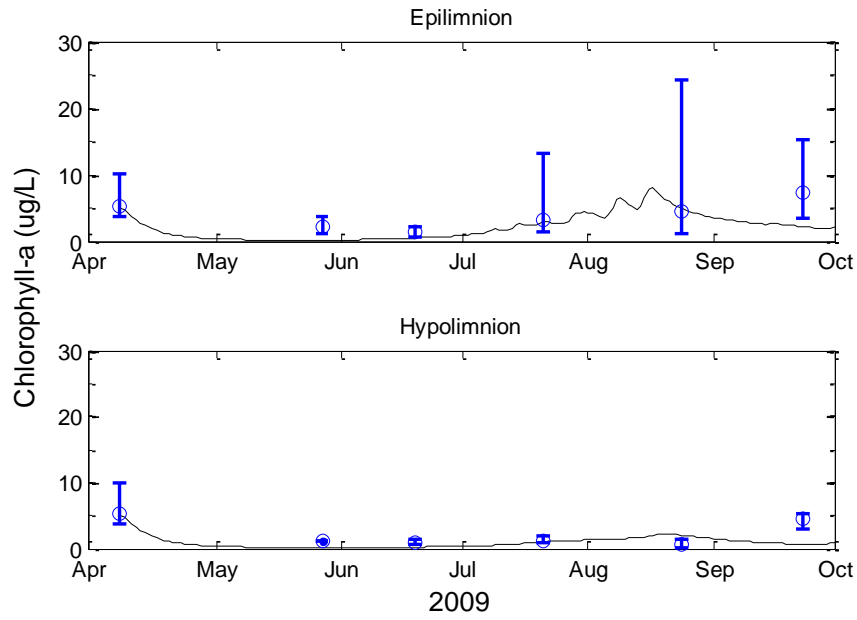


Figure 28. Results of calibration simulations for Chl-a. Black line is the simulated model results, blue circles represent arithmetic means, and error bars indicate minimum and maximum observed values.

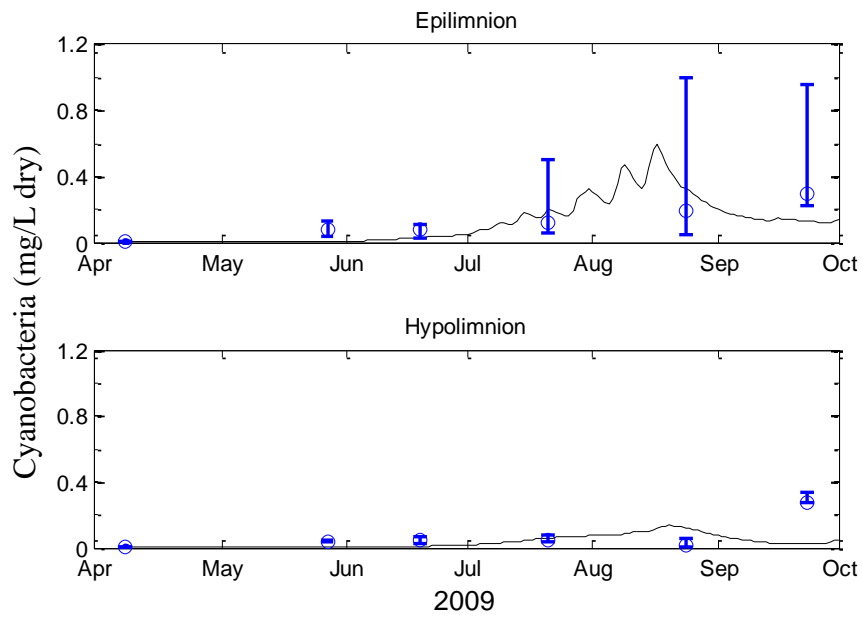


Figure 29. Results of calibration simulations for cyanobacteria. Black line is the simulated model results, blue circles represent arithmetic means, and error bars indicate minimum and maximum observed values.

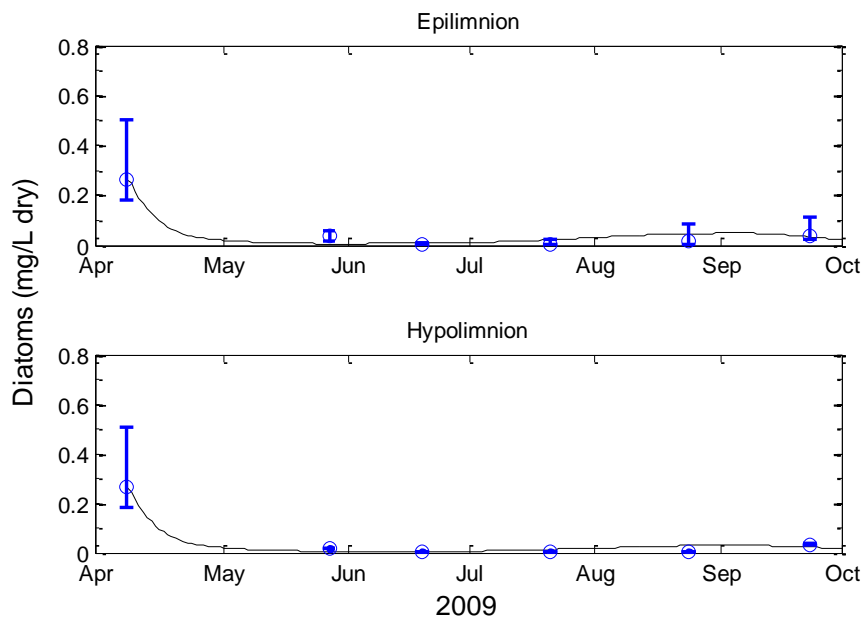


Figure 30. Results of calibration simulations for diatoms. Black line is the simulated model results, blue circles represent arithmetic means, and error bars indicate minimum and maximum observed values.

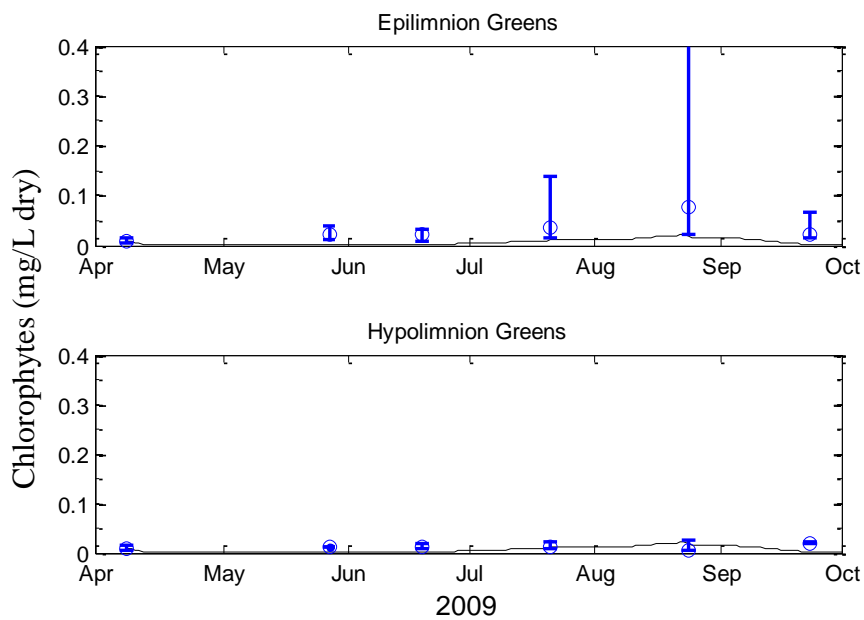


Figure 31. Results of calibration simulations for chlorophytes. Black line is the simulated model results, blue circles represent arithmetic means, and error bars indicate minimum and maximum observed values.

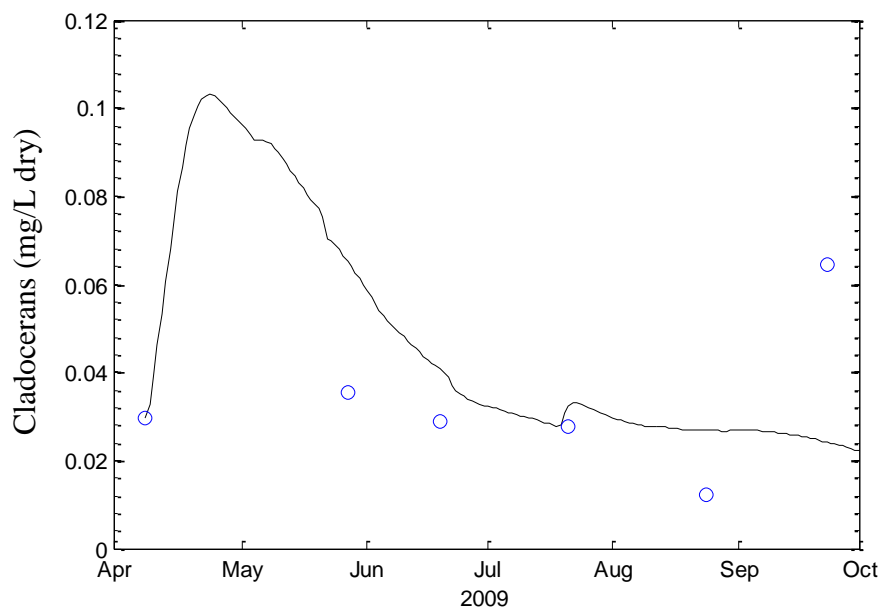


Figure 32. Results of calibration simulations for Cladocerans. Black line is the simulated model results, blue circles represent the reservoir arithmetic mean values.

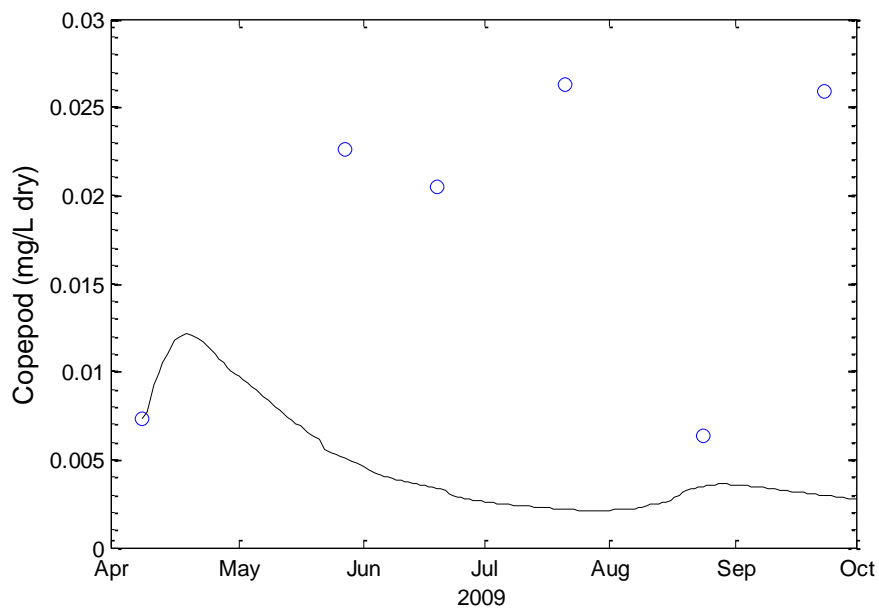


Figure 33. Results of calibration simulations for Copepod. Black line is the simulated model results, blue circles represent arithmetic mean values.

6.3.2 RESERVOIR MODEL VALIDATION RESULTS

Data collected from June to August of 2010 served as validation data for the SFH Reservoir model. Reservoir data including dissolved nutrients loadings were not collect from August of 2009 to June of 2010, and were linearly interpolated over the period without data. Loading values of POC were interpolated for the validation period based on 2009 surrogate results of TSS and POC. Temperatures were not observed throughout the winter of 2009-2010, though ice cover did occur. SFH Reservoir temperatures were simulated at 4°C, representing ice cover in AQUATOX 3.1 (U.S. EPA, 2009a) from December 20th, 2010, to January 31st. Phytoplankton and zooplankton identification and biovolume enumeration were not completed during the validation period, creating a lack of testing for individual state variables. Validation data was kept separate from calibration data, and the results were not analyzed until the completed of calibration parameter estimation.

Validation results were assessed by RMSE and BIAS values for simulated model results vs. four reservoir observations in 2010. RMSE values were comparable to levels achieved during calibration, with slightly higher values for Chl-a and SD. Additionally, BIAS values were generally lower than those of the calibration period. These agreements help support the application of simulation parameter values derived by calibration. Additionally, validation data was not analyzed though the reservoir calibration process. Goodness-of-fit results were assessed only after calibration was complete.

Table 9. Reservoir model validation goodness-of-fit for the epilimnion (Epil) and hypolimnion (Hypo).

SFH Reservoir State Variables	RMSE		BIAS	
	Epil	Hypo	Epil	Hypo
DO mgO ₂ /L	0.867	1.522	0.511	0.408
SD m	1.71	-	-0.167	-
PO ₄ mgP/L	0.027	0.037	-0.026	-0.021
NH ₄ mgN/L	0.032	0.043	-0.019	0.021
NO _x mgN/L	0.019	0.080	0.001	0.057
TP mgP/L	0.033	0.037	0.384	-0.015
TN mgN/L	0.384	0.517	-0.031	0.516
Chl-a µg/L	3.336	-	-2.123	-

Validation data generally fit well with observed data in 2010. Dissolved Oxygen values followed a similar trend observed in 2009 with stratification and depletion of the hypolimnion in later summer months (Figure 34). Secchi Depth initially over predicted visibility, which is likely due to a lack of sediment loadings for the simulation (Figure 35). The simulation predicted observations fairly well once loading conditions of 2010 were applied in the model. Values of Chl-a had a similar problem matching values in June of 2010, though the model did predict the maximum and final Chl-a value (Figure 36). Dissolved nutrients simulations match observed values well (Figures 37-39), except for spikes of NO_x in the hypolimnion occurring in August of 2010. Simulations of TP match observed values throughout 2010, though samples of TN were significantly lower than observed values.

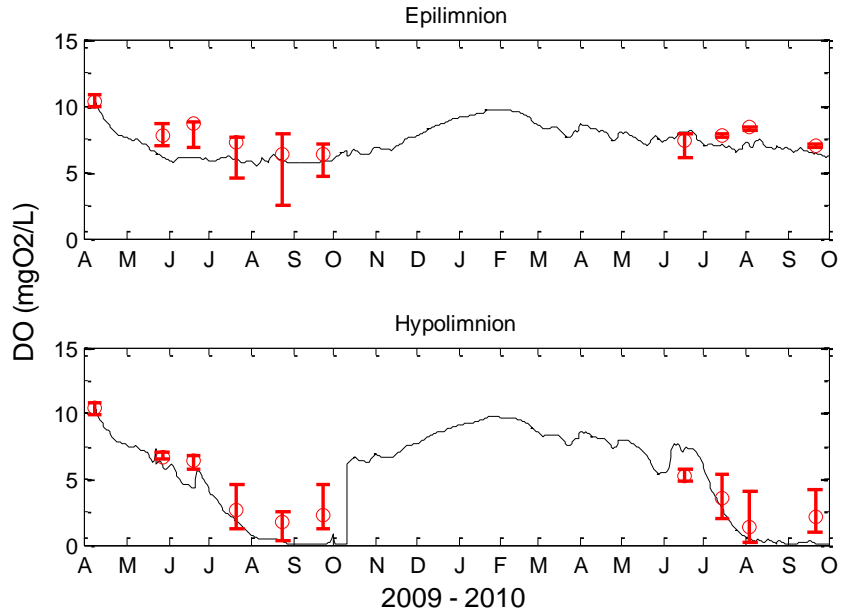


Figure 34. DO calibration (2009) and validation (2010) results for the SFH Reservoir. Black line is the simulated reservoir volume model results, red line represents observed reservoir volume, and red error bars represent minimum and maximum observed values.

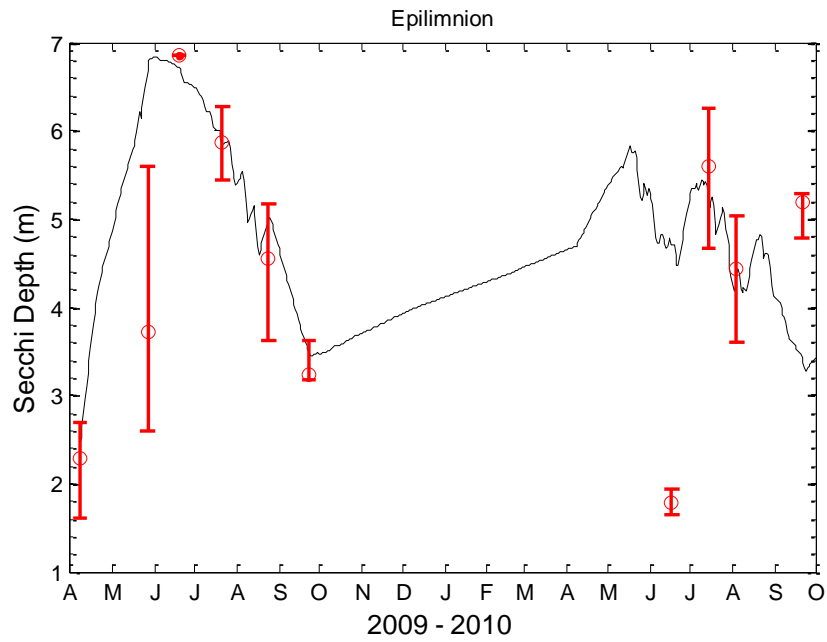


Figure 35. Secchi Depth calibration (2009) and validation (2010) results for the SFH Reservoir. Black line is the simulated SD model results, red line represents observed SD values, and red error bars represent minimum and maximum values.

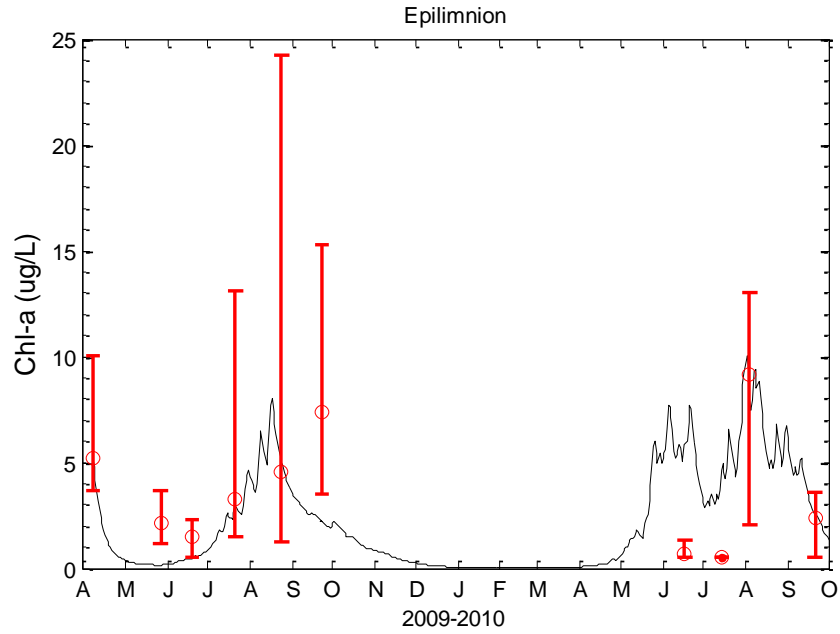


Figure 36. Chl-a calibration (2009) and validation (2010) results for the SFH Reservoir. Black line is the simulated Chl-a model results, red circle represents observed Chl-a values, and red error bars represent minimum and maximum.

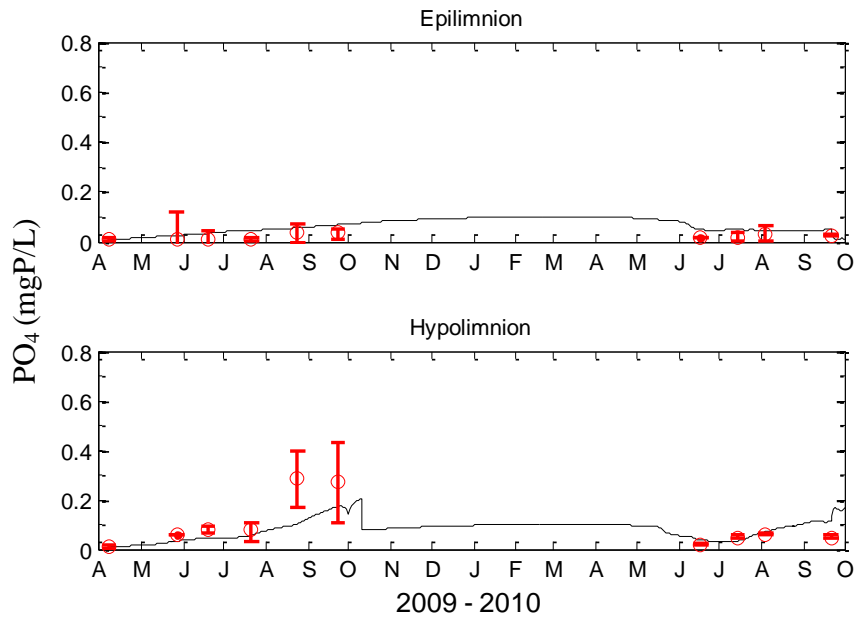


Figure 37. PO₄ calibration (2009) and validation (2010) results for the SFH Reservoir. Black line is the simulated PO₄ model results, red circle represents observed Chl-a, and red error bars represent minimum and maximum.

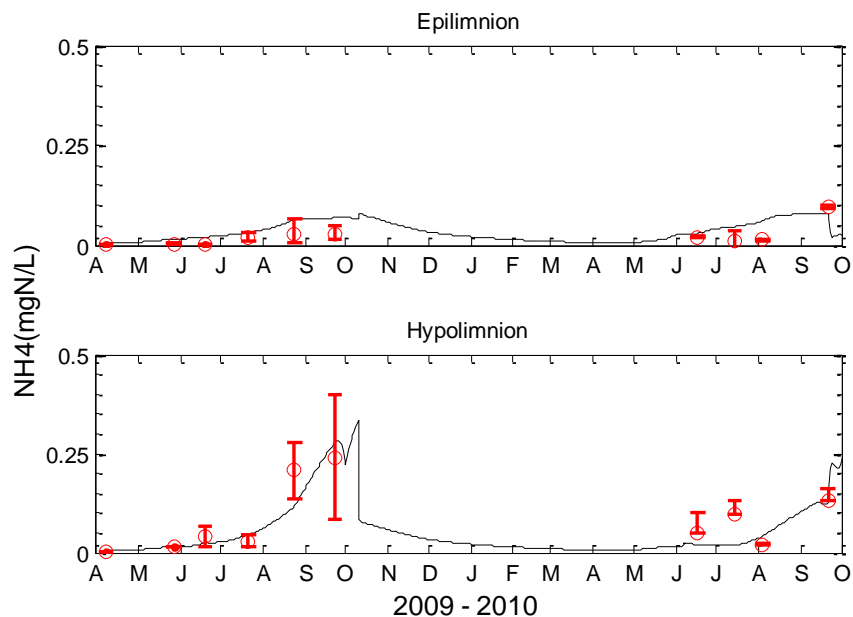


Figure 38. NH_4 calibration (2009) and validation (2010) results for the SFH Reservoir. Black line is the simulated NH_4 model results, red circle represents observed NH_4 , and red error bars represent minimum and maximum.

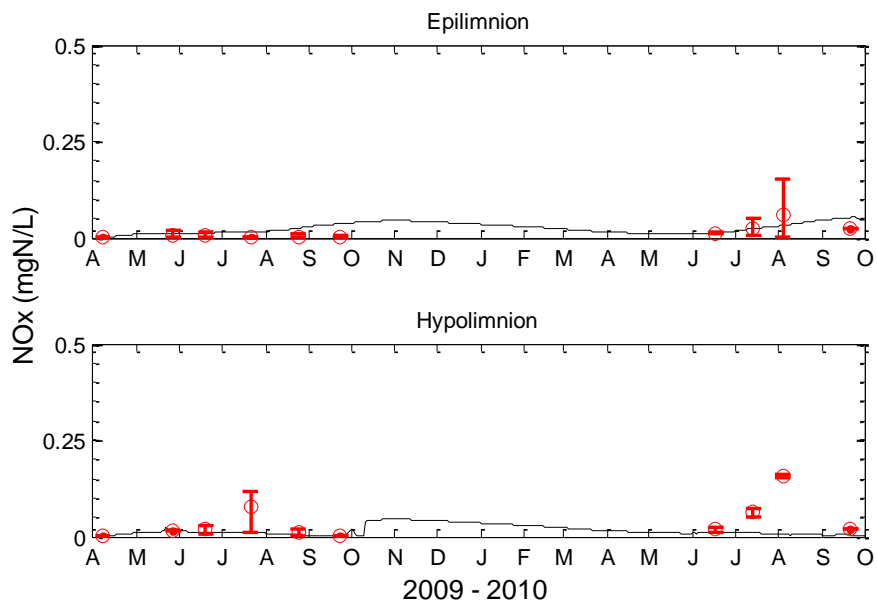


Figure 39. NO_x calibration (2009) and validation (2010) results for the SFH Reservoir. Black line is the simulated NO_x model results, red circle represents observed NO_x , and red error bars represent minimum and maximum.

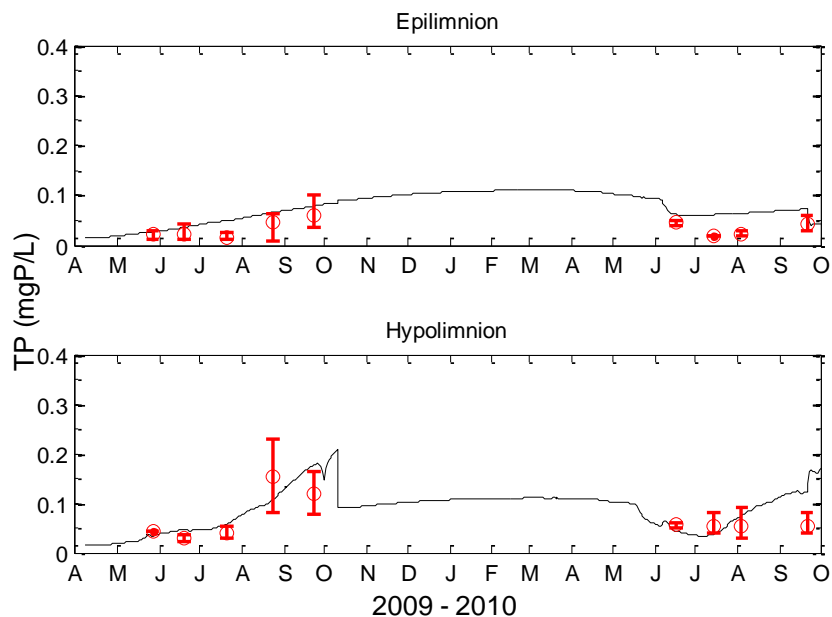


Figure 40. TP calibration (2009) and validation (2010) results for the SFH Reservoir. Black line is the simulated TP model results, red circle represents observed TP, and red error bars represent minimum and maximum.

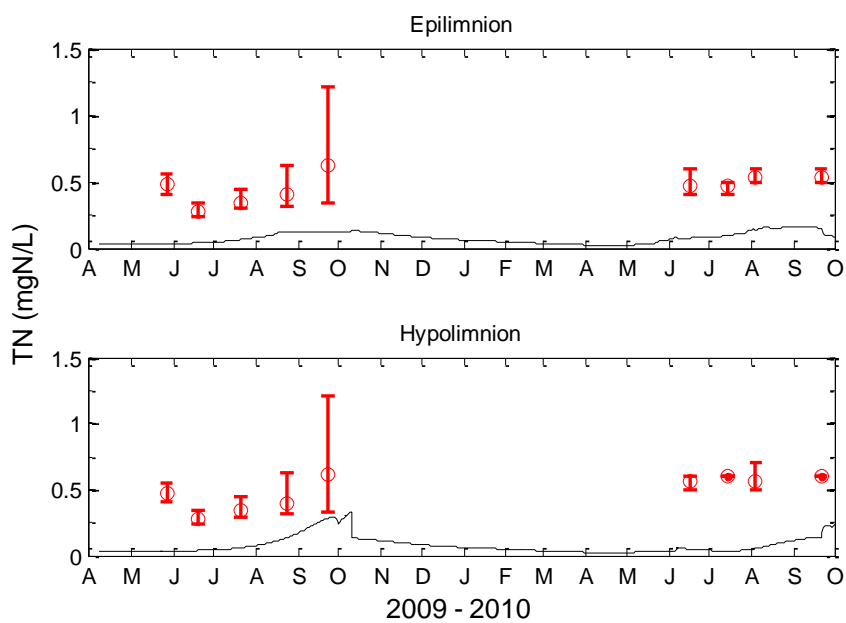


Figure 41. TN calibration (2009) and validation (2010) results for the SFH Reservoir. Black line is the simulated TN model results, red circle represents observed TN, and red error bars represent minimum and maximum.

6.3.3 RIVER MODEL CALIBRATION RESULTS

The SFH river model was calibrated for the period of June 12th to October 1st 2009, corresponding to three periphyton and five water quality collections by (Davis, et al., 2011). The objective for the SFH river simulation was for the calibrated reservoir model outflows to represent loadings, or boundary conditions, for river tail-water dissolved nutrients (PO_4 , NH_4 , and NO_x), temperature, detritus/suspend sediment, and phytoplankton loadings. DO boundary conditions were assumed to be at atmospheric saturation, due to dam outlet design and operator communication (Perry, 2007). The simulation step-time was set as hourly for diel DO simulations. Physical characteristics including reach riffle and run percentages were collected in (Davis, et al., 2011).

The 1-D river model reach is 1.25 km in length, extending from the reservoir outlet with the 80 meter periphyton sampling area located in the centroid of the reach. Periphyton variables selected for simulation included *Cladophora*, modeled as an individual taxa included within AQUATOX 3.1, and the general taxonomic group of diatoms. Cyanobacteria was not simulated within the river model due to the low percentage of biovolume (<5 percent of periphyton biovolume). Initial conditions and physical characteristics of the SFH river model can be found in Appendix-B.

Following the calibration and validation of the SFH Reservoir model, the river model calibration was approached by the following method:

1. Calibrate Manning's roughness coefficient to match observed flow velocities
2. Calibrate of *Cladophora* and diatoms to match observed biomass and Chl-a.

3. Calibration of the parameter Pmax simultaneously for *Cladophora* and diatoms to match observed biomass and Chl-a.

The physical attribute of stream velocity was initially calibrated due the importance of scouring of periphyton during high velocities. Initial AQUATOX 3.1 recommendations for natural cobble stream conditions corresponded to a Manning's roughness value of 0.040 , resulting in values of stream velocity more than double the observed values. Random sampling was used with a Monte Carlo uniform range of 0.04 to 0.112 , a value representing severely sluggish stream flow due to periphyton (Boman et al., 2002). The result was a calibrated Manning roughness value of 0.088 for the SFH River simulations.

Calibration of the SHR river periphyton biomass was challenging due to the high rate of growth and physical influence of scouring. The parameter of light saturation had significant influence on the rate of photosynthesis, with AQUATOX 3.1 default and literature values resulting in the maximum rate of photosynthesis being achieved before noon in the simulation. This is likely due to the high values of irradiance associated with the Nevada's Great Basin Desert, the shallow stream depth (average simulation depth of 0.34 meters), and the low turbidity of the SFH reservoir hypolimnion outflows (Davis, et al., 2011). Calibration of saturating light parameter resulted in a value of 2000 ly/day, the highest observed radiation for the Elko, NV region. The high value of light saturation is supported by studies documenting linear response to high values of irradiance (Hornberger et al., 1976; Kelly et al., 1974).

Cladophora and diatom sloughing parameters of force-critical (newtons) and slough percent removed were initially calibrated. Following the calibration of sloughing values, C half-saturation (mgC/L), optimum temperature (°C), Pmax (1/day), and respiration rate (g/g·day) were selected for Monte Carlo analysis to simulate observed periphyton biomass. The final calibration of periphyton state variables was highly iterative, with Monte Carlo simulations of *Cladophora* and diatom parameter Pmax to obtain a simultaneous fit for biomass. Final periphyton parameter values were selected from literature values (Table 7) and AQUATOX 3.1 default values when possible.

Table 10. SFH River parameter estimation results for periphyton. Maximum and minimum values indicate initial literature ranges in uniform distribution for Monte Carlo random sampling. Additional parameters included for the periphyton state variables are left as default values.

Periphyton Parameters	<i>Cladophora</i>		Diatoms	
	Value	Note	Value	Note
Lt Sat (ly/day)	~2000	No Saturation (Dodds et al., 1999)	~2000	No Saturation (Dodds, et al., 1999)
C Half-Saturation (mgC/L)	0.01	Range: 0.054 - 0.008 (Collins and Wlosinski, 1983)	0.054	Default (U.S. EPA, 2009a)
Opt. Temp. (°C)	17	Range: 13 - 17 (Auer et al., 1982)	12	Range: 20 (Collins and Wlosinski, 1983)
Pmax (1/day)	3.24	Range: 1 - 4.6 (Auer, et al., 1982; U.S. EPA, 2009a)	2.815	Range: 1 - 3.2 (U.S. EPA, 2009a)
Resp Rate 20°C (g/g·day)	0.06	Range: 0.01 - 1.2 (Collins and Wlosinski, 1983)	0.1	Default = 0.08 (Collins and Wlosinski, 1983)
Force-Crit. (Newtons)	0.086	Default = 0.001 (No Lit. Range) (U.S. EPA, 2009b)	0.013	Default = 0.002 (No Lit. Range) (U.S. EPA, 2009b)
Slough Percent Removed. (percent)	0.5	Default = 1.04 (No Lit. Range) (U.S. EPA, 2009a)	0.01	Default = 3.75 (No Lit. Range) (U.S. EPA, 2009a)

SFH River calibration period goodness-of-fit results were assessed by RMSE and BIAS values for five water quality and three periphyton observations in 2009. RMSE values were low for dissolved nutrients that were modeled boundary conditions from the SFH reservoir model. DO values of RMSE, 0.725 mgO₂/L, were low even with the assumption of DO boundary conditions modeled at saturation, and the influence of the model reporting the mean value of all constituents within the 1.25 km model reach length (Figure 43 and Figure 44). Simulation trends generally fell within the maximum and minimum mean standard error bars of dissolved nutrients (Figures 45, 46, 47). BIAS values were low for all variables for the calibration period Benthic Chl-a, *Cladophora* and diatoms RMSE and Bias values were moderately high due to high concentration unit values (Figure 48, 49, and 50). RMSE of Benthic Chl-a represents roughly 12 percent of observed biomass levels with the simulation matching the general trend of periphyton biomass well.

Table 11. River model calibration goodness-of-fit results.

River Model Calibration Results	RMSE	BIAS
State Variable	River	River
Flow cm/s	5.866	-5.716
DO mgO ₂ /L	0.725	-0.036
PO ₄ mgP/L	0.012	-0.001
NH ₄ mgN/L	0.032	0.020
NO _x mgN/L	0.026	0.021
Benthic Chl-a mg/m ²	86.080	9.325
<i>Cladophora</i> mg/L dry	16.092	2.119
Diatoms mg/L dry	3.029	-3.001

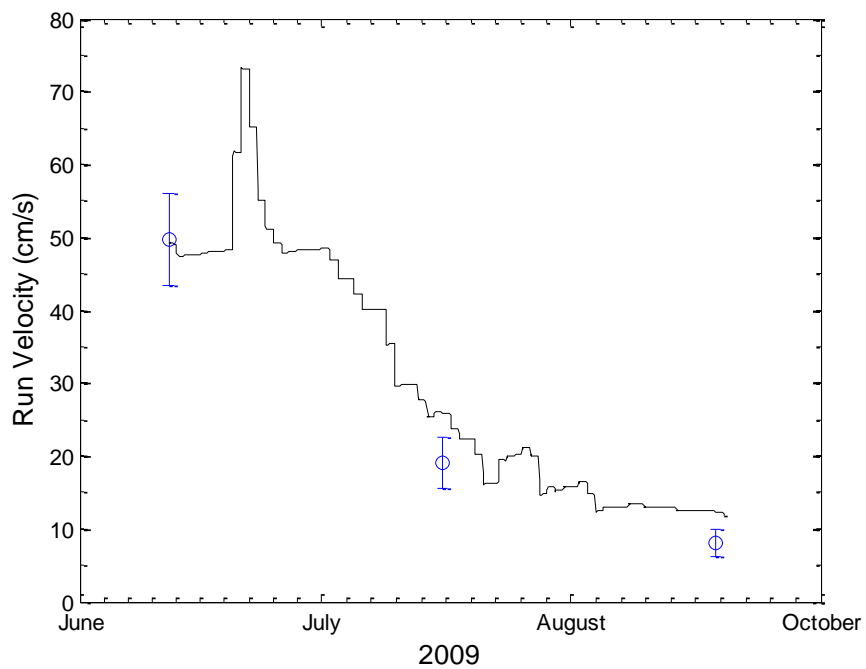


Figure 42. Results of river calibration simulations for run velocity. Blue circles represent the observed arithmetic mean, and error bars represent the observed mean standard error.

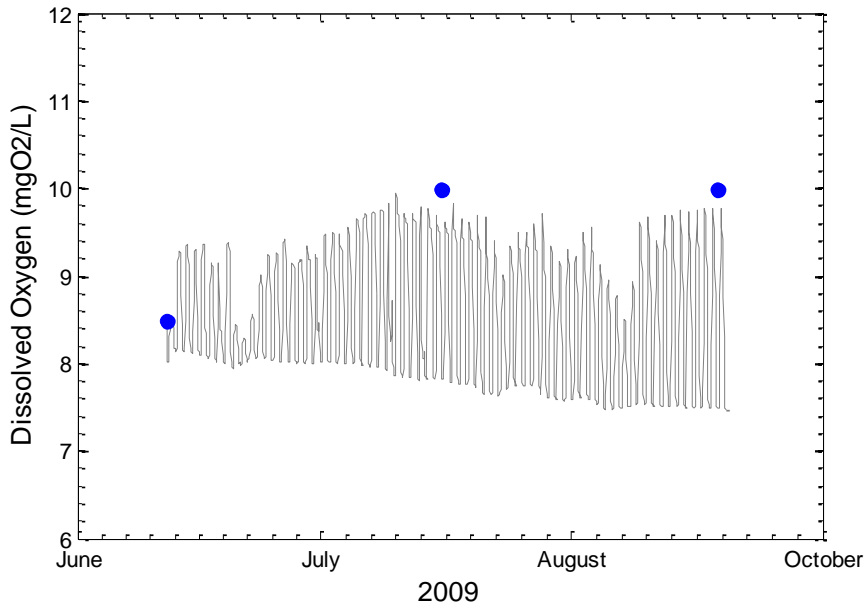


Figure 43. Results of river calibration simulations for DO. Blue circles represent the discrete DO observations from a Hydrolab Sonde.

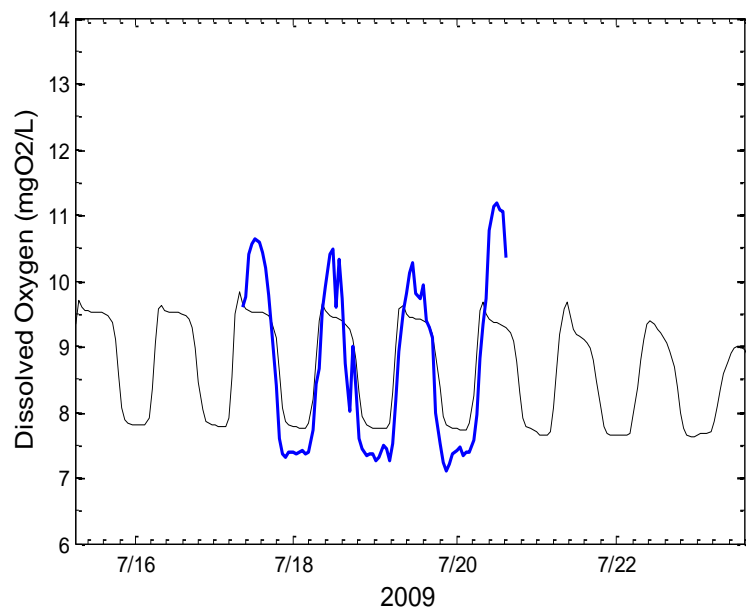


Figure 44. Results of river calibration simulations for diel DO. Blue line represents continuously observed DO values from YSI sonde deployment.

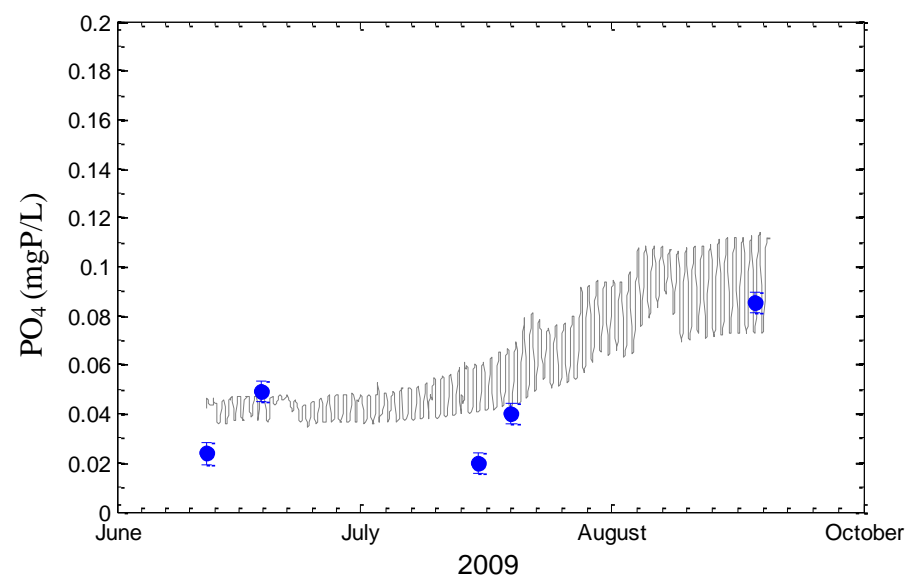


Figure 45. Results of river calibration simulations for PO₄. Blue circles represent the observed arithmetic mean, and error bars represent the observed mean standard error.

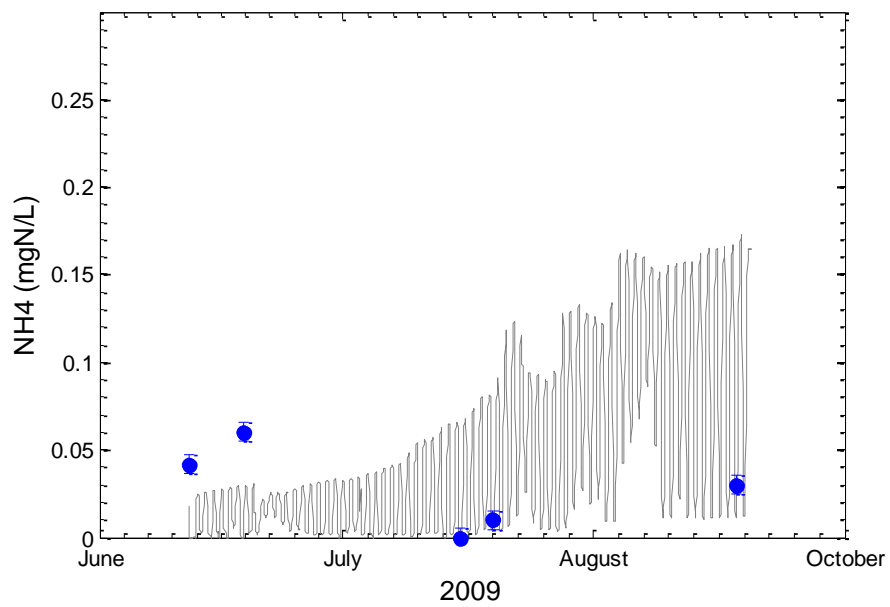


Figure 46. Results of river calibration simulations for NH_4 . Blue circles represent the observed arithmetic mean, and error bars represent the observed mean standard error.

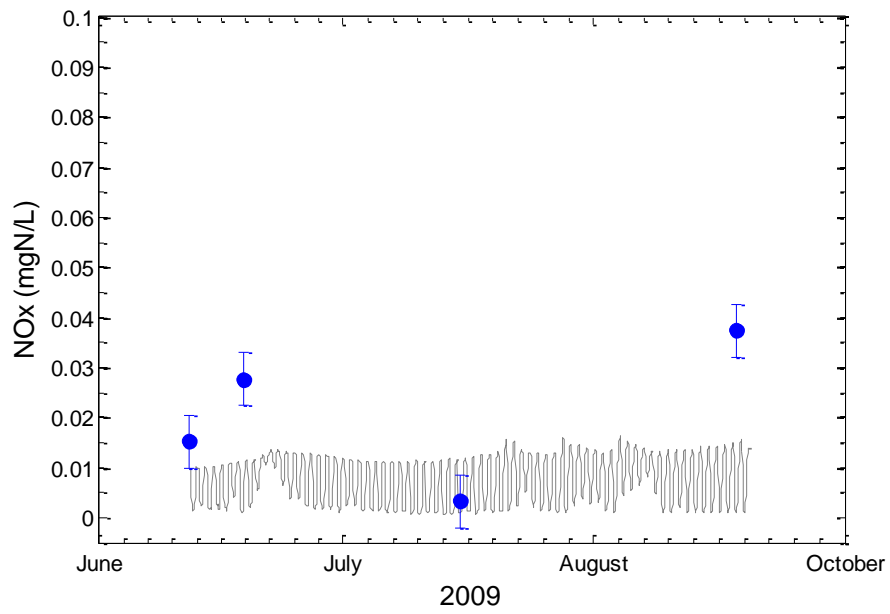


Figure 47. NO_x calibration results for the SFH River simulation. Blue circles represent the observed arithmetic mean, and error bars represent the observed mean standard error.

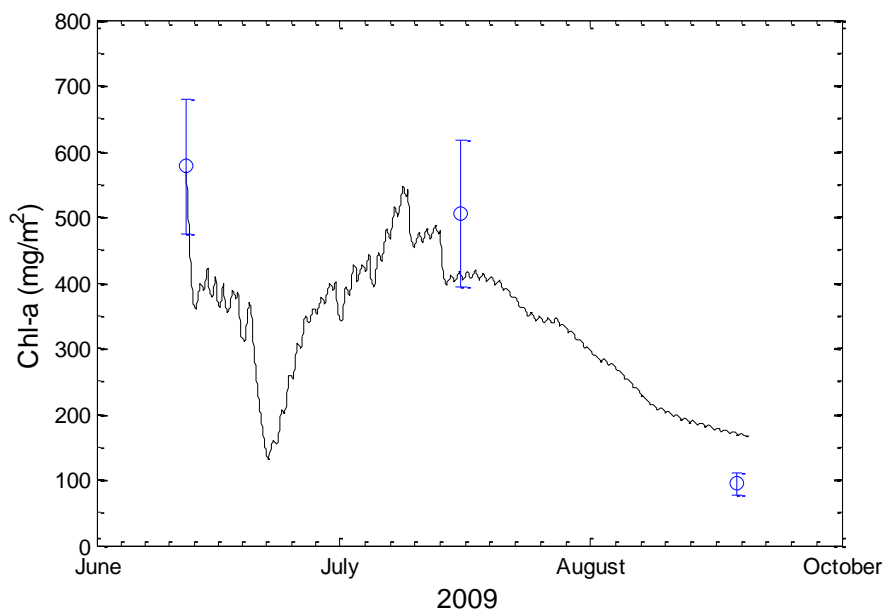


Figure 48. Chl-a calibration results for the SFH River simulation. Blue circles represent the observed arithmetic mean, and error bars represent the observed mean standard error.

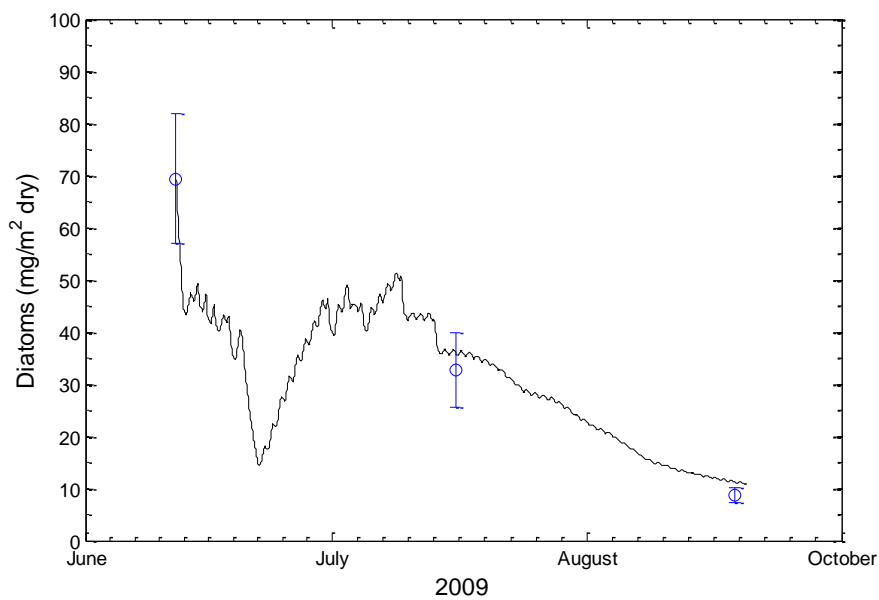


Figure 49. Periphyton diatoms calibration results for the SFH River simulation. Blue circles represent the observed arithmetic mean, and error bars represent the observed mean standard error.

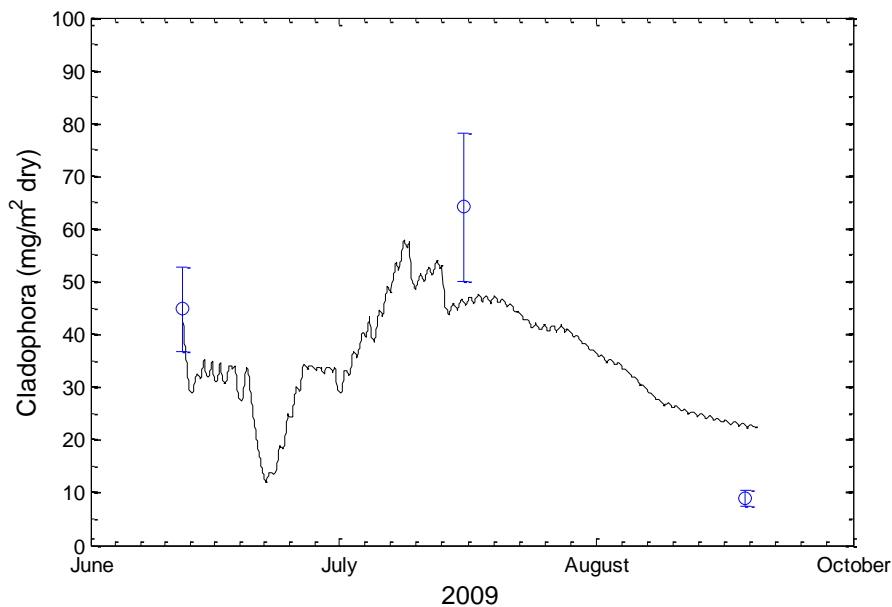


Figure 50. *Cladophora* calibration results for the SFH River simulation. Blue circles represent the observed arithmetic mean, and error bars represent the observed mean standard error.

6.3.4 RIVER MODEL VALIDATION RESULTS

SFH river validation data was collected from June to August of 2010, representing observations from location 0.75 km downstream. Model boundary conditions were delivered from SFH reservoir model outflows, except DO, which was assumed to be at atmospheric saturation. Calibration and validation of the SFH river model were kept separate with river simulation goodness-of-fit only examined after final calibration.

Validation results were assessed by RMSE and BIAS values for simulated model results versus observations in the SFH River during 2010. DO values had a low RMSE value of 0.720 mgO₂/L and a low BIAS value of -0.160 (Figure 52). Dissolved nutrients had higher RMSE errors with the highest associated with the lowest concentrations for

NO_x NH₄ (Figure 53, 54, and 55). RSME evaluation was not appropriate for benthic Chl-a due to the collection of only one periphyton sample, though the simulation match observed values exceptionally well (Figure 56).

Table 12. SFH River model validation goodness-of-fit results.

River Model Validation Results		RMSE	BIAS
State Variable	River	River	River
DO mgO ₂ /L		0.720	-0.160
PO ₄ mgP/L		0.032	-0.025
NH ₄ mgN/L		0.082	-0.012
NO _x mgN/L		0.090	0.078
Benthic Chl-a mg/m ²		-	22.30

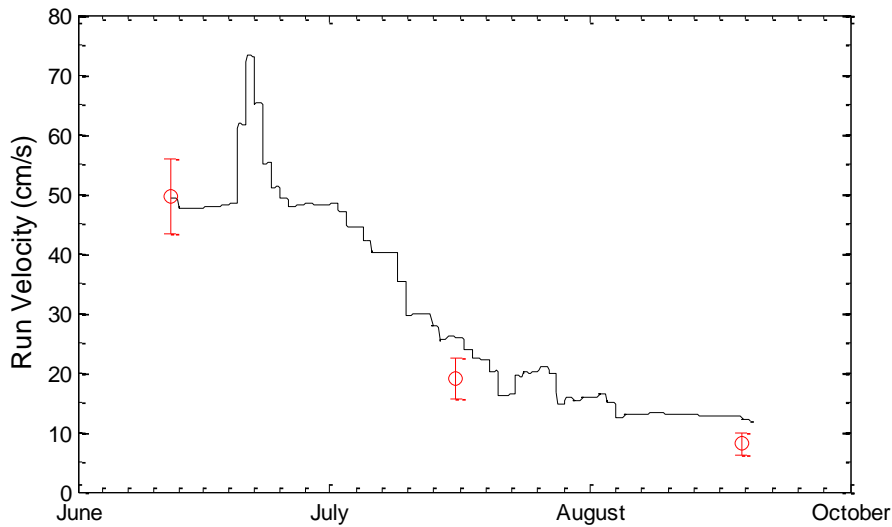


Figure 51. Flow velocity Validation results for the SFH River. Black line is the simulated flow model results, , and red error bars represent the mean standard error of observed values.

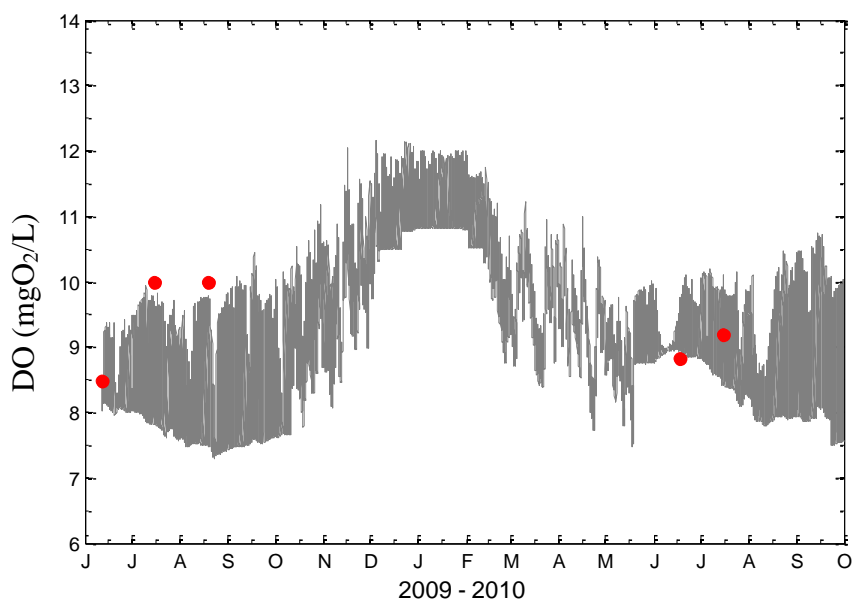


Figure 52. DO calibration (2009) and validation (2010) results for the SFH River. Grey line is the simulated river DO, red circles represent observed river DO values.

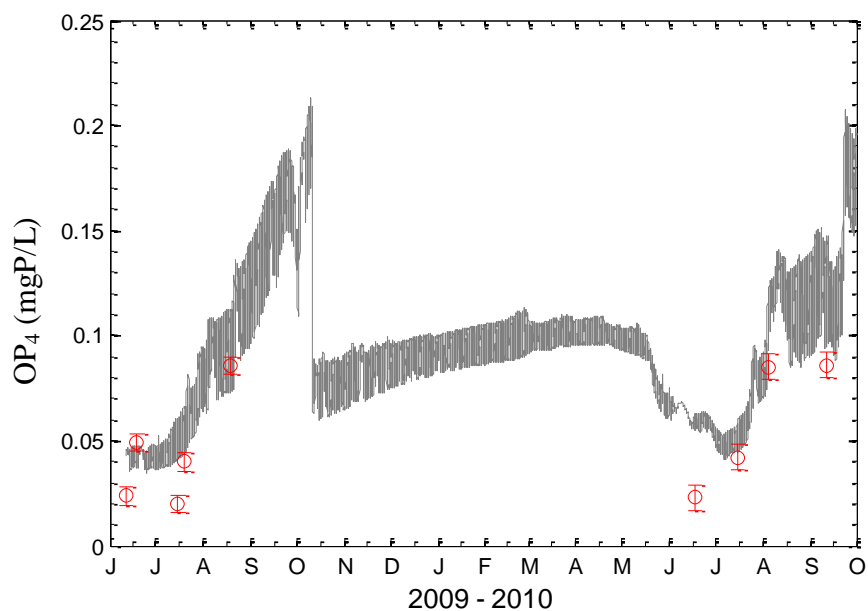


Figure 53. PO₄ calibration (2009) and validation (2010) results for the SFH River. Grey line is the simulated river model results, red circle represents observed PO₄ values, and red error bars represent the mean standard error of observed samples.

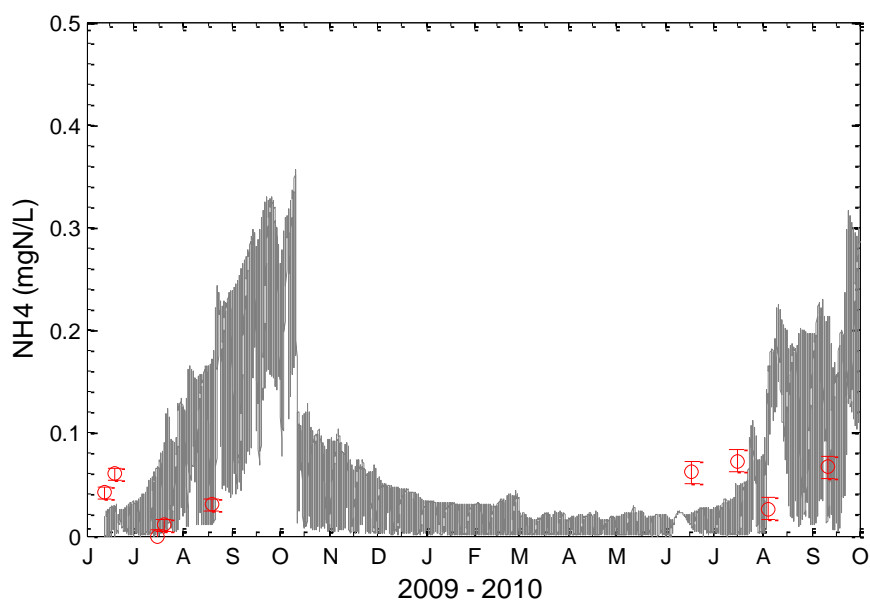


Figure 54. NH_4 calibration (2009) and validation (2010) results for the SFH River. Grey line is the simulated river model results, red circle represents observed NH_4 values, and red error bars represent the mean standard error of observed samples.

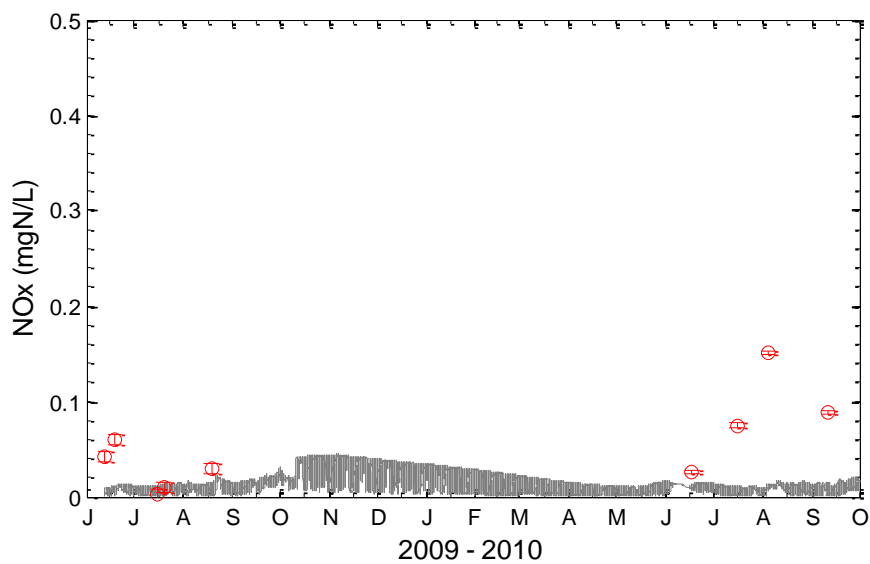


Figure 55. NO_x calibration (2009) and validation (2010) results for the SFH River. Grey line is the simulated river model results, red circle represents observed NH_4 values, and red error bars represent the mean standard error of observed samples.

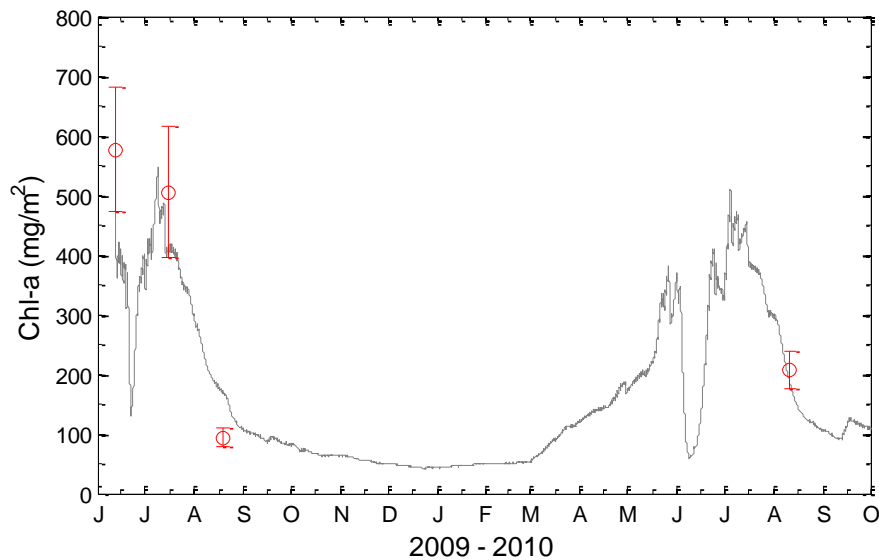


Figure 56. Benthic Chl-a calibration (2009) and validation (2010) results for the SFH River. Grey line is the simulated river model results, red circle represents observed Chl-a values, and red error bars represent the mean standard error of observed samples.

7. NUTRIENT LOADING SCENARIOS

Following the calibration and validation of both the SFH Reservoir and River models, loading scenarios were investigated to help determine possible coupled system responses due to changes in nutrient loadings. Selecting scenarios of reductions and additions requires consideration as to how nutrients and sediment loadings covary with respect to hypothetical changes. The nutrient multiplier method of (Carleton, et al., 2009) was applied to the SFH simulations by examining 10 percent reductions and additions of phosphorus and the subsequent covariance of nitrogen and sediment with the scenario changes.

The covariance of nutrients with respect to phosphorous, was calculated by regressing historical water quality observations with phosphorous, nitrogen, and TSS

(Steven Heiskary and Markus, 2001; S. Heiskary and Markus, 2003). Critical SFH river observations of dissolved nutrients were not available for regression analysis. Therefore a NDEP dataset of over 45 observations, of TP, TN, and TSS was utilized. Total nutrient variables were used as a surrogate for PO_4 and NH_4 percent multipliers that were unavailable from the NDEP dataset. In the case of NO_x , a high detection limit of 0.1 mgN/L prevented regression analysis. Regression relationships resulted in a moderate linear fit of TP verses TN data and a poor fit of TP verses TSS, with an r^2 statistic of 0.66 and 0.28 respectively (Figures 57 and 58). One data point of the TN:TP regression represents a clear outlier, though there is no defensible reason to remove the data point. The TN:TP regression with the outlying data point removed results in the regression of $1.9859x + 0.2713$, with an r^2 value of 0.306. AQUATOX 3.1 includes a multiplier parameter (a unitless multiplier, where 0 is equal to no loadings, and 1 being 100% of observed loads) for nutrient and sediment state variables, applying a percent changes to loading variables. Regression results were applied to 10% changes reductions and additions of PO_4 for scenario covariance of NH_4 , NO_x , TSS, and suspended detritus (Table 13).

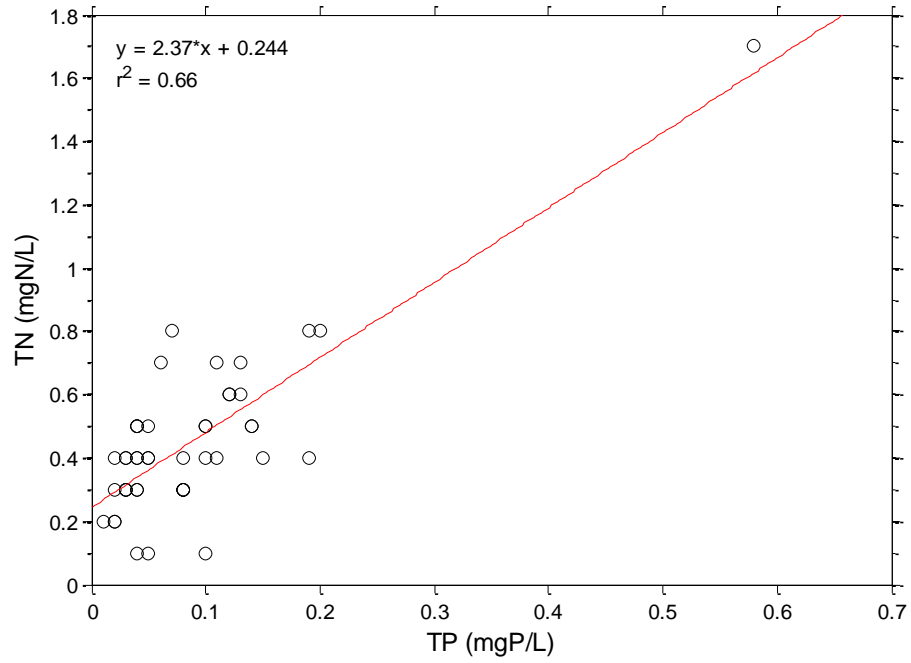


Figure 57. TP vs. TN regression analysis for nutrient multiplier covariance. Black circles represent NDEP observed nutrient samples, and red line is the linear regression of the dataset.

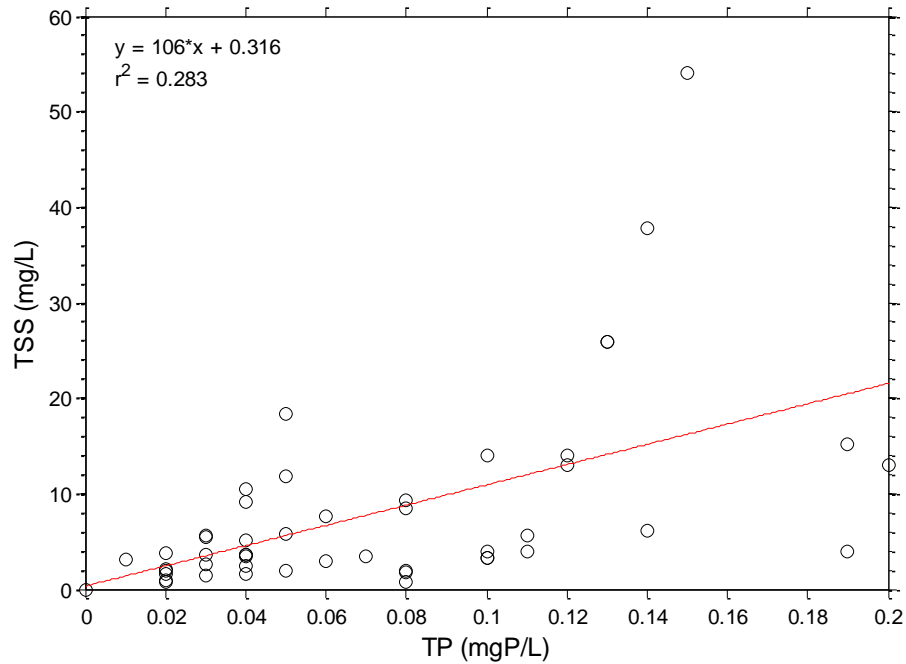


Figure 58. TP vs. TSS regression analysis for nutrient multiplier covariance. Black circles represent NDEP observed nutrient samples, and red line is the linear regression of the dataset.

Loading multipliers were simulated for 20 reservoir scenarios for the SFH system, keeping solar radiation, flow, temperature, wind speed, and stratification dynamics constant (Appendix-E). SFR Reservoir scenario outflow results were used as the boundary conditions for an additional 20 River simulations. Thus, the combined scenarios assessed the downstream periphyton growth. Results of scenarios are displayed with the relationship to lake trophic state values (Carlson and Simpson, 1996) and to EPA nutrient criteria reference conditions for ecoregion 13 (Table 1).

Table 13. Scenario loading multipliers for dissolved nutrients, TSS, and OM loadings. “Observed” represents the calibrated SFH Reservoir model observed nutrient loadings.

TP Percent Reduction/Additions	PO₄ Multiplier	NH₄ + NO_x Multipliers	TSS + OM Multipliers
100%	2.00	1.912	1.909
90%	1.90	1.821	1.818
80%	1.80	1.729	1.727
70%	1.70	1.638	1.636
60%	1.60	1.547	1.545
50%	1.50	1.456	1.454
40%	1.40	1.365	1.364
30%	1.30	1.274	1.273
20%	1.20	1.182	1.182
10%	1.10	1.091	1.091
Simulated 2009	1.00	1.000	1.000
-10%	0.90	0.909	0.909
-20%	0.80	0.818	0.818
-30%	0.70	0.726	0.727
-40%	0.60	0.635	0.636
-50%	0.50	0.544	0.546
-60%	0.40	0.453	0.455
-70%	0.30	0.362	0.364
-80%	0.20	0.271	0.273
-90%	0.10	0.179	0.182

Scenario results for the SFH Reservoir model were analyzed for the EPA nutrient criteria constituents of TP, SD, and Chl-a. EPA recommendations are based on mean growing season concentrations (U.S EPA, 2001). Due to the inability to simulate TN with acceptable accuracy, TN results were not analyzed. Concentrations and ranges of TP change linearly as specified by the constant scenario loadings of PO_4 by +/- 10% (Appendix-E, Figure 66). Boxplots of load scenarios (Figure 59, 60, and 61) represent the temporal variability of model results for the epilimnion, indicating ranges of nutrient criteria variables associated with individual scenarios. The loading scenario outcomes for TP show that the EPA reference condition mean growing season value of 0.03 mgP/L was only achievable by -90% reduction scenarios.

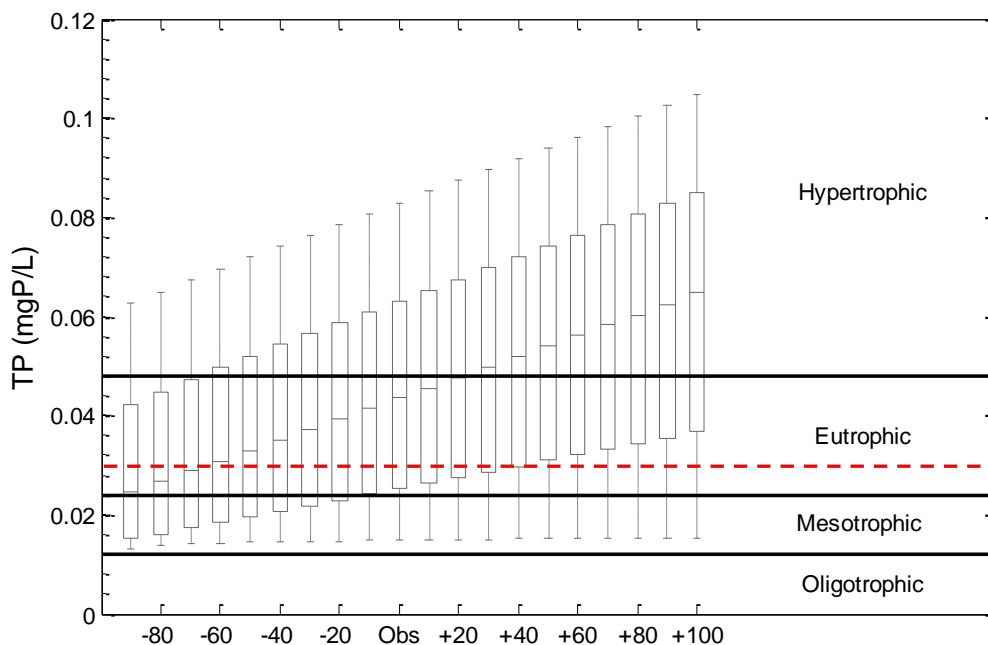


Figure 59. TP scenario loading results for April 7th to Oct. 1st 2009. Boxplots center line is median, outer box represents the 25th and 75th percentiles, and whiskers are 1.5 times the Inter Quartile Range (IQR). Lake TP trophic level boundaries based on (Carlson and Simpson, 1996). Red dashed line indicates EPA reference condition of 0.030 mgP/L for the Great Basin and Range Ecoregion (U.S. EPA, 2001).

Secchi Depth displayed a non-linear response to nutrient reduction and additions (Figure 59). The SD EPA target condition of 2.4 meters was exceeded by all reduction scenarios. The minimum scenario mean growing season SD value was 3.2 meters for the +100% scenario.

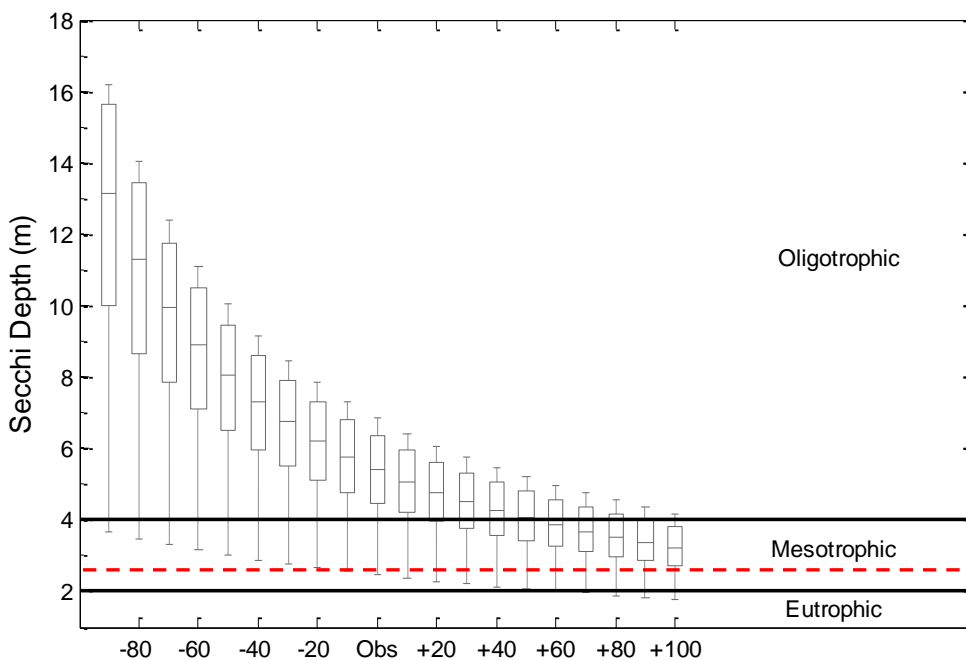


Figure 60. SD scenario loading results for April 7th to Oct. 1st 2009. Boxplots center line is median, outer box represents the 25th and 75th percentiles, and whiskers are highest data points within 1.5 times the Inter Quartile Range (IQR). Trophic level boundaries are based on (Carlson and Simpson, 1996). Red dashed line indicates EPA reference condition of 2.3 meters for the Great Basin and Range Ecoregion (U.S. EPA, 2001).

Model scenario results for Chl-a indicate a direct relationship of increased scenario loadings and Chl-a outliers (Figure 61). EPA Chl-a reference conditions of 1.9 $\mu\text{g/L}$ were achieved for scenario reductions of -40 to -90 percent from 2009 observational dataset. Results of the SFH Reservoir model mean summer values are found in Table 14. Scenario results for reservoir Chl-a are graphically displayed in 3-d for visualization of loading influences on maximum Chl-a values in Figure 62.

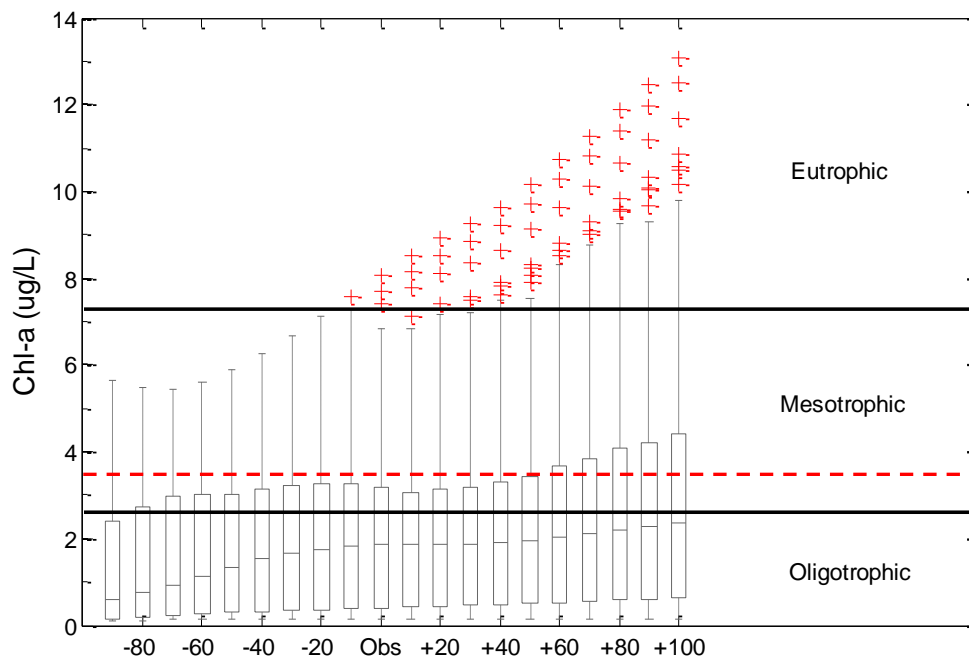


Figure 61. Chl-a scenario loading results for April 7th to Oct. 1st 2009. Boxplots center line is median, outer box represents the 25th and 75th percentiles, whiskers are highest data points within 1.5 times the IQR, and red plus signs indicate statistical outliers. Lake TP trophic level boundaries based on (Carlson and Simpson, 1996). Red dashed line indicates EPA reference condition of 3.5 $\mu\text{g/L}$ for the Great Basin and Range Ecoregion (U.S. EPA, 2001).

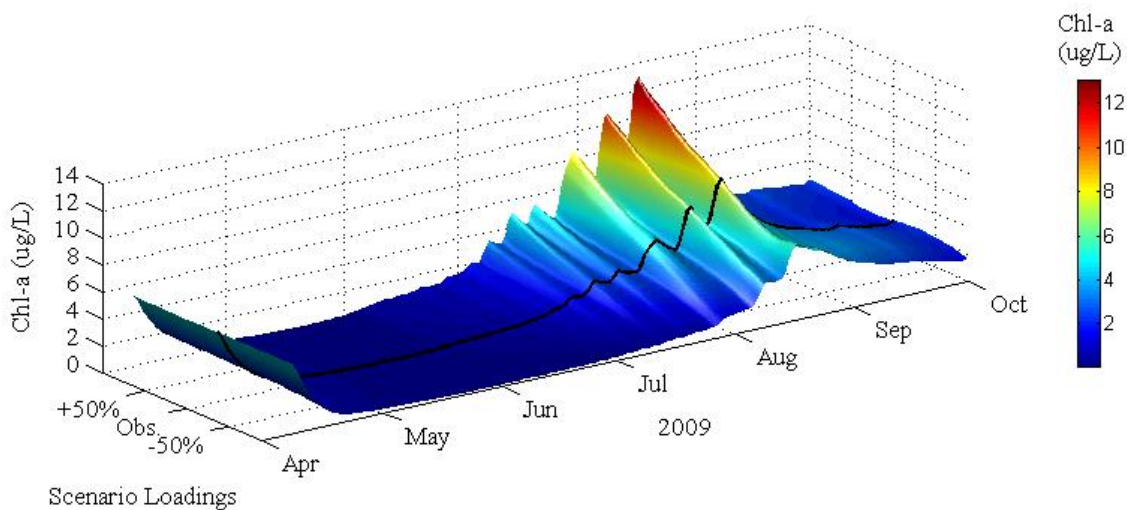


Figure 62. 3-dimensional view of the SFH load scenarios for the 2009 phytoplankton growing season. Black line indicates the calibrated model results.

Table 14. Average growing season values of water quality derived from loading scenarios.

SFH Reservoir Scenarios	TP mgP/L	SD m	Chl-a ug/L	NOx mgN/L
100%	0.061	3.20	2.98	0.026
90%	0.059	3.33	2.85	0.025
80%	0.057	3.48	2.73	0.024
70%	0.056	3.64	2.61	0.023
60%	0.054	3.81	2.50	0.023
50%	0.052	4.00	2.39	0.022
40%	0.051	4.20	2.29	0.021
30%	0.049	4.43	2.23	0.020
20%	0.048	4.67	2.19	0.019
10%	0.046	4.95	2.15	0.018
Simulated 2009	0.044	5.27	2.11	0.017
-10%	0.043	5.63	2.07	0.017
-20%	0.041	6.04	2.01	0.016
-30%	0.039	6.53	1.95	0.015
-40%	0.038	7.09	1.87	0.014
-50%	0.036	7.78	1.78	0.014
-60%	0.035	8.58	1.69	0.014
-70%	0.033	9.58	1.61	0.014
-80%	0.031	10.85	1.52	0.013
-90%	0.029	12.53	1.40	0.013

Simulated reservoir outflows of water quality constituents were used for the 20 SFH River simulations. The objective was to determine if reservoir loading conditions would stimulate changes in the immediate downstream river reach. Simulation results from June to October of 2009 show the initial conditions represent the highest benthic Chl-a concentration for all simulations at 570 mg/m² in all scenarios. After a period of biomass loss (attributed to scouring high flows) a second peak of benthic Chl-a was simulated with the highest value of 530 mg/m² for the scenario having +10% in reservoir

loadings. However, all scenario Chl-a values fell within 490-530 mg/m^2 , a range lower than the model benthic Chl-a RMSE goodness-of-fit of 70.38 mg/m^2 . The results indicate the river Chl-a dynamics are insensitive to the range of reservoir outputs predicted by the loading scenarios tested. Additional scenarios may represent future work including multiple year scenario simulations. Scenario results for benthic Chl-a are graphically displayed in 3-d for visualization of scenario outcomes on river benthic Chl-a in Figure 63.

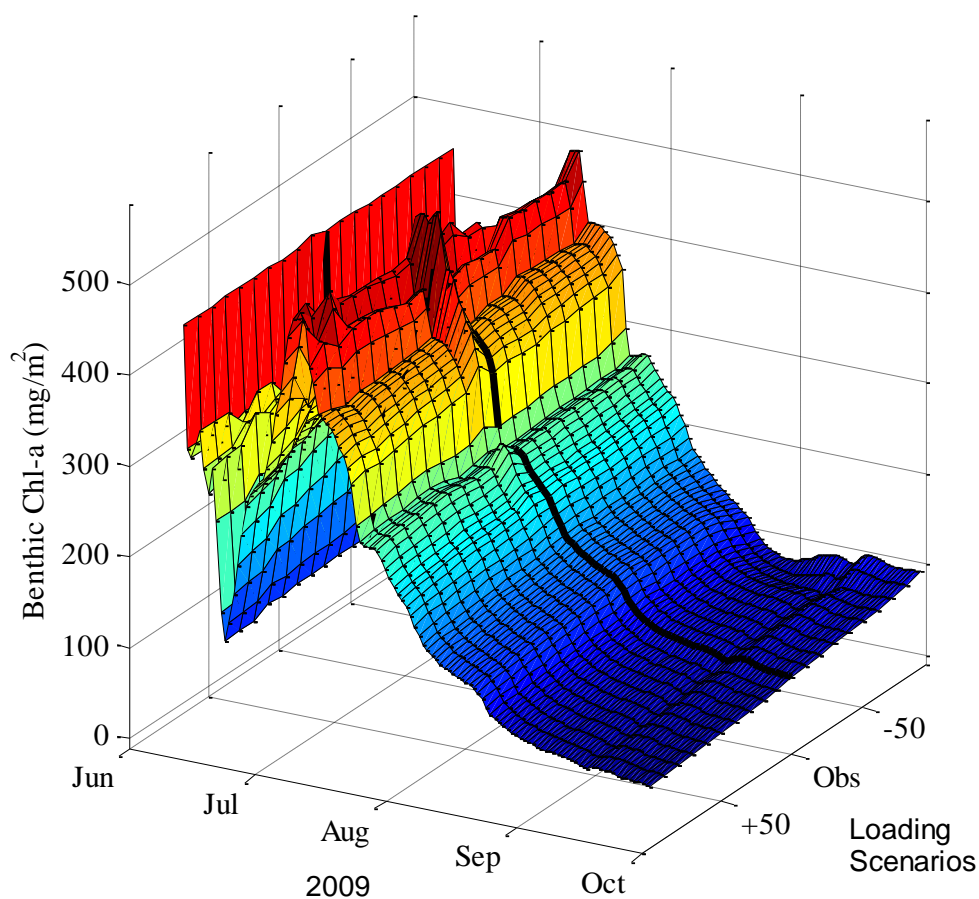


Figure 63. 3-dimensional view of the SFH river loading scenarios for the 2009 season. Black line indicates the calibrated model results.

8. CONCLUSIONS & RECOMMENDATIONS

Data from reservoir and river investigations during 2009 (Fritsen, et. al., 2011) were collected in a manner successfully completing the report objectives. However, the data also represents opportunistic dataset for preliminary nutrient criteria modeling investigations, for a coupled reservoir and river system. The collection of nutrients, pH, DO, POC, and water temperature, and a rich dataset of phytoplankton and periphyton and taxa and biomass were developed into an appropriate calibration dataset for AQUATOX 3.1 simulations. Additional validation data collected in 2010 supported the modeling exercise.

Results of calibration and validation of AQUATOX 3.1 for the SFH Reservoir and River demonstrates the applicability of the model for phytoplankton and periphyton simulations. Calibration and validation results of state variables yielded relatively low RMSE and BIAS values of simulated vs. observed data from the SFH system. Additionally, simulated values of state variables generally fell within minimum and maximum observed values for the modeling exercise.

Although valuable, the 2009 sampling schedule lacked some of the observational data required for a full dynamic season model. The SFH reservoir observational period missed the early development of the spring diatom bloom; therefore the initial conditions of the model were specified during diatom bloom in April, 2009. Additionally, initial periphyton sampling was collected in June, when values were at the observed maximum. The effect of data collection limitations was the inability to simulate periphyton and

phytoplankton for the initial month of March for the growing season, though validation data for both variables did result in an acceptable fit for 2010.

A significant model limitation was encountered with the calculation of TN, a necessary component for nutrient criteria investigations, representing a disadvantage in the modeling process. The combination of lack of reservoir sediment, dissolved OM, and unchangeable relationships between total and dissolved nitrogen, made it impossible to achieve a reasonable fit to both dissolved and total nitrogen observations. A decision was made to focus upon accurately simulating dissolved nutrients in the reservoir rather than totals. While TN was not accurately simulated, dissolved nutrients and TP were simulated with low values of RMSE and BIAS. Conversely, the model was not the priority for initial report data collection, and appropriate data surrogates were made when possible, thus utilizing the best methods for model data constraints.

The ability of AQUATOX 3.1 to effectively simulate the SFH Reservoir and River for the 2009, permitted scenario nutrient loading investigation to gain a better understanding of how the reservoir and river might respond to short-term loading changes. Assumptions that the calibrated models represent actual biological processes occurring during scenarios, and the covariance method of (Carleton, et al., 2009) correctly represents nutrient loadings are necessary for such investigations. The objective for the simulations was to aid management decisions regarding nutrient criteria, not to recommend specific values from the simulations. However, future mechanistic model investigations with two full growing season biomass, taxa identification, and uncertainty

analyses would likely generate numeric nutrient criteria values, in the absence of other management options.

Results indicate the reference EPA criteria for the ecoregion are generally not appropriate for the SHF Reservoir. Reference values of TP and Chl-a were only achieved via substantial load reductions. Reference values for NO_x were not achieved in the loading simulations, supporting the argument for a rejection of EPA's reference conditions for the reservoir, however reference values of SD were within the EPA criteria. While uncertainty of calibrated parameter values and nutrient loading conditions were not assessed, the large scenario range of loadings and the inability to meet target reference conditions supports the effort of developing site-specific nutrient criteria. River scenarios also indicate the immediate tailwater reach is somewhat insensitive to changes in reservoir loadings, indicating outflows conditions are potentially dominated by long-term sediment diagenesis processes.

Future research of the SFH models can be focused on many unique investigations of long-term modeling and climate change impacts, aiding state agencies to make informed management decisions. Long term modeling of reservoir and river response to nutrient scenarios would provide a better understand of how criteria selection will impact the reservoir and river water quality. Additionally, the impacts of climate change, with potential influences to river hydrology, cyanobacteria growth, and the effects on nutrient criteria are valuable questions yet to be addressed.

9. REFERENCES

- Acker, F. (2002). Analysis of Soft-Algae and Enumeration of Total Number of Diatoms in USGS NAWQA Program Quantitative Targeted-Habitat (RTH and DTH) Samples. In D. F. Charles, C. Knowles & R. S. Davis (Eds.), *Protocols for the analysis of algal samples collected as part of the U.S. Geological Survey National Water-Quality Assessment Program*. (pp. 124). Philadelphia, PA.: Patrick Center for Environmental Research, The Academy of Natural Sciences.
- Alexander, M. (1961). *Introduction to Soil Microbiology* (2nd Edition ed.). New Delhi: Wiley Eastern Limited.
- Arhonditsis, G. B., & Brett, M. T. (2004). Evaluation of the current state of mechanistic aquatic biogeochemical modeling. [Review]. *Marine Ecology-Progress Series*, 271, 13-26. doi: 10.3354/meps271013
- Asaeda, T., & Son, D. H. (2000). Spatial structure and population of a periphyton community: a model and verification. *Ecological Modelling*, 133, 195-207.
- Auer, M. T., Canale, R. P., Grundler, H. C., & Matsuoka, Y. (1982). Ecological and Mathematical Modeling of *Cladophora* in Lake Huron: 1 Program description and field monitoring of growth dynamics. *Journal of Great Lakes Research*, 8(1), 84-92.
- Bartholow, J., Hanna, R. B., Saito, L., Lieberman, D., & Horn, M. (2001). Simulated limnological effects of the Shasta Lake temperature control device. *Environmental Management*, 27(4), 609-626.
- Blinn, D. W., Shannon, J. P., Benenati, P. L., & Wilson, K. P. (1998). Algal ecology in tailwater stream communities: The Colorado River below Glen Canyon Dam, Arizona. *Journal of Phycology*, 34(5), 734-740.
- Boman, B., Wilson, C., Vandiver, V., & Hebb, J. (2002). Aquatic Weed Management in Citrus Canals and Ditches (pp. 14): Agricultural and Biological Engineering Department, Florida Cooperative Extension Service, Institute of Food and Agricultural Sciences, University of Florida.
- Bunn, S. E., Balcombe, S. R., Davies, P. M., Fellows, C. S., & McKenzie-Smith, F. J. (2006). Aquatic productivity and food webs of desert river ecosystems. In R. Kingsford (Ed.), *Ecology of Desert Rivers* (pp. 76-99). New York: Cambridge University Press.
- Camargo, J. A., Alonso, K., & de la Puente, M. (2005). Eutrophication downstream from small reservoirs in mountain rivers of Central Spain. [Article]. *Water Research*, 39(14), 3376-3384. doi: 10.1016/j.watres.2005.05.048
- Carleton, J. N., Park, R. A., & Clough, J. S. (2009). Ecosystem modeling applied to nutrient criteria development in rivers. [Research Support, U.S. Gov't, Non-P.H.S.]. *Environmental Management*, 44(3), 485-492. doi: 10.1007/s00267-009-9344-2
- Carlson, & Simpson, J. (1996). A Coordinator's Guide to Volunteer Lake Monitoring Methods. (pp. 96): North American Lake Management Society.
- Caupp, C. L., Brock, J. T., & Runke, H. M. (1998). Application of the Dynamic Stream Simulation and Assessment Model (DSSAMt) to the Truckee River Below Reno,

- Nevada: Model Formulation and Overview. Bosie, ID: Rapid Creek Research, Inc.
- Cerco, C. F., & Cole, T. (1993). 3-Dimensional Eutrophication Model of Chesapeake Bay. *Journal of Environmental Engineering-Asce*, *119*(6), 1006-1025. doi: 10.1061/(asce)0733-9372(1993)119:6(1006)
- Chapra, S. C. (1997). *Surface Water-Quality Modeling*. Long Grove, IL: Waveland Press, Inc.
- Chaves, P., Kojiri, T., & Yamashiki, Y. (2003). Optimization of storage reservoir considering water quantity and quality. *Hydrological Processes*, *17*(14), 2769-2793. doi: 10.1002/hyp.1433
- Clason, T., Frank, A., Morales, E., & Marr, L. (2002). Analysis of Diatoms on Microscope Slides Prepared From USGS NAWQA Program Algae Samples. Protocol P-13-39. In D. F. Charles, C. Knowles & R. S. Davis (Eds.), *Protocols for the analysis of algal samples collected as part of the U.S. Geological Survey National Water-Quality Assessment Program* (pp. 124). Philadelphia, PA.: Patrick Center for Environmental Research, The Academy of Natural Sciences.
- Clesceri, L. S., Greenberg, A. E., & Eaton, A. D. (1998). *Standard Methods for the Examination of Water and Wastewater*. Baltimore, MD: American Public Health Association.
- Collins, C. D., & Wlosinski, J. H. (1983). *Coefficients for Use in the U.S. Army Corps of Engineers Reservoir Model, CE-QUAL-R1*. (E-83). Vicksburg, MS.
- Cooke, G. D. (2005). *Restoration and management of lakes and reservoirs* (3rd ed.). Boca Raton, FL: CRC Press.
- Cullen, A. C., & Frey, H. C. (1999). *Probabilistic Techniques in Exposure Assessment*. New York.: Plenum Press.
- Dall, P. C. (1979). Sampling Technique for Littoral Stone Dwelling Organisms. *Oikos*, *33*(1), 106-112.
- Davis, C. J., Fritsen, C. H., Wirthlin, E. D., & Memmott, J. C. (2011). High Rates of Primary Productivity in a Semi-Arid Tailwater: Implications for self-regulated production. *River Research and Applications*. doi: 10.1002/rra.1573
- DeNicola, D. M. (1962). Periphyton responses to temperature at different ecological levels. In R. J. Stevenson, M. L. Bothwell & R. L. Lowe (Eds.), *Algal Ecology: Freshwater Benthic ecosystems*. San Diego, CA: Academic Press.
- Dhar, A., & Datta, B. (2008). Optimal operation of reservoirs for downstream water quality control using linked simulation optimization. *Hydrological Processes*, *22*(6), 842-853. doi: 10.1002/hyp.6651
- Diskin, M. H., & Simon, R. (1977). A Procedure for the Selection of Objective Functions for Hydrologic Simulation Models. *Journal of Hydrology*, *34*, 129-149.
- DiToro, D. M. (2001). *Sediment Flux Modeling*. New York: John Wiley & Sons, Inc.
- Dodds, W. K., Biggs, B. J. F., & Lowe, R. L. (1999). Photosynthesis-irradiance patterns in benthic microalgae: Variations as a function of assemblage thickness and community structure. *Journal of Phycology*, *35*(1), 42-53. doi: 10.1046/j.1529-8817.1999.3510042.x

- Dubrovsky, N. M., Burow, K. R., Clark, G. M., Gronberg, J. M., P.A., H., & Hitt, K. J. (2010). *The Quality of Our Nation's Waters—Nutrients in the Nation's Streams and Groundwater, 1992–2004*. U.S. Geological Survey.
- Ernst, M. R., & Owens, J. (2009). Development and application of a WASP model on a large Texas reservoir to assess eutrophication control. *Lake and Reservoir Management*, 25(2), 136-148. doi: 10.1080/07438140902821389
- Fritsen, C. H., Davis, C. J., Wirthlin, E. D., Smith, D. W., Momberg, D. K., & Memmott, J. C. (2011). South Fork Reservoir Report. In U. Review (Ed.), *South Fork Reservoir and South Fork of the Humboldt River Reports to Nevada Department of Environmental Protection* (Under Review ed., pp. Under Review.). Reno, NV: Desert Research Institute.
- Grumbles, B. H. (2007). *Memorandum: Nutrient Pollution and Numeric Water Quality Standards*. Washington, D.C.
- Hawkins, B. E., & Evans, M. S. (1979). Seasonal Cycles of Zooplankton Biomass in Southeastern Lake Michigan, USA. *Journal of Great Lakes Research*, 5(3-4), 256-263.
- Heiskary, S., & Markus, H. (2001). Establishing relationships among nutrient concentrations, phytoplankton abundance, and biochemical oxygen demand in Minnesota, USA, rivers. *Lake and Reservoir Management*, 17(4), 251-262.
- Heiskary, S., & Markus, H. (2003). Establishing relationships among instream nutrient concentrations, sestonic algae abundance and composition, fishin IBI and biochemical oxygen demand in Minnesota USA rivers. St. Paul, MN: Minnesota Pollution Control Agency.
- Henley, W. F., Patterson, M. A., Neves, R. J., & Lemly, A. D. (2000). Effects of sedimentation and turbidity on lotic food webs: A concise review for natural resource managers. *Reviews in Fisheries Science*, 8(2), 125-139. doi: 10.1080/10641260091129198
- Hill, W. (1996). Effects of Light. In R. J. Stevenson, M. L. Bothwell & R. L. Lowe (Eds.), *Algal Ecology* (pp. 121-148). San Diego: Academic Press.
- Hillebrand, H., Durselen, C. D., Kirschtel, D., Pollinger, U., & Zohary, T. (1999). Biovolume calculation for pelagic and benthic microalgae. *Journal of Phycology*, 35(2), 403-424. doi: 10.1046/j.1529-8817.1999.3520403.x
- Hornberger, G. M., Kelly, M. G., & Eller, R. M. (1976). Relationship Between Light and Photosynthetic Rate in a River Community and Implications for Water-Quality Modeling. *Water Resources Research*, 12(4), 723-730. doi: 10.1029/WR012i004p00723
- Hupfer, M., & Lewandowski, J. (2008). Oxygen Controls the Phosphorus Release from Lake Sediments - a Long-Lasting Paradigm in Limnology. [Review]. *International Review of Hydrobiology*, 93(4-5), 415-432. doi: 10.1002/iroh.200711054
- Hutchinson, G. E. (1957). *A Treatise on Limnology, Volume I, Geography, Physics, and the Limnoplankton*. New York: John Wiley & Sons.
- Ishikawa, M., & Ishikuni, M. (1981). Coprecipitation of Phosphate with Calcite. *Geochemical Modelling*, 28, 717-726.

- Jager, H. I., & Smith, B. T. (2008). Sustainable reservoir operation: Can we generate hydropower and preserve ecosystem values? *River Research and Applications*, 24(3), 340-352. doi: 10.1002/rra.1069
- Jorgensen, S. E. (2003). The application of models to find the relevance of residence time in lake and reservoir management. *Journal of Limnology*, 62(Suppl. 1), 16-20.
- Karl, D. M., Dore, J. E., Hebel, D. V., & Winn, C. (1991). Procedures for particulate carbon, nitrogen, phosphorus, and total mass analyses used in the US-JGOFS Hawaii Ocean time series program. *Marine Particles: Analysis and Characterization* (Vol. p. 71-77): American Geophysical Union.
- Keehner, D. (2009). *Memorandum: External Peer Review to AQUATOX Release 3*. Washington, DC: US EPA.
- Kelly, M. G., Hornberg, Gm, & Cosby, B. J. (1974). Continuous Automated Measurement of Rates of Photosynthesis and Respiration in an Undisturbed River Community. *Limnology and Oceanography*, 19(2), 305-312.
- Kennedy, R. H. (2005). Toward integration in reservoir management. *Lake and Reservoir Management*, 21(2), 128-138.
- Kitchell, J. F., Koonce, J. F., O'Neill, R. V., Shugart, H. H., Magnuson, J. J., & Booth, R. S. (1972). Implementation of a Predator-Prey Biomass Model for Fishes *Eastern Deciduous Forest Biome* (pp. 57): International Biological Program.
- Koelmans, A. A., Van der Heijde, A., Knijff, L. M., & Aalderink, R. H. (2001). Integrated modelling of eutrophication and organic contaminant fate & effects in aquatic ecosystems. A review. *Water Research*, 35(15), 3517-3536. doi: 10.1016/s0043-1354(01)00095-1
- Koiv, T., Noges, T., & Laas, A. (2011). Phosphorus retention as a function of external loading, hydraulic turnover time, area and relative depth in 54 lakes and reservoirs. *Hydrobiologia*, 660(1), 105-115. doi: 10.1007/s10750-010-0411-8
- Komatsu, E., Fukushima, T., & Shiraishi, H. (2006). Modeling of P-dynamics and algal growth in a stratified reservoir - mechanisms of P-cycle in water and interaction between overlying water and sediment. *Ecological Modelling*, 197(3-4), 331-349. doi: 10.1016/j.ecolmodel.2006.03.023
- Larsen, D. P., Schults, D. W., & Malueg, K. W. (1981). Summer Internal Phosphorus Supplies in Shagawa Lake, Minnesota. *Limnology and Oceanography*, 26(4), 740-753.
- Leidy, G. R., & Ploskey, G. R. (1980). *Simulation Modeling of Zooplankton and Benthos in Reservoirs: Documentation and Development of Model Constructs*. Vicksburg, MS: U.S. Army Corps of Engineers.
- Liao, N. (2002). Determination of Orthophosphate in Waters by Flow Injection Colorimetry (Vol. 10-115-01-1-M:17): QuikChem® Method.
- Lyman, W. J. (1982). *Handbook of Chemical Property Estimation Methods*. New York: McGraw-Hill Book Co.
- Macedo, C. F., & Pinto-Coelho, R. M. (2000). Diel variations in respiration, excretion rates, and nutritional status of zooplankton from the Pampulha reservoir, Belo Horizonte, MG. *Journal of Experimental Zoology*, 286(7), 671-682. doi: 10.1002/(sici)1097-010x(20000601)286:7<671::aid-jez1>3.0.co;2-e

- Marshall, D. W., Otto, M., Panuska, J. C., Jaeger, S. R., Sefton, D., & Baumberger, T. R. (2006). Effects of hypolimnetic releases on two impoundments and their receiving streams in southwest Wisconsin. [Article]. *Lake and Reservoir Management*, 22(3), 223-232.
- McIntire, C. D., & Colby, J. A. (1978). A Hierarchical Model of Lotic Ecosystems. *Ecological Monographs*, 48, 167-190.
- McKay, M. D., Conover, W. J., & Beckman, R. J. (1979). A Comparison of Three Methods for Selecting Values of Input Variables in the Analysis of Output from Computer Code. *Technometrics*, 21(239-245).
- Megard, R. O., Combs, W. S., Smith, P. D., & Knoll, A. S. (1979). Attenuation of Light and Daily Integral Rates of Photosynthesis Attained by Planktonic Algae. *Limnology and Oceanography*, 24(6), 1038-1050.
- Munn, M. D., & Brusven, M. A. (2004). The influence of Dworshak Dam on epilithic community metabolism in the Clearwater River, USA. *Hydrobiologia*, 513(1-3), 121-127.
- NDEP. (2008). Nutrient Assessment Protocols for Lakes and Reservoirs in Nevada (B. o. W. Q. Planning, Trans.) (Vol. 1): Nevada Division of Environmental Protection.
- NDEP. (2009). Nevada's Nutrient Criteria Strategy (Version 2 ed., pp. 1-20). Carson City: Nevada Division of Environmental Protection.
- NDSP. (2008). South Fork State Recreation Area. In N. D. o. S. Parks (Ed.), <http://parks.nv.gov/pdf/09SFBrochure.pdf> (pp. 2). Carson City.
- Neumann, D. W., Rajagopalan, B., & Zagona, E. A. (2003). Regression model for daily maximum stream temperature. *Journal of Environmental Engineering-Asce*, 129(7), 667-674. doi: 10.1061/(asce)0733-9372(2003)129:7(667)
- Nurnberg, G. K. (2007). Lake responses to long-term hypolimnetic withdrawal treatments. *Lake and Reservoir Management*, 23(4), 388-409. doi: 10.1080/07438140709354026
- Obreza, T., Clark, M., Boman, B., Borisova, T., Cohen, M., Dukes, M., . . . Wright, A. (2010) A Guide to EPA's Numeric Nutrient Water Quality Criteria for Florida. *Soil and Water Science Department, Florida Cooperative Extension Service: Institute of Food and Agricultural Sciences*.
- Oklahoma Department of Environmental Quality. (1996). TMDL Development for Cobb Creek Watershed and Fort Cobb Lake (Final Report ed.).
- Ozkundakci, D., Hamilton, D. P., & Gibbs, M. M. (2011). Hypolimnetic phosphorus and nitrogen dynamics in a small, eutrophic lake with a seasonally anoxic hypolimnion. *Hydrobiologia*, 661(1), 5-20. doi: 10.1007/s10750-010-0358-9
- Pahl, R. (2011, 9/22/2011). [South Fork Reservoir Personal Communication].
- Palisade Corporation. (1991). *Risk Analysis and Simulation Add-In for Lotus 1-2-3*. New York: Newfield.
- Park, R. A., Clough, J. S., & Wellman, M. C. (2008). AQUATOX: Modeling environmental fate and ecological effects in aquatic ecosystems. *Ecological Modelling*, 213(1), 1-15. doi: 10.1016/j.ecolmodel.2008.01.015
- Park, R. A., Groden, T. W., & Desormeau, C. J. (1979). Modification to the Model CLEANER Requiring Further Research. In D. Scavia & A. Robertson (Eds.),

- Perspectives on Lake Ecosystem Modeling* (pp. 22): Ann Arbor Science Publishers, Inc.
- Perry, R. M. (2007). [Personal Communication "South Fork Main Dam Embankment"].
- Pritzlaff, P. (2000). Determination of Nitrate/Nitrite in Surface and Wastewaters by Flow Injection Analysis. *QuikChem® Method*(10-107-04-1-C:15).
- Prokopy, W. R. (2003). Determination of Ammonia by Flow Injection Analysis (Vol. 10-107-06-2-C:10). *QuikChem® Method*.
- Rashleigh, B., Barber, M. C., & Walters, D. M. (2009). Foodweb modeling for polychlorinated biphenyls (PCBs) in the Twelvemile Creek Arm of Lake Hartwell, South Carolina, USA. *Ecological Modelling*, 220(2), 254-264. doi: 10.1016/j.ecolmodel.2008.09.007
- Redfield, A. (1958). The Biological control of chemical factors in the environment. *American Science* 46, 205-221.
- Rosemond, A. D. (1993). Interactions Among Irradiance, Nutrients, and Herbivores Constrain a Stream Algal Community. *Oecologia*, 94(4), 585-594.
- Rueda, F., Moreno-Ostos, E., & Armengol, J. (2006). The residence time of river water in reservoirs. [Article]. *Ecological Modelling*, 191(2), 260-274. doi: 10.1016/j.ecolmodel.2005.04.030
- Saito, L., & Koski, M. (2006). Simulated effects of altered spillway releases on thermal structure and kokanee growth in a Colorado reservoir. *Journal of the American Water Resources Association*, 42(3), 645-658.
- Sater, E. M., Reuter, J. D., & Goldman, C. R. (1994). Seasonal nutrient limitation at four high altitude shallow reservoirs of the Tahoe Basin and Northern Nevada. Davis, CA: University of California-Davis.
- Scavia, D. (1980). The Need for Innovation Verification of Eutrophication Models. In R. V. Thomann & T. D. Barnwell (Eds.), *Verification of Water Quality Models* (pp. 214-225). Athens, Ga: US EPA.
- Smith, V. H., Tilman, G. D., & Nekola, J. C. (1999). Eutrophication: impacts of excess nutrient inputs on freshwater, marine, and terrestrial ecosystems. [Article; Proceedings Paper]. *Environmental Pollution*, 100(1-3), 179-196. doi: 10.1016/s0269-7491(99)00091-3
- Sourisseau, S., Bassères, A., Périé, F., & Caquet, T. (2008). Calibration, validation and sensitivity analysis of an ecosystem model applied to artificial streams. *Water Research*, 42(4-5), 1167-1181. doi: 10.1016/j.watres.2007.08.039
- Sterner, R. W., & Elser, J. J. (2002). *Ecological Stoichiometry: The Biology of Elements from Molecules to the Biosphere*. New York: Princeton University Press.
- Straskraba, M., & Gnauck, A. H. (1985). *Freshwater Ecosystems: Modelling and Simulation* (Vol. 8). Amsterdam, The Netherlands: Elsevier Science Publishers.
- Thomann, R. V., & Mueller, J. (1987). *Principles of Surface Water Quality Modeling and Control*. New York, NY: HarperCollins.
- Tucker, S., & Jones, D. (2007a). Determination of total nitrogen in manual persulfate digests. (Vol. 10-107-04-4-B:26): *QuikChem® Method*
- Tucker, S., & Jones, D. (2007b). Determination of Total Phosphorus in Manual Persulfate Digests (Vol. 10-115-01-4-B:16): *QuikChem® Method*.
- U.S. EPA. (1972). *Federal water Pollution Control Act: Section 303*. Washington, DC.

- U.S. EPA. (1998). *National Strategy for the Development of Regional Nutrient Criteria*. (EPA-822-R-98-00). Washington, DC.
- U.S. EPA. (2001). *Ambient Water Quality Criteria Recommendations*. (EPA-822-B-01-008). Washington, DC.
- U.S. EPA. (2009a). *AQUATOX (Release 3): Modeling Environmental fate and ecological effects in aquatic ecosystems*. Retrieved from http://www.epa.gov/waterscience/models/aquatox/technical/aquatox_release_3_fact_sheet.pdf.
- U.S. EPA. (2009b). *A Calibrated Parameter Set for Simulateion of Algae in Shallow Rivers*. (EPA-823-R-09-003). Washington, DC.
- U.S. EPA. (2009c, 4/7/2009). User's Guide and Technical Documentation KABAM Version 1.0 (Kow (based) Aquatic BioAccumulation Model) Retrieved 11/12/2011, 2011
- U.S. EPA. (2010). *Using Stressor-response Relationships to Derive Numeric Nutrient Criteria*. (EPA-820-S-10-001). Washington, DC.
- USGS. (2011). National Water Information System: Web Interface Retrieved 10/5, 2011, from <http://waterdata.usgs.gov/nwis>
- Ward, J. V., & Stanford, J. A. (1983). The Serial Discontinuity Concept of Lotic Ecosystems. *Fontaine, T. D. Iii and S. M. Bartell (Ed). Dynamics of Lotic Ecosystems. Xiii+494p. Ann Arbor Science Publishers: Ann Arbor, Mich., USA. Illus. Issbn 0-250-40612-8, P29-42.*
- Welch, E. B., & Jacoby, J. M. (2004). *Pollutant Effects in Freshwater: Applied Limnology* (3rd Edition ed.). New York: Spon Press.
- Welschmeyer, N. A. (1994). Fluorometric Analysis of Chlorophyll-a in the Presence Of Chlorophyll-b and Pheopigments. *Limnology and Oceanography*, 39(8), 1985-1992.
- Wetzel, R. G. (2001). *Limnology: Lake and River Ecosystems*. San Diego: Academic Press.
- White, S. D. M. (1986). Numerical Recipes - The Art Of Scientific Computing - Presse,Wh, Flannery,Bp, Teukolsky,Sa, Vetterling,Wt. *Scientist*, 1(2), 23-23.
- Whitton, B. A., & Potts, M. (2000). *The Ecology of Cyanobacteria: Their Diversity in Time and Space*. New York: Springer.
- Wool, T. A., Ambrose, R. B., Martina, J. L., & Comer, E. A. (2004). *Water Quality Analysis Simulation Program (WASP) Version 6.0 DRAFT: User's Manual*. Atlanta, GA.

APPENDIX A-2009-2010 SFH System Data

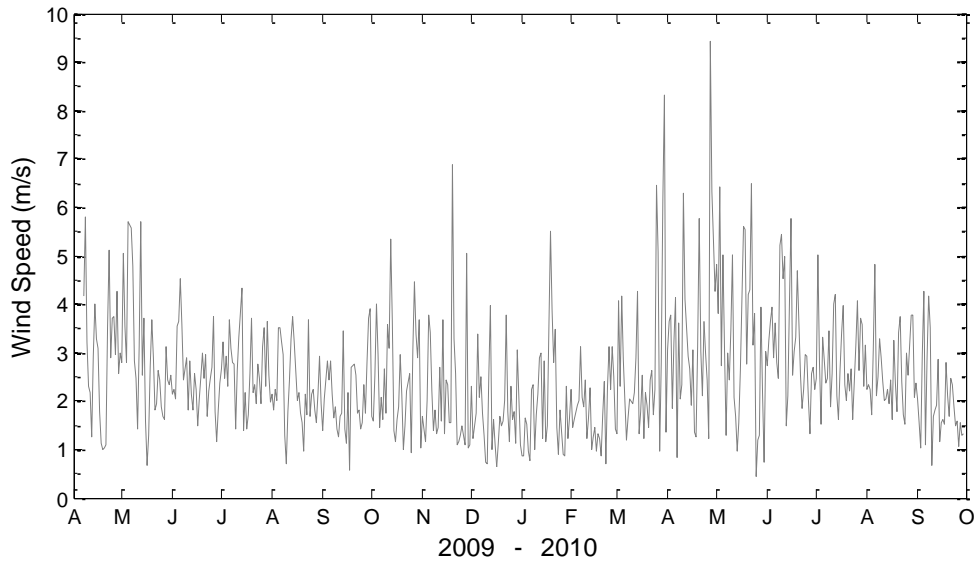


Figure 64. Average daily wind speed obtained from the Elko Regional Airport NWS Weather Station (<http://mesowest.utah.edu/index.html>).

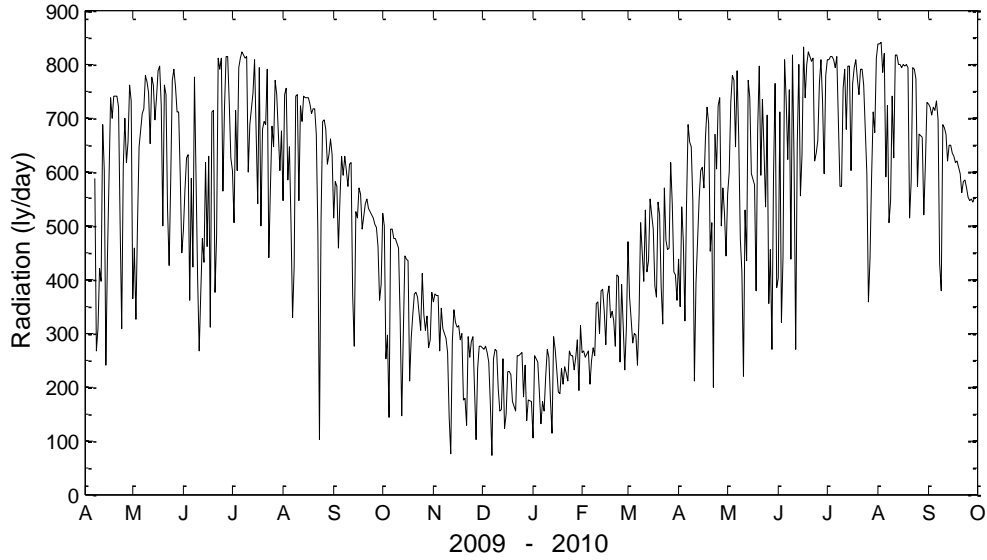


Figure 65. Average daily radiation from the Crain Springs BLM Weather Station (<http://mesowest.utah.edu/index.html>).

Table 15. South Fork Reservoir average pH, calculated thermocline depth and average hypolimnion temperature from 2009-2010.

Reservoir Sample Date	pH Ave.	Thermocline Depth	Hypolimnion Temp.
4/7/2009	8.29	-	-
5/27/2009	7.96	11.98	13.38
6/9/2009	8.00	10.02	17.75
7/21/2009	8.21	7.52	16.8
8/24/2009	8.40	11.33	18.18
9/23/2009	8.57	12.77	17.85
6/17/2010	8.25	9.50	12.90
7/14/2010	8.29	10.50	13.82
8/4/2010	8.34	11.50	14.53
9/21/2010	8.39	12.00	15.70

APPENDIX B- RESERVOIR AND RIVER MODEL INITIAL CONDITIONS

Table 16. SFH reservoir and river model initial conditions (Fritsen, et. al., 2011).

Model Initial Conditions	Units	Reservoir	River
Physical Characteristics			
Volume	m ³	4.93E+07	8.00E+03
Surface Area	m ²	6.15E+06	2.73E+04
Site Length	km	4.95	1.25
Mean Depth	m	7.12	0.3
Maximum Depth	m	18.5	1.5
Mean Evaporation	Inches/Year	24.74	0
Latitude	degrees	40.66	40.66
Temperature	°C	8.5	16.09
Wind	m/sec	4.17	2
Light	ly/day	587.41	463
Channel Slope	m/m	-	0.0018
Manning's Coefficient	s/m ^{1/3}	-	0.088
Habitat: Percent Riffle	percent	-	52
Habitat: Percent Run	percent	-	48
Chemical Variables			
pH	standard	8.29	7.65
Total Suspended Solids (TSS)	mg/L	2.12	1.64
NH ₄	mgN/L	0.0023	0.0184
NO ₃	mgN/L	0.0011	0.0103
PO ₄	mgP/L	0.0131	0.0423
Carbon Dioxide	mgC/L	0.7	0.2397
Oxygen	mgO ₂ /L	10.38	8.5548
Organic Carbon (OC)	mg/L	1.18	0.4674
Particulate Percentage of OC	percent	100	100
Refractory vs. Labile Percentage	percent	50	50

Table 17. SFH reservoir and river initial conditions (continued).

Model Initial Conditions	Units	Reservoir	River
Sediment and Diagenesis			
POC G1	g C/m ³	1203.368	-
POC G2	g C/m ³	4783.389	-
POC G3	g C/m ³	30.084	-
PON G1	g N/m ³	180.626	-
PON G2	g N/m ³	18.177	-
PON G3	g N/m ³	0.114	-
POP G1	g P/m ³	41.155	-
POP G2	g P/m ³	1.818	-
POP G3	g P/m ³	0.011	-
Labile Detritus	g/m ² dry	-	3
Refractory Detritus	g/m ² dry	-	1
Phytoplankton			
Diatoms	mg/L dry	0.2636	0.0038
Cyanophytes	mg/L dry	0.0079	0.0052
Chlorophytes	mg/L dry	0.0016	-
Periphyton			
Diatom (<i>Navicula</i>)	g/m ² dry	-	69.3371
Chlorophytes (<i>Cladophora</i>)	g/m ² dry	-	44.8015
Zooplankton			
Copepod	mg/L dry	0.00735	-
Cladocerans	mg/L dry	0.02977	-

APPENDIX C- RESERVOIR PARAMETER VALUES

Table 18. Default phytoplankton parameters values used in SFH Reservoir modeling study (USEPA, 2009).

SFH Reservoir Phytoplankton		Cyanobacteria	Diatoms	Chlorophytes	Note
Parameter	Unit	Value	Value	Value	
N-Half Saturation	mgN/L	0.4	0.011	0.006	(U.S. EPA, 2009a), - ,(Collins & Wlosinski, 1983)
C-Half Saturation	mgC/L	0.240	0.054	0.054	(Collins & Wlosinski, 1983)
Temp. Response Slope	unitless	2.000	1.8	2	(USEPA, 2009)
Max. Temp.	°C	50.0	35	42	(DeNicola, 1962)
Min. Adaptation Temp.	°C	5	2	10	(USEPA, 2009)
Photoresp. Coeff.	1/day	0.129	0.26	0.03	(USEPA, 2009), - ,(Collins & Wlosinski, 1983)
Mort. Coeff.	g/g·day	0.002	0.003	0.003	(USEPA, 2009)
Expn. Mort. Coeff.	g/g·day	0.12	0.04	0.04	(USEPA, 2009)
P:Organics	unitless	0.004	0.007	0.007	(Sterner and Elser, 2002)
N:Organics	unitless	0.04	0.079	0.079	(Sterner and Elser, 2002)
Lt. Extinction	1/m-g/m ³	0.099	0.144	0.144	(Megard et al., 1979), (Collins & Wlosinski, 1983)
Wet to Dry	unitless	5	10	5	(USEPA, 2009), (U.S. EPA, 2009c)
Lipid Fraction	wet wt.	0	0.023	0	(USEPA, 2009), (Collins & Wlosinski, 1983)
Sed. Rate	m/day	0.01	0.16	0.14	(USEPA, 2009)
Exp. Sed. Coeff.	unitless	0.05	0.693	0.693	(USEPA, 2009)

Table 19. Zooplankton parameter values for the SFH Reservoir model.

SFH Reservoir Zooplankton		Copepod	Cladocerans	
Parameter	Unit	Value	Value	Note
Half-Sat. Feeding	mgPhyto/L	0.569	0.206	CALIBRATED
Max. Consumption	g/g·day	0.660	0.904	CALIBRATED
Min. Prey for Feeding	mgPhyto/L	0.094	0.016	CALIBRATED
Sorting: Selective Feeding	unitless	0.5	0.9	(U.S. EPA, 2009a)
Slope for Sed. Response	unitless	-0.46	-0.46	(U.S. EPA, 2009a), (Henley et al., 2000)
Intercept for Sed. Resp.	unitless	2.20	2.20	(U.S. EPA, 2009a), (Henley, et al., 2000)
Temp. Response Slope	unitless	2.20	2.40	(U.S. EPA, 2009a)
Opt. Temp	°C	25.78	10.49	CALIBRATED
Max. Temp.	°C	34.00	34.00	(Leidy and Ploskey, 1980)
Min. Adaptation Temp.	°C	5	5	(Leidy and Ploskey, 1980)
Mean wet weight	g wet	0.0006	0.0060	(Thomann and Mueller, 1987)
Endogenous Resp.	1/day	0.0063	0.013	CALIBRATED
Specific Dynamic Action	unitless	0.180	0.180	(U.S. EPA, 2009a)
Excretion:Resp.	ratio	0.170	0.170	(Scavia, 1980)
N to Org.	frac. dry	0.006	0.090	(Sterner and Elser, 2002)
P to Org.	frac. dry	0.006	0.014	(Sterner and Elser, 2002)
Wet:Dry	ratio	6.610	6.750	(U.S. EPA, 2009c)
Gametes:Biomass	ratio	0.10	0.10	(U.S. EPA, 2009a)
Gamete Mortality	1/day	0.90	0.90	(U.S. EPA, 2009a)
Mort. Coeff.	1/day	0.002	0.002	(Collins and Wlosinski, 1983)
Carrying Capacity	mg/L	8.00	8.00	(U.S. EPA, 2009a)
Removal due to Fishing	frac/day	0	0	(U.S. EPA, 2009a)
Mean lifespan	days	14	14	(U.S. EPA, 2009a)
Frac. Lipid	wet wt.	0.024	0.080	(U.S. EPA, 2009c), , (Macedo and Pinto- Coelho, 2000)
Lethal O2 Conc.	mg/L	0	1	(U.S. EPA, 2009a)
Ammonia Toxicity	mg/L	25	19	(U.S. EPA, 2009a)

Table 20. Remineralization parameters used within the SFH Reservoir model.

Remineralization Parameters	SFH Reservoir		
	Unit	Value	Note
Max. Degrdn. Rate, Labile	g/g·day	0.08	(Wetzel, 2001)
Max. Degrdn. Rate, Refrac.	g/g·day	0.0018	(Collins and Wlosinski, 1983)
Opt. Temp.	°C	25	Default (U.S. EPA, 2009a)
Max. Temp.	°C	65	(Alexander, 1961)
Min. pH for Degrad.	standard	5.00	(Lyman, 1982)
Max. pH for Degrad.	standard	8.50	(Lyman, 1982)
kNitri, Max Rate of Nitrif.	1/day	0.05	Default (U.S. EPA, 2009a)
kDenitri Bottom (max rate denitri at sed./water)	1/day	0.20	Default (U.S. EPA, 2009a)
kDenitri Water (max rate denitri at water)	1/day	0.65	Default (U.S. EPA, 2009a)
P:Organics, Labile	frac. dry	0.001	(Redfield, 1958)
N:Organics, Labile	frac. dry	0.001	(Redfield, 1958)
P:Organics, Refractory	frac. dry	0.001	(Sterner and Elser, 2002)
N:Organics, Refractory	frac. dry	0.002	(Sterner and Elser, 2002)
P:Organics, Diss. Labile	frac. dry	0.007	(Redfield, 1958)
N:Organics, Diss. Labile	frac. dry	0.06	(Redfield, 1958)
P:Organics, Diss. Refr.	frac. dry	0.10	(Sterner and Elser, 2002)
N:Organics, Diss. Refr.	frac. dry	0.002	(Sterner and Elser, 2002)
O ₂ :Biomass, Resp., Decomp.	unitless	0.58	(Redfield, 1958)
CBOD _u to BOD ₅ Conversion	unitless	2.47	(Thomann and Mueller, 1987)
O ₂ :N, Nitrification	unitless	4.57	(Scavia, 1980)
Detrital Sed. Rate Ksed	g/m·day	0.69	(Collins and Wlosinski, 1983)
Temp. of Obs. Ksed	°C	20	Default (U.S. EPA, 2009a)
Wet to Dry, Susp. Labile	unitless	5	Default (U.S. EPA, 2009a)
Wet to Dry, Susp. Refr.	unitless	5	Default (U.S. EPA, 2009a)
Wet to Dry, Sed. Labile	unitless	5	Default (U.S. EPA, 2009a)
Wet to Dry, Sed. Refr.	unitless	5	Default (U.S. EPA, 2009a)
KD, Partition Coeff. P to CaCO ₃	L/kg	1740	(Ishikawa and Ishikuni, 1981)

Table 21. Sediment diagenesis parameters for the reservoir model.

Sediment Diagenesis Parameters	SFH Reservoir		
	Unit	Value	Note
Solids Conc. (Layer 1)	kg/L	0.50	Default (DiToro, 2001)
Solids Conc. (Layer 2)	kg/L	0.50	Default (DiToro, 2001)
Layer 1 Thickness (H1)	m	0.01	Default (DiToro, 2001)
Deep Burial (Dd)	m ² /day	0.001	Default (DiToro, 2001)
Deep Burial Vel. (w2)	m/day	0.0003	Default (DiToro, 2001)
Layer 2 Thickness (H2)	m	0.30	Default (DiToro, 2001)
Freshwater Nitrif. Vel.	m/day	0.077	CALIBRATED
Freshwater DeNitrif. Vel.	m/day	0.333	CALIBRATED
Freshwater DeNitrif. Vel. Layer 2	m/day	0.250	Default (DiToro, 2001)
CH4 Oxid. Layer 1	m/day	0.7	Default (DiToro, 2001)
Nitrif. Half-Sat. for NH ₄	mgN/L	0.728	Default (DiToro, 2001)
Nitrif. Half-Sat. for O ₂	mgO ₂ /L	0.740	Default (DiToro, 2001)
Part. Coeff. For NH ₃ (KdNH ₃)	L/kg	1.000	Default (DiToro, 2001)
Part. Coeff. For Inorg. P (KdPO₄)	L/kg	21.46	CALIBRATED
Freshwater Aerobic Partition Coeff. Inorg. P	unitless	8.15	CALIBRATED
Critical O ₂ con. For partion Inorg. P	mgO ₂ /L	2.0	Default (DiToro, 2001)
Theta Pore Water Diffusion 1-2	unitless	0.995	CALIBRATED
Theta for Nitrif.	unitless	0.75	Default (DiToro, 2001)
Theta for Denitrif.	unitless	1.08	Default (DiToro, 2001)
Theta for Methane Oxid.	unitless	1.079	Default (DiToro, 2001)
Layer 1 Reaction Vel. for diss. Sulfide Oxid.	m/day	0.20	Default (DiToro, 2001)
Layer 1 Reaction Vel. for part. Sulfide Oxid.	m/day	0.40	Default (DiToro, 2001)
Theta for Sulfide Oxid.	unitless	1.08	Default (DiToro, 2001)
Sulfide Oxid. Constant for O ₂	mgO ₂ /L	4	Default (DiToro, 2001)
Partition Coeff for Sulfide Layer 1	L/kg	100	Default (DiToro, 2001)
Partition Coeff for Sulfide Layer 2	L/kg	100	Default (DiToro, 2001)

Table 22. Sediment diagenesis parameters for the reservoir model (continued).

Sediment Diagenesis Parameters	SFH Reservoir		
	Unit	Value	Note
G class 1 pon mineralization	1/day	0.0011	Default (DiToro, 2001)
G class 2 pon mineralization	1/day	0.0018	Default (DiToro, 2001)
G class 3 pon mineralization	1/day	0	Default (DiToro, 2001)
G class 1 poc mineralization	1/day	0.035	Default (DiToro, 2001)
G class 2 poc mineralization	1/day	0.0018	Default (DiToro, 2001)
G class 2 poc mineralization	1/day	0	Default (DiToro, 2001)
G class 1 pop mineralization	1/day	0.035	Default (DiToro, 2001)
G class 2 pop mineralization	1/day	0.0018	Default (DiToro, 2001)
G class 2 pop mineralization	1/day	0	Default (DiToro, 2001)
Theta for G class 1 PON	unitless	1.10	Default (DiToro, 2001)
Theta for G class 2 PON	unitless	1.15	Default (DiToro, 2001)
Theta for G class 3 PON	unitless	1.17	Default (DiToro, 2001)
Theta for G class 1 POC	unitless	1.10	Default (DiToro, 2001)
Theta for G class 2 POC	unitless	1.15	Default (DiToro, 2001)
Theta for G class 3 POC	unitless	1.17	Default (DiToro, 2001)
Theta for G class 1 POP	unitless	1.10	Default (DiToro, 2001)
Theta for G class 2 POP	unitless	1.15	Default (DiToro, 2001)
Theta for G class 3 POP	unitless	1.17	Default (DiToro, 2001)
First-order decay rate benthic Stress	1/day	0.03	Default (DiToro, 2001)
First Order Dissolution Rate Bio. Si Layer 2	1/day	0.50	Default (DiToro, 2001)
Temp. Adjust for Bio. Si	unitless	1.10	Default (DiToro, 2001)
Si diss. Half-Sat. Const. for Bio. Si	g Si/m ³	50000	Default (DiToro, 2001)
Sat.-conc. of silica in pore water	g Si/m ³	40	Default (DiToro, 2001)
Part. Coeff. for Si in Layer 2	L/kg	100	Default (DiToro, 2001)
Sorption Factor of Si in Layer 1	unitless	10	Default (DiToro, 2001)
Critical DO for Silica Sorption in Layer 1	mg/L	1.00	Default (DiToro, 2001)
Fraction of Susp. Detritus (non-reactive)	unitless	0.01	Default (DiToro, 2001)
Fraction of Si of diatoms (dry)	g/g dry	0.43	Default (DiToro, 2001)

APPENDIX D- RIVER PARAMETERS

Table 23. Default periphyton parameters for the SFH river model (USEPA, 2009).

SFH Reservoir Phytoplankton		<i>Cladophora</i>	Diatoms	
Parameter	Unit	Value	Value	Note
P-Half Saturation	mgP/L	0.0025	0.003	(Collins & Wlosinski, 1983)
N-Half Saturation	mgN/L	0.003	0.007	(Collins & Wlosinski, 1983)
Temp. Response Slope	unitless	2.000	1.8	(USEPA, 2009)
Max. Temp.	°C	22	39	(DeNicola, 1962)
Min. Adaptation Temp.	°C	5	2	(USEPA, 2009)
Photoresp. Coeff.	1/day	0.03	0.05	(USEPA, 2009), - ,(Collins & Wlosinski, 1983)
Mort. Coeff.	g/g·day	0.06	0.001	(USEPA, 2009)
Expn. Mort. Coeff.	g/g·day	0.001	0.001	(USEPA, 2009)
P:Organics	unitless	0.0044	0.018	(Sternier and Elser, 2002)
N:Organics	unitless	0.04	0.04	(Sternier and Elser, 2002)
Lt. Extinction	1/m-g/m ³	0.02	0.002	(Megard, et al., 1979), (Collins & Wlosinski, 1983)
Wet to Dry	unitless	5	5	(USEPA, 2009), (U.S. EPA, 2009c)
Lipid Fraction	wet wt.	0	0	(USEPA, 2009), (Collins & Wlosinski, 1983)
Still Water Reduction	unitless	0.2	0.16	(USEPA, 2009)

Table 24. Remineralization parameters used within the SFH River model.

Remineralization Parameters	SFH River		
	Unit	Value	Note
Max. Degrdn. Rate, Labile	(g/g·day)	0.08	(Wetzel, 2001)
Max. Degrdn. Rate, Refrac.	(g/g·day)	0.0018	(Collins and Wlosinski, 1983)
Opt. Temp.	(°C)	25	Default (U.S. EPA, 2009a)
Max. Temp.	(°C)	65	(Alexander, 1961)
Min. pH for Degrad.	(standard)	5.00	(Lyman, 1982)
Max. pH for Degrad.	standard	8.50	(Lyman, 1982)
kNitri, Max Rate of Nitrif.	1/day	1.0	(Caupp, et al., 1998)
kDenitri Bottom (max rate denitri at sed./water)	1/day	0.2	Default (U.S. EPA, 2009a)
kDenitri Water (max rate denitri at water)	1/day	0.3	Default (U.S. EPA, 2009a)
P:Organics, Labile	frac. dry	0.018	(Redfield, 1958)
N:Organics, Labile	frac. dry	0.079	(Redfield, 1958)
P:Organics, Refractory	frac. dry	0.0002	(Sterner and Elser, 2002)
N:Organics, Refractory	frac. dry	0.002	(Sterner and Elser, 2002)
P:Organics, Diss. Labile	frac. dry	0.059	(Redfield, 1958)
N:Organics, Diss. Labile	frac. dry	0.0002	(Redfield, 1958)
P:Organics, Diss. Refr.	frac. dry	0.0002	(Sterner and Elser, 2002)
N:Organics, Diss. Refr.	frac. dry	0.002	(Sterner and Elser, 2002)
O2:Biomass, Resp., Decomp.	unitless	0.575	(Redfield, 1958)
CBODu to BOD5 Conversion	unitless	2.47	(Thomann and Mueller, 1987)
O2:N, Nitrification	unitless	4.57	(Scavia, 1980)
Detrital Sed. Rate Ksed	g/m·day	0.65	(Collins and Wlosinski, 1983)
Temp. of Obs. Ksed	°C	20	Default (U.S. EPA, 2009a)
Wet to Dry, Susp. Labile	unitless	5	Default (U.S. EPA, 2009a)
Wet to Dry, Susp. Refr.	unitless	5	Default (U.S. EPA, 2009a)
Wet to Dry, Sed. Labile	unitless	5	Default (U.S. EPA, 2009a)
Wet to Dry, Sed. Refr.	unitless	5	Default (U.S. EPA, 2009a)
KD, Partition Coeff. P to CaCO3	L/kg	1740	(Ishikawa and Ishikuni, 1981)

APPENDIX E- SCENARIO NUTRIENT LOADING VALUES

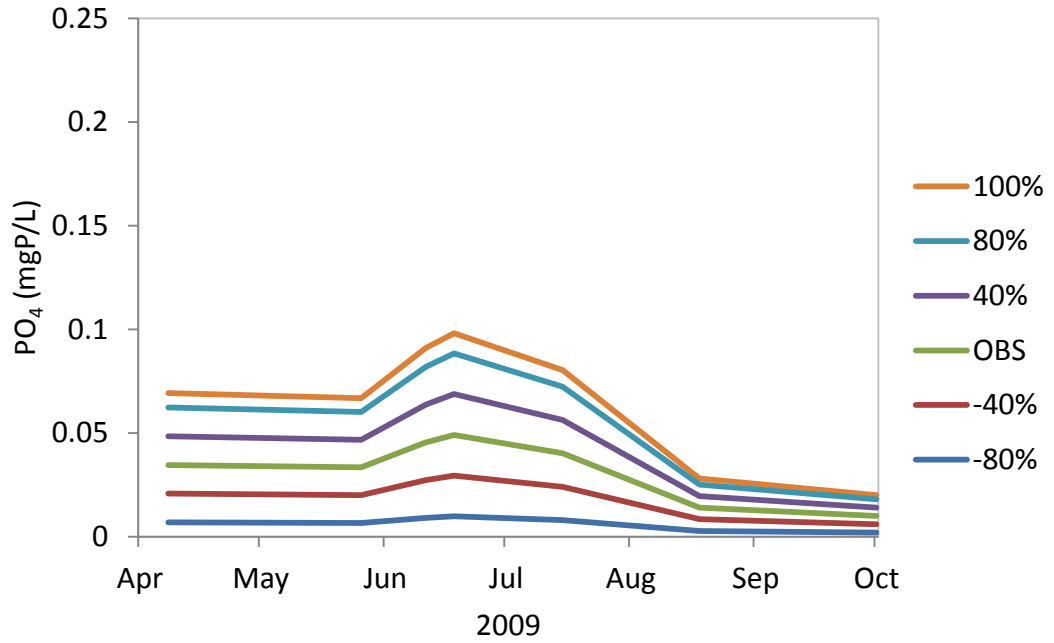


Figure 66. Scenario results for PO₄ loading to the SFH Reservoir. 2009 simulation is represented by the OBS values.

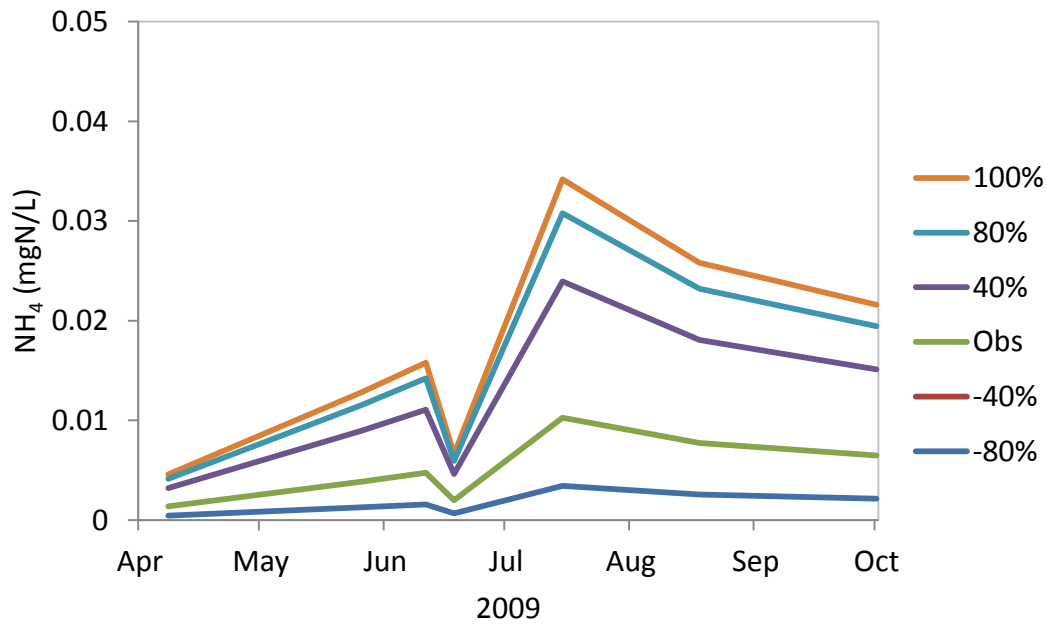


Figure 67. Scenario results for NH₄ loading to the SFH Reservoir. 2009 simulation is represented by the OBS values.

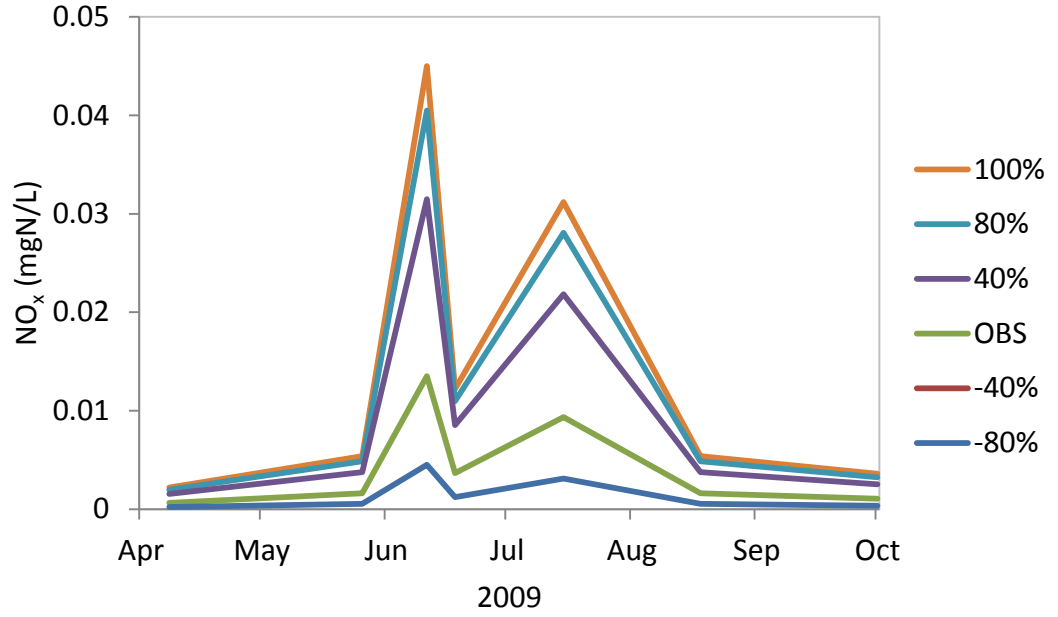


Figure 68. Scenario results for NO_x loading to the SFH Reservoir. 2009 simulation is represented by the OBS values.